THESIS ON INFORMATICS AND SYSTEM ENGINEERING C47

Model Based Method for Adaptive Decomposition of the Thoracic Bio-impedance Variations into Cardiac and Respiratory Components

ANDREI KRIVOŠEI

TALLINN UNIVERSITY OF TECHNOLOGY
Faculty of Information Technology
Department of Electronics

Dissertation was accepted for the defence of the degree of Doctor of Philosophy in Engineering on August 19, 2009.

Supervisors:	Professor Mart Min Department of Electronics Tallinn University of Technology
	Professor Vello Kukk Department of Computer Control Tallinn University of Technology
Reviewer:	Professor Emeritus Enn Velmre Department of Electronics Tallinn University of Technology
Opponents:	Professor Ivars Bilinskis, Dr.Sci.Eng. Academician of Latvian Academy of Sciences, Latvia
	Professor Jari Hyttinen, Dr.Eng. Tampere University of Technology, Finland
	Senior Researcher Gert Tamberg, PhD Department of Mathematics Tallinn University of Technology, Estonia

Defence of the thesis: 21.09.09, 15:00, Tallinn, Ehitajate tee 5, room II-208

Declaration:
Hereby I declare that this doctoral thesis, my original investigation and achievement, submitted for the doctoral degree at Tallinn University of Technology has not been submitted for any academic degree.

/ *Andrei Krivošei* /

Copyright: Andrei Krivošei, 2009
ISSN 1406-4731
ISBN 978-9985-59-936-5

INFORMAATIKA JA SÜSTEEMITEHNIKA C47

Mudelipõhine meetod torso bioimpedantsi muutuste adaptiivseks dekompositsiooniks südametegevuse ja hingamise komponentideks

ANDREI KRIVOŠEI

Abstract

The developed method for adaptive decomposition of the thoracic electrical bio-impedance (EBI) into its main components – cardiac and respiratory ones – is described in the thesis. The method allows decompose the EBI on-line in non-stationary conditions. Delay of the resulting signals with respect to the input is only two seconds. Moreover, the proposed method allows decompose the EBI signal into its components also in the case when the harmonic spectra of these components are partially overlapped.

The method is based on models of the cardiac and respiratory components of the total EBI signal. The model of cardiac component is composed as a parametric time domain model, which uses the specially designed set of orthonormal signals, called as application specific orthonormal basis (ASOB). The Jacobi weight function is applied to the design of ASOB. The cardiac model is characterised first by natural parameters – frequency and amplitude. Additionally, other parameters, characteristic to the model type and specific to the designed ASOB, are introduced. The respiratory signal model is designed in frequency domain. This is just a low-pass filter, which suppresses the remainder of the cardiac component – the difference between the cardiac component of EBI and its parametric model. The LPF with finite impulse response is used to preserve the waveform of respiratory component unchanged.

The bio-impedance signal decomposer (BISD) as a realization of the proposed method is accomplished digitally using PC software. However, the future developments are oriented towards applications in portable and stationary cardiac devices, both in ambulatory and clinical settings, where imbedded solutions are required.

Resümee

Väitekirjas on esitatud väljatöötatud meetod rindkere elektrilise bioimpedantsi lahutamiseks südametegevuse ja hingamise komponentideks. See meetod võimaldab eraldada komponendid praktiliselt reaalajas mittestatsionaarses olukorras. Väljundsignaalide hilistumine sisendi suhtes on maksimaalselt kaks sekundit. Seejuures võimaldab esitatud meetod lahutada bioimpedantsi signaali komponentideks isegi siis, kui nende spektrid osaliselt kattuvad.

Meetod kasutab torso impedantsi signaali südametegevuse ja hingamise komponentide mudeleid. Südamekomponendi aeg-esituses parameetrilise mudeli matemaatiliseks aluseks on spetsiaalselt koostatud ortonormaalne rakenduspõhine signaalibaas, mille juures aproksimeerimise kaalud määrab Jacobi funktsioon. Südametegevuse mudelit karakteriseeritakse esmajoones naturaalsete parameetritega – amplituudi ja sagedusega. Lisaks tuuakse sisse lisaparameetrid, mis on iseloomulikud just antud mudelitüübile. Sagedusesituses hingamissignaali mudel on madalpääsfilter, mis surub maha jääkkomponendi – südametegevuse signaali ja selle parameetrilise mudeli vahelise erinevuse. See on lõpliku impulsskajaga madalpääsfilter, mis filtreerimisega toob sisse vaid hilistamise ilma läbiva hingamissignaali kuju moonutamiseta.

Ülalkirjeldatud meetodi alusel on välja töötatud bioimpedantsi signaalikomponentide eraldaja, mis on realiseeritud digitaalselt personaalarvuti tarkvara kujul. Siiski, kuna tulevikurakendused on orienteeritud kasutamisele kantavates ja implanteeritud seadmetes ning ambulatoorsetes ja kliinilistes tingimustes, siis on silmapiiril meetodi rakendused sardsüsteemide koosseisus.

Acknowledgments

This work was supported by Estonian Science Foundation (grants G7212, G7243, and G5614), Enterprise Estonia through the Competence Centre ELIKO, and EITSA. The author express him thanks to Dr. Jürgen Lamp from JR Medical Ltd for providing practical information and giving valuable advice.

Great thanks to my supervisors Prof. Mart Min and Prof. Vello Kukk. I thank my colleagues, coauthors of our published papers, and all the people who supported me during this study.

Special thanks to my girlfriend Olga and my parents for their understanding and support.

Contents

Abbreviations 13

1 Introduction 15
  1.1 Electrical Bio-Impedance (EBI) – overview 16
  1.2 Estimate of the EBI Value 18
    1.2.1 Electrode configurations. 20
  1.3 Bio-Impedance Signal Considerations 21
    1.3.1 Bio-Impedance vs. Bio-Admittance 22
    1.3.2 Considering EBI as a signal 24
  1.4 Impedance Cardiography (ICG) 26
    1.4.1 Hemodynamic parameters 27
    1.4.2 Difficulties in hemodynamic parameters analysis 31
  1.5 Impedance Respirography (IRG) 32
    1.5.1 Pneumodynamic parameters 33
    1.5.2 Troubles in pneumodynamic parameters analysis 33
  1.6 Uncertainties in the ICG and IRG 34

2 Problem statement 35
  2.1 The EBI decomposition – problem statement 35
  2.2 Decomposition the EBI signal – a review about known methods and potential solutions 37
    2.2.1 Ensemble averaging 37
    2.2.2 Adaptive filtering (classical) 37
    2.2.3 Spectral methods 38
    2.2.4 Independent component analysis (ICA) methods 38
    2.2.5 Concluding the review 39

3 Proposed method – Model based EBI decomposition 41
  3.1 The method basics 41
  3.2 The cardiac EBI signal model 44
    3.2.1 Cardiac signal parameters – an overview 44
  3.3 The respiratory EBI signal model 48
  3.4 Practical realization of the electrical BI signal decomposer (BISD) 49
    3.4.1 BISD with a semi-adaptive cardiac model 49
    3.4.2 BISD with fully adaptable cardiac model 50

4 Discussion 53

5 Conclusions 55

A appendix “A Bio-Impedance Signal Synthesiser (BISS) for Testing of an Adaptive Filtering System” 57

B appendix “An Adaptive Filtering System for Separation of Cardiac and Respiratory Components of Bioimpedance Signal” 63

C appendix “Signal-Shape Locked Loop (SSLL) as an Adaptive Separator of Cardiac and Respiratory Components of Bio-Impedance Signal” 71

D appendix “Bio-Impedance Signal Decomposer (BISD) as an Adaptive Signal Model Based Separator of Cardiac and Respiratory Components” 79

E appendix “An Adaptively Tunable Model of the Cardiac Signal for the Bio-Impedance Signal Decomposer (BISD)” 85

F appendix “Decomposition method of electrical bio-impedance signal into cardiac and respiratory components” 91

G appendix ELULOOKIRJELDUS 103

H appendix CURRICULUM VITAE 107

List of publications 111

References 113

Abbreviations

Abbreviations used in the thesis.

AF – Adaptive Filter (filtering)
AR – Auto Regressive
ASOB – Application Specific Orthonormal Basis
OB – Orthonormal Basis
BA – Bio-Admittance
BI – Bio-Impedance
BISD – Bio-Impedance Signal Decomposer
BISS – Bio-Impedance Signal Synthesizer
SSLL – Signal Shape Locked Loop
EBI – Electrical Bio-Impedance
EBA – Electrical Bio-Admittance
ICG – Impedance Cardiography
ICGm – Impedance Cardiogram
DICGm – Derivative of ICGm (1st order)
D^2ICGm – Derivative of ICGm (2nd order)
IRG – Impedance Respirography
IRGm – Impedance Respirogram
ICA – Independent Component Analysis
FIR – Finite Impulse Response (filter)
IIR – Infinite Impulse Response (filter)
LPF – Low-Pass Filter
TD – Tidal Volume
MV – Minute Ventilation
VR – Ventilation Rate
HR – Heart Rate

1

Introduction

The thesis presents the results of author's research work carried out during his PhD study at the Department of Electronics of Tallinn University of Technology on the electrical bio-impedance (EBI) subject, and in more particular, on its application in cardiology. More precisely, the topic lies in the processing of the raw data of the human chest's EBI by separating its cardiac and respiratory components and in selecting them out from the total EBI signal. As a result, the selected and separated components – cardiac and respiratory ones – can be further analyzed and processed individually.

Below, the introductory first chapter of the thesis continues by presenting the overview of the EBI and its applications in general in the section 1.1. The overview of the EBI estimation techniques is shown in the section 1.2. Some considerations about the bio-impedance signal are discussed in the section 1.3. The impedance cardiography (ICG) with related troubles is discussed in more details in the section 1.4. The impedance respirography (IRG) with related troubles is discussed in the section 1.5.

The second chapter contains the problem statement together with a review about known and possible new solutions. The latter review, in addition to its main purpose, allows better explaining the problem in general and showing the complex nature of the stated problem.

The third chapter describes the proposed method for adaptive signal decomposition. In this chapter, the basics of the method are introduced, and the models of the cardiac and respiratory bio-impedance components are presented. In the last section of the chapter two practical accomplishments are described: 1) the bio-impedance signal decomposer (BISD) with semi-adaptive cardiac signal model, and 2) the BISD with fully adaptable cardiac signal model.

In the last chapter of the thesis, the author's standpoints, discussions and conclusions are presented.

Published journal papers and the full texts of the presented conference papers of the author are given in appendices A – F.

At the end of the thesis the list of references and the list of author's publications are presented.

1.1 Electrical Bio-Impedance (EBI) – overview

The conception and the definition of the electrical bio-impedance (EBI) are familiar to scientists and researchers since a long time ago. The term *electrical impedance* was introduced by Oliver Heaviside even in 1886 year and was developed further by Kennely (1893), who introduced complex variables for describing of electrical impedance. The *bio* prefix in the EBI term indicates the biological nature of the object, electrical impedance of which is under discussion. Therefore, assuming the biological nature of the subject, the EBI can be defined as the quantity showing how much the *biological* tissue resists to the electrical current flow, which is injected into the tissue. As an electrical parameter, the EBI reflects electrical performances of the tissue under examination (Grimnes and Martinsen 2008, Chapter 4 and 5). Consequently, an electrical model of the tissue can be defined, which in conjunction with others discipline specific models (i.e. chemical, mechanical, geometrical etc.) can give more exact and complete understanding of the tissue structure and performances.

In addition, since an estimation of the EBI as a parameter of a living tissue gives certain information about the physiological (electrical) performances of this tissue or its state, the variations in the EBI can reflect the changes in the tissue state and functioning. For example, in application to the human and other mammal organisms, the body motions, the blood flow, the mechanical movements of the heart and lungs cause complicated changes in the EBI. Estimating and analyzing the EBI of human thorax makes possible to analyze some dynamic processes in organs, such as respiration and cardiac activities.

Such relations between the EBI variations and physiological changes were investigated already in 1930-40s years by Atzler and Lehmann (1932), who related the impedance changes to the mechanical activity of the heart. Later investigations followed by Nyboer *et al*, enabled to declare that changes in the human chest impedance are related to a pulsatile blood volume (Nyboer *et al* 1940).

But only in the past decades, due to the giant progress in the microelectronic and computers fields, an estimation of the EBI and its practical applications began to play an important role in medicine. During the past years, the developments in EBI estimation techniques and the related signal processing algorithms have achieved great results. For example, modern devices cover wider and wider frequency range in which the EBI can be estimated and analyzed. More complex digital algorithms can be used instead of its analogue approximations. Therefore, such devices are more precise and reliable in the EBI estimation task than before, which opens more possibilities in studies of small variations of EBI. Variations of that kind may have small amplitude, but often they are of the most of importance for researchers and medical doctors. For example, in some measurement conditions, the amplitude of the impedance variation caused by cardiac activity can be 100 times smaller than the value of basal EBI component.

Moreover, the great achievements in micro technologies, allow to produce more complicated systems on a chip, make possible to integrate the whole (or, at least, almost whole) EBI estimating circuitry into the single chip. Such a possibility together with non-invasiveness of the EBI techniques gives great opportunity to develop the cost-effective widely used medical diagnostic and prognostic devices. Devices of that kind can be used for long-term monitoring of patients in clinical conditions as well as in ambulatory conditions or even at patient’s home.

The information collected from the EBI estimation can be used in a wide range of the medical and biological applications, i.e. *impedance cardiology*, *impedance tomography, body composition estimation, biological cells research* or even for human *disgust indication* (Rohrmann and Hopp 2008). However, the cardio-applications are of greatest importance topics nowadays.

Numerous diseases related to the heart functioning are known, e.g., heart failure, congestive heart failure, cardiovascular disease, coronary artery disease, ischemia, hypertension and etc. For example, 21% of the adult population in Canada are affected by hypertension (McFetridge-Durdle *et al* 2008).

Thereupon, the situation requires developing of cheap and widely available, non-invasive and reliable monitoring and diagnosing tools capable to recognize a heart disease on its early progress stage. Such devices also must to be easy to handle for medical staff as well as for personal use at home.

The present day, in opposite, heart activity monitors and diagnosing tools are expensive, cumbersome and time-consuming, also complicated in use. Moreover, they are invasive and therefore health risky, as it was reviewed recently by Sodolski and Kutarski (2007).

In contrast, the EBI based technology offers non-invasive, safe for the person health, and easy to use methods and tools for heart activity monitoring and analysis. Despite that the commercially distributable EBI-based cardiac devices are not cheap enough and their availability is not enough wide yet, the EBI-based methods are very promising not only in its reliability, but also in cost and wider availability in the near future.

1.2 Estimate of the EBI Value

Since already values of the EBI are used as the input data for the method proposed in the thesis, only a short overview of the EBI estimation technique is presented. First, to start this subsection the definitions of used terms are given.

The conception *impedance estimate* or *estimation* instead of *impedance measure* or *measurement* is used in the current work. This is since the impedance is indirectly measured (thus estimated) through the direct measurement of the voltage in the case of the current driven measurement (Grimnes and Martinsen 2008, Chapter 7).

Taking into account an existence of parasitic components[1] in the measuring stuff and their complexity, such as impedances of electrodes, of the skin and tissue regions, which are out of interest, makes an accurate and reliable EBI value estimation to the non-trivial task (Grimnes and Martinsen 2008). Moreover, high-quality current source design is complicated, especially in the frequency range over 100 kHz (Annus *et al* 2008a), giving thus an additional error component for the EBI estimate. Thus the use of terms *estimate* and *estimation* corresponds much more to the realistic situation.

However, for the simplicity of description, the overview of the estimation techniques is done without considering the parasitic effects in the measuring stuff. It is possible without any loss of generality, in the context of the thesis topic.

Thus, in principle, the value of EBI can be estimated by injecting the electrical current into the tissue region, which is of interest and measuring the voltage drop around this region (Figure 1).

Using the well known Ohm's law, a value of the tissue impedance for a selected frequency can be expressed as ratio of the measured voltage response over the excitation current:

$$\mathbf{Z} = \frac{\mathbf{V}_{\mathrm{res}}}{\mathrm{I}_{\mathrm{exc}}} \tag{1}$$

Here, in eq. (1), and in the following mathematical expressions, the symbols describing signals and certain parameters, which are typed in bold, mean the vectors. Such vectors have two coordinates – typically, the amplitudes of the inphase and quadrature components of the same order of the used orthonormal basis (e.g. cosine and sine functions). The components can be represented using the complex math notation.

Moreover, the use of an admittance notation can be more convenient in some applications. The admittance of the tissue region of interest at a selected frequency is following:

---

[1] Such components are parasitic with regard to the tissue region, immittance of which is of interest, see i.e. Annus *et al* 2008a.

$$\mathbf{Y} = \frac{1}{\mathbf{Z}} = \frac{\mathrm{I}_{\mathrm{exc}}}{\mathbf{V}_{\mathrm{res}}} \tag{2}$$

Both the impedance and admittance of the biological tissue are complex values in their nature. This is due to the capacitive effect of membranes of the tissue cells and their nucleuses (Grimnes and Martinsen 2008, Chapter 3), which is reflected in the phase shift of the voltage around the cells with respect to the current flowing through the cells. In opposite, electrolytic solution of the cells and surrounding space is purely resistive and does not give any phase shift between the voltage in the rounding space and the injected current (Grimnes and Martinsen 2008, Chapter 2).

Since a lot of cells exist in the tissue region of interest, they all take part in the EBI formation. Such the sharing and distribution of factors, including also the complicated frequency dependence, is very complicated. This makes difficult to analyze and model it (Grimnes and Martinsen 2008, Chapter 8).

It is clear, that the EBI of living tissue is frequency dependent due to the capacitive effect. And moreover, different cells and different tissue regions have different electrical performances, and consequently also their spectral characteristics in frequency domain. In this way researchers are interested in obtaining the EBI estimates in so wide frequency range as possible and thanks to the great development of technology in last decade, it is becoming realizable.

The first possible solution suitable to obtain EBI values over the selected frequency range is to scan over the frequency range of interest, varying the frequency of the excitation current generator in the single frequency EBI estimator.

The second possibility is to generate the excitation current of a complicated waveform (thus of complicated spectral content). In this case the wide frequency

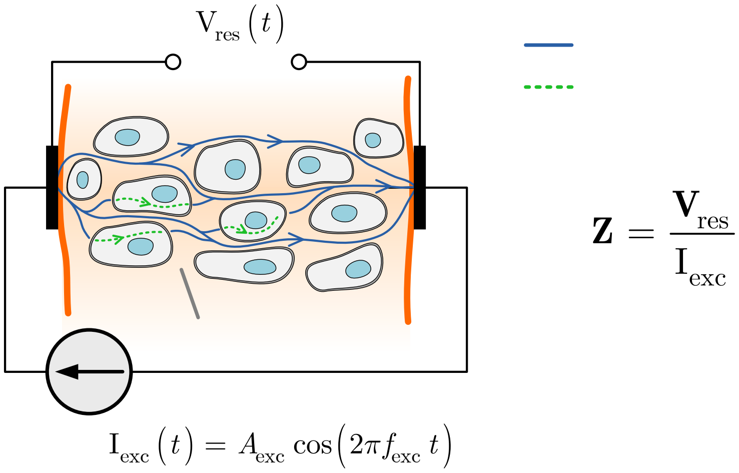
$\mathrm{V}_{\mathrm{res}}(t)$
$\mathbf{Z} = \frac{\mathbf{V}_{\mathrm{res}}}{\mathrm{I}_{\mathrm{exc}}}$
$\mathrm{I}_{\mathrm{exc}}(t) = A_{\mathrm{exc}} \cos(2\pi f_{\mathrm{exc}}\, t)$

Figure 1 Simplified diagram of the EBI value estimating technique

range can be covered in one-step measurement-estimation procedure (Annus *et al* 2008b, Min *et al* 2008, Paavle *et al* 2008). It is very important in such applications, where the performances of the biological tissue change very fast in time, and the response of the EBI in a wide frequency range is of interest. The estimation of EBI must be done during a very short time interval.

1.2.1 Electrode configurations.

Numerous electrode configurations exist to estimate the EBI of the human thorax. Here, in this subsection, some of such configurations are presented for example.

A. Four band electrode configuration

For a long period the electrode configuration shown in Figure 2 was widely used in the ICG applications.

B. Hands to feet spot electrode configuration

This electrode configuration is used in JR Medical Ltd (Estonia) instrumentation. The same configuration was applied also for collecting the EBI estimates, which were used by the author as input data for making computer experiments with the developed decomposer.

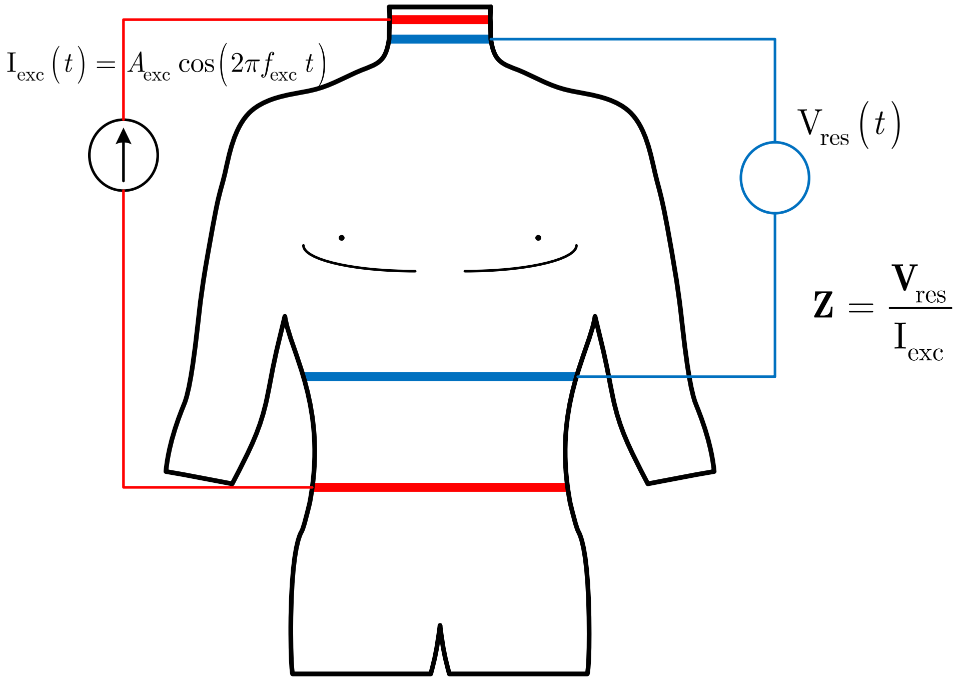
$I_{exc}(t) = A_{exc}\cos(2\pi f_{exc}\, t)$
$V_{res}(t)$
$\mathbf{Z} = \frac{\mathbf{V}_{res}}{I_{exc}}$

Figure 2 The four band electrode configuration typically used for the EBI value estimation

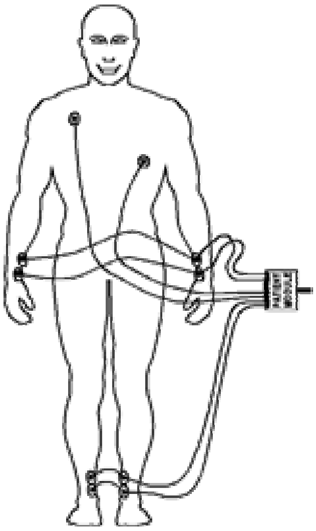

Figure 3 Hands to feet spot electrode configuration (used in JR Medical Ltd products)

1.3 Bio-Impedance Signal Considerations

For the thesis work, the EBI variations caused by respiration and cardiac activities are both of interest. Therefore, the developing of the model-based conceptual method of the EBI cardiac and respiratory components for their separation is presented in the thesis. First of all, only the single-frequency EBI value estimates are used. After that the developed algorithms can be extended and adapted for the input data set containing the multi-frequency EBI value estimates.

The single-frequency measurement configuration used for estimating the EBI value is shown in Figure 4, where on the sources of dynamic variations (the heart and lungs), are taken into account too as well.

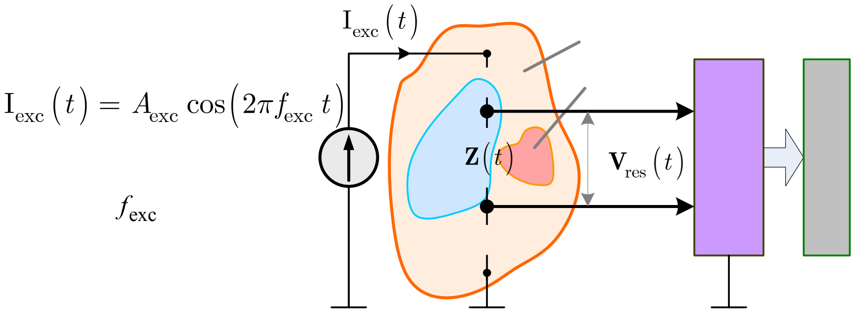
$\mathrm{I}_{\mathrm{exc}}(t)$
$\mathrm{I}_{\mathrm{exc}}(t) = A_{\mathrm{exc}} \cos(2\pi f_{\mathrm{exc}}\, t)$
f_{exc}
$\mathbf{Z}(t)$
$\mathbf{V}_{\mathrm{res}}(t)$

Figure 4 The block-diagram of a typical single-frequency measurement configuration used for estimating of the EBI value

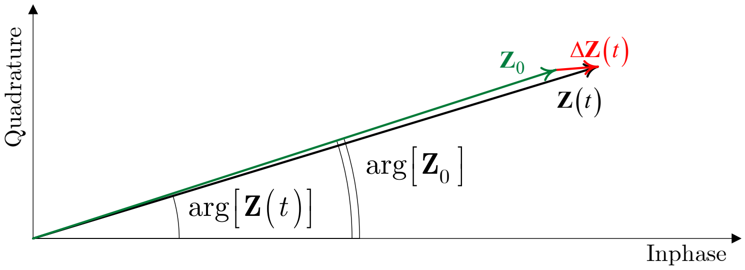

Figure 5 Phasor diagram of electrical bioimpedance Z(t) and its variation ΔZ(t)

1.3.1 Bio-Impedance vs. Bio-Admittance

In this subsection, a comparison between the impedance and admittance use for the immitance cardiography and respirography is done. I will show that the time varying parts of impedance and admittance are different only in their scales and signs, if their values are much smaller than their related basal components. As a result, the proposed method can be used with either impedance or admittance estimates of the human thorax.

Despite that the impedance as a parameter of the living tissue region between the voltage measuring electrodes is the unified whole, the small variation of it can be treated as a separate signal (see $\Delta\mathbf{Z}(t)$ in Figure 5) summed up with the basal part of the estimated impedance (3), which is constant in time (see $\mathbf{Z}_0$ in Figure 5):

$$Z(t) = Z_0 + \Delta Z(t) \tag{3}$$

And the same for an admittance:

$$Y(t) = Y_0 + \Delta Y(t) \tag{4}$$

It is clear that electrical performances of the living tissue can be described either by the impedance or admittance, which are related as reciprocal ratios:

$$Y = \frac{1}{Z} = \frac{1}{Z_0 + \Delta Z} \tag{5}$$

$$Z = \frac{1}{Y} = \frac{1}{Y_0 + \Delta Y} \tag{6}$$

And both parameters, in turn, can be presented as a sum of basal and time-varying parts (3) - (4). The basal component is the constant impedance (admittance) of the living tissue region between the voltage measuring electrodes. The

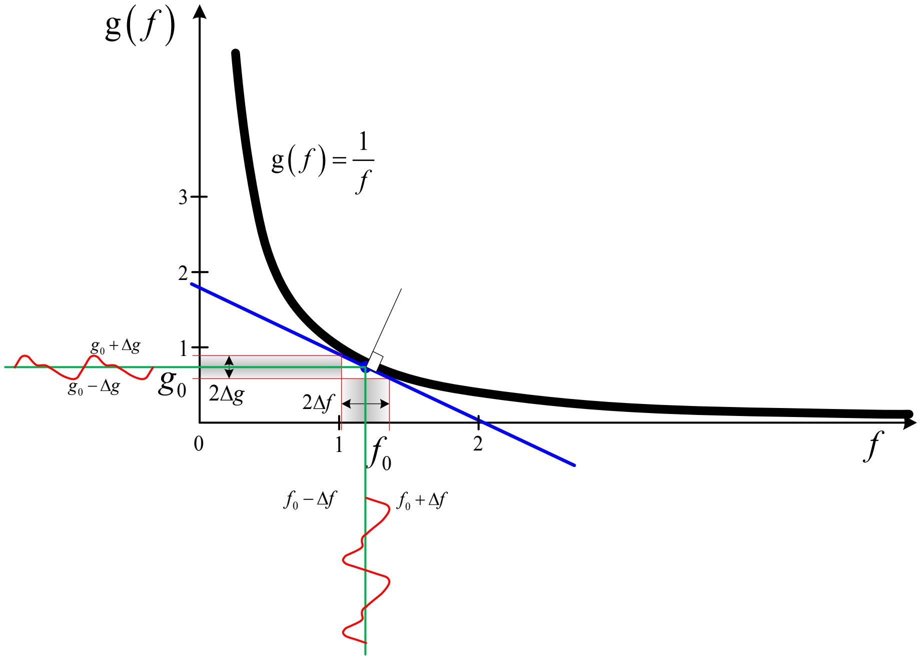

Figure 6 The graph of the inversion function $\mathrm{g}(f) = 1/f$ and the linearization of $\mathrm{g}(f)$ around the point $g_0 = \mathrm{g}(f_0)$

time-varying part reflects small variations of the estimated impedance (admittance) value caused mainly by the cardiac and respiratory activities.

Since the time varying part of the impedance and admittance are the most of interest, it is useful to show the relation between these variations. For this reason the reciprocal function $\mathrm{g}(f) = 1/f$ is introduced (plotted in Figure 6) to generalize the task.

Assuming that f_0 and Δf are known, the variation Δg of the function value $\mathrm{g}(f)$ can be found by linearization of this function at the neighbourhood of the observation point (f_0, g_0). After that, the variation Δg can be evaluated as

$$\Delta g = \Delta f \cdot \mathrm{g}'(f) \tag{7}$$

where the derivative of the function $\mathrm{g}(f)$ is

$$\mathrm{g}'(f) = \frac{d[\mathrm{g}(f)]}{df} = -\frac{1}{f^2} \approx \frac{\Delta g}{\Delta f} \tag{8}$$

and the variation is consequently

$$\Delta g = -\frac{\Delta f}{f^2} \tag{9}$$

Coming back to the impedance and admittance notations, the latter one can be approximated by the inverse value of the basal impedance minus the scaled value of the impedance variation:

$$Y = Y_0 + \Delta Y \simeq \frac{1}{Z_0} - \frac{\Delta Z}{Z_0^2}, \text{ when } Z_0 \gg \Delta Z \tag{10}$$

This is true, if the value of the basal impedance component is much greater than the impedance variation.

Similar expression is valid for the impedance approximated by the admittance:

$$Z = Z_0 + \Delta Z \simeq \frac{1}{Y_0} - \frac{\Delta Y}{Y_0^2}, \text{ when } Y_0 \gg \Delta Y \tag{11}$$

As a result, it can be summarized that the variations of the impedance and admittance, mainly caused by the cardiac and respiratory activities, are related directly, if the basal values of the impedance and admittance are much greater than the respective variations, which are under discussion.

To define how accurate such approximations are, the difference of the impedance and admittance product from the unity is examined in eqs. (12) - (13):

$$Y \cdot Z = \left(\frac{1}{Z_0} - \frac{\Delta Z}{Z_0^2} \right) \cdot \left(Z_0 + \Delta Z \right) \tag{12}$$

$$Y \cdot Z = 1 - \left(\frac{\Delta Z}{Z_0} \right)^2 = 1 - \left(\frac{\Delta Y}{Y_0} \right)^2 = 1 - r^2 = 1 - \varepsilon \tag{13}$$

As a result if a ratio $r > 10$ then the error $\varepsilon < 0.01$ in (13), thus less than 1%. By Grimnes and Martinsen (2008, Chapter 9) the typical value for Z_0 is $25\,\Omega$ and for variation caused by cardiac activity is $0.2\,\Omega$.

1.3.2 Considering EBI as a signal

Assuming that the bio-impedance as a parameter of living tissue is estimated using the sine wave electrical current excitation at some predetermined frequency and level, the phasor model can be used (Figure 5). Moreover, such an assumption makes possible to represent the variations of EBI in time domain as a signal. This is more appropriate representation of EBI based information for engineering, medical diagnosing, and signal processing.

Assuming the EBI as a signal, the phasor $\mathbf{Z}(t)$ can be marked as signal $\mathbf{S}(t)$ and expressed as a sum of basal $\mathbf{S}_0$, cardiac $\mathbf{S}_\mathrm{C}(t)$ and respiratory $\mathbf{S}_\mathrm{R}(t)$ signals, stochastic disturbance (noise) $\mathbf{n}_{\mathrm{S}}(t)$ and unwanted motion artefact $\mathbf{n}_{\mathrm{M}}(t)$, caused e.g. by muscular activity:

$$\mathbf{S}(t) = \mathbf{S}_0 + \mathbf{S}_{\mathrm{C}}(t) + \mathbf{S}_{\mathrm{R}}(t) + \mathbf{n}_{\mathrm{S}}(t) + \mathbf{n}_{\mathrm{M}}(t) \tag{14}$$

Moreover, taking into account the relation between dynamic parts of the electrical bio-impedance and -admittance, expression (14) can be treated as a general case, and it can be used for algorithm description applied to the electrical bio-admittance (EBA) as well.

Often the output of EBI estimator is presented by the signal's inphase component or its magnitude, sometimes by both – inphase and quadrature components (Figure 5).

Considering that in the whole frequency range up to several MHz the inphase and quadrature components have similar spectral contents, the scalar value of EBI, either of its inphase or quadrature components or magnitude, can be used for conceptual method developing.

Consequently, the equation (14) can be rewritten in a scalar form:

$$S(t) = S_0 + S_{\mathrm{C}}(t) + S_{\mathrm{R}}(t) + n_{\mathrm{S}}(t) + n_{\mathrm{M}}(t) \tag{15}$$

In other words, assuming that the EBI components are obtained from independent signal sources, the EBI signal $S(t)$ can be expressed as a sum of the independent components: basal S_0, cardiac $S_{\mathrm{C}}(t)$ and respiratory $S_{\mathrm{R}}(t)$ components and unwanted artefacts, such as stochastic disturbances and motion artefact.

Thus, expressions (14) and (15) describe the content of the EBI signal. But what

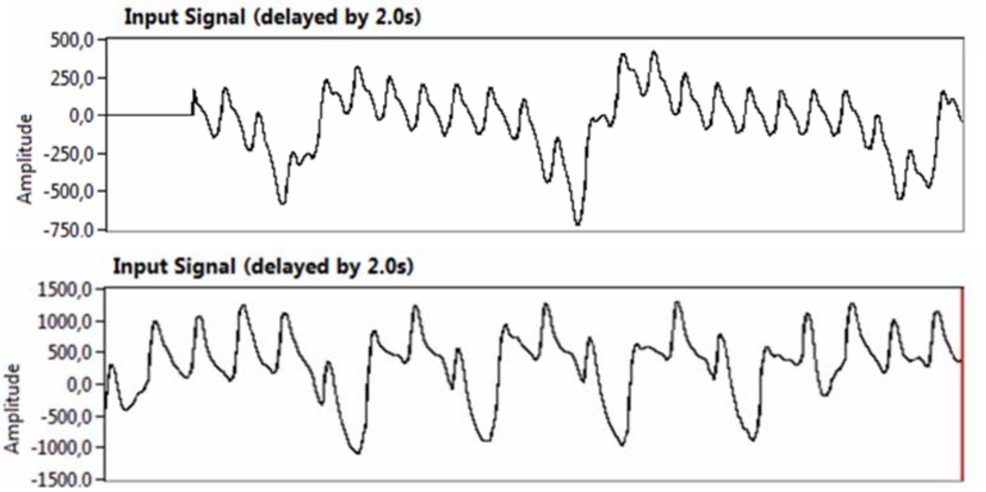

Figure 7 Two examples of the EBI signal obtained from the human chest (two different persons) during 20 seconds, using hands to feet spot electrode configuration (see section 1.2.1-B)

is about amplitudes of the components, which form the EBI?

Since the heart and lungs are not placed separately in the space, but they are parts of the human organism and placed side-by-side and affecting each other mechanically. The heart "beats" the lungs on each heart beating cycle and the lungs, in opposite, press the heart during the inspiration. Consequently, not only the individual mechanical movements are reflected in the EBI variations, but their interactions too. Such interaction is not strong, but any way, it exists. Empirically it can be described as mutual amplitude modulation of the cardiac and respiratory components of the EBI and expressed as

$$S(t) = a_{\mathrm{C}}\left(1 + b_{\mathrm{R}} s_{\mathrm{R}}\right) s_{\mathrm{C}} + a_{\mathrm{R}}\left(1 + b_{\mathrm{C}} s_{\mathrm{C}}\right) s_{\mathrm{R}} + n_{\mathrm{S}} + n_{\mathrm{M}} \tag{16}$$

The expression (16) for the EBI signal can be reordered in such a manner, that the cardiac and respiratory components, which are not affected by the modulation, will be presented separately from their mutual combination meaning the modulating part, as it is shown below in the system of equations (17):

$$\begin{cases} S(t) = a_{\mathrm{C}} s_{\mathrm{C}} + a_{\mathrm{R}} s_{\mathrm{R}} + \xi_{\mathrm{CR}} s_{\mathrm{C}} s_{\mathrm{R}} + n_{\mathrm{S}} + n_{\mathrm{M}} \\ \xi_{\mathrm{CR}} = a_{\mathrm{R}} b_{\mathrm{C}} + a_{\mathrm{C}} b_{\mathrm{R}} \end{cases} \tag{17}$$

In the equations (16) and (17), variables a_{C} and a_{R} are the main amplitudes of the cardiac and respiratory components respectively (without the modulation effect), variables b_{C} and b_{R} are the amplitudes of modulating parts of the cardiac and respiratory components respectively. The variable ξ_{CR} is the amplitude of the mutual component $\left(s_{\mathrm{C}} s_{\mathrm{R}}\right)$ in the equation system (17), taking into account the modulation effect.

To summarize this subsection, examples of the EBI signal obtained from the human chest (from two different persons) during 20 seconds using hands to feet spot electrode configuration (see section 1.2.1-B), are shown in Figure 7.

1.4 Impedance Cardiography (ICG)

Impedance cardiography (ICG) is the EBI-based method of evaluating hemodynamic parameters (Cotter *et al* 2006). The time variant part of the EBI, which is caused by cardiac activity, is taken as a basis for the ICG.

The first correlation between the estimated EBI variations and the cardiac activity was published in early 1930s by Atzler and Lehmann (1932), Nyboer *et al* (1940), and then followed by others.

By Zlochiver *et al* (2006), with reference to Newman and Callister (1999), the term *impedance cardiography* (ICG) was introduced in 1959.

However, the question about terminology arises, if the first time-derivative of the cardiac BI signal is marked in literature as ICG, then how the raw cardiac BI signal can be marked? To avoid any questions of such kind, in the following text the abbreviation ICG is used for the *impedance cardiography*. When talking about the time diagram of the cardiac BI signal, thus about the *impedance cardiogram*, the abbreviation ICGm is used. When about *first time-derivative of the cardiac BI signal* is talked, the abbreviation DICGm is used. And in addition, the higher order time-derivatives of the ICGm are designated by superscript at the letter D, for example *the second order time-derivative of the ICGm* is abbreviated as D^2ICGm.

1.4.1 Hemodynamic parameters

Evaluation of hemodynamic parameters[2] is possible due to the fact that the blood has higher conductivity (lower resistivity) compared with tissues surrounding the heart and vessels. For example, the blood has a resistivity about $1.6\,\Omega\mathrm{m}$, the lungs about $20\,\Omega\mathrm{m}$, but the bones have much higher resistivity, about $170\,\Omega\mathrm{m}$ (Malmivuo and Plonsey 1995). Consequently, using appropriate measuring configuration and signal processing algorithms, it is possible to separate the immitance variations in the heart and vessels caused by the cardiac activity, from the immitances originated from other tissue regions.

The hemodynamic parameters, which are of the most of interest for cardiologists, are the heart stroke volume (SV) and the cardiac output (CO). The SV is measured in litres [L] and is defined as the volume of blood pumped by the heart during the ventricular ejection time interval. The CO [L/min] is the volume of blood pumped by the heart in one minute and can be evaluated using the values of SV and heart rate (HR [1/min]) as

$$CO = SV \cdot HR \tag{18}$$

The EBI based evaluating of volumes is known also as *impedance plethysmography*, but this is more general definition, which can be applied to all kinds of the volumes, not only to the blood volumes.

Moreover, the ICG has also other names as *impedance plethysmography of the chest*, *electrical impedance of the chest* or *reocardiography* (Sodolski and Kutarski 2007).

The hemodynamic parameters evaluation from the ICGm is based on the model of the human torso. The cylindrical models are most widely used due to their simplicity. For example, in Figure 8, the one cylinder model is shown. By Grimnes and Martinsen (2008, Chapter 9) the volume evaluating from immitance estimates is based on two effects:

1. A geometry-dependent effect.
2. A conductivity-dependent effect.

---

[2] *Hemodynamic* (lat.) means the blood movement.

A. The geometry-dependent effect

The geometry-dependent effect can be defined from the cylindrical model (single-cylinder model in Figure 8), admittance and impedance of which are presented by expressions (19) and (20) respectively:

$$Y = \sigma \frac{A}{L} \tag{19}$$

$$Z = \rho \frac{L}{A} \tag{20}$$

where σ is the conductivity and ρ is the resistivity of tissue, A is the cross section area of the cylinder, and L is its length. The resulting geometry-dependent effect by Grimnes and Martinsen (2008) will be dependent on the constraints on the estimated tissue volume: if the volume increase results in a swelling of length L, admittance will fall. If the volume increase results in a swelling of cross sectional area A, the admittance will increase. If the volume increase occurs outside the estimated tissue volume, the estimated admittance will not change with the geometrical volume increase.

Using eqs. (19) and (20), the volume V of the cylinder can be found:

$$V = Y\rho L^2 \tag{21}$$

The volume estimation through impedance can be expressed as

$$V = Z\sigma A^2 = \frac{1}{Z}\frac{L^2}{\sigma} = \frac{1}{Z}\rho L^2 \tag{22}$$

In practical applications the absolute volume is not available. Therefore the relative changes $\Delta V / V$ will be evaluated as

$$\frac{\Delta V}{V} = \frac{\Delta Y}{Y}, \tag{23}$$

Using eq. (21), the volume change can be expressed with respect to the admittance change as it is shown in eq. (24):

$$\frac{\Delta V}{\Delta Y} = \rho L^2 \tag{24}$$

Consequently, the volume change can be found when the admittance change is known:

$$\Delta V = \Delta Y \rho L^2 \tag{25}$$

The equations (23) - (25) can be applied if admittance model with presumption that $L = \mathrm{const}$ (and known) is valid for the volume evaluation. In this case, expressions (26) - (28) will be applied for volume evaluation:

$$\Delta V = \left(\frac{1}{Z_0 + \Delta Z} - \frac{1}{Z_0} \right) \rho L^2 \tag{26}$$

$$\Delta V = -\frac{\Delta Z}{Z_0} \frac{1}{Z_0 + \Delta Z} \rho L^2 \tag{27}$$

Equation (27) for the single cylinder model (Figure 8) is exact and non-linear with respect to the impedance change. It can be approximated by a linear variant (28) only then, when $Z_0 \gg \Delta Z$:

$$\Delta V \simeq -\rho \left(\frac{L}{Z_0} \right)^2 \Delta Z \text{, when } Z_0 \gg \Delta Z \tag{28}$$

By Grimnes and Martinsen (2008) the single cylindrical model of human torso for hemodynamic parameters evaluating was used firstly by Nyboer (1950). Nyboer regarded the thorax as a cylindrical volume of length L and used the following expression for volume evaluation:

$$\Delta V_{\mathrm{B}} = \rho \left(\frac{L}{Z_0} \right)^2 \Delta Z_{\mathrm{C}} \quad \left[m^3 \right] \text{ (Nyboer)} \tag{29}$$

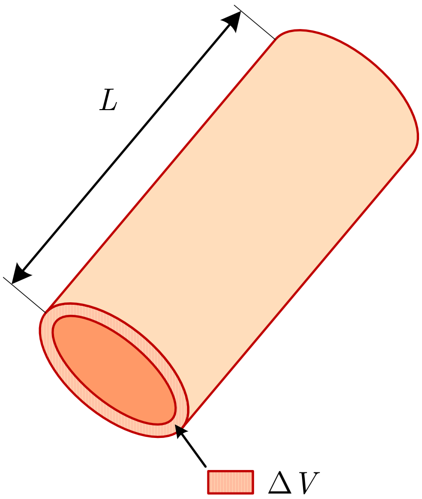

Figure 8 One-cylinder model: L is a length of the cylinder, and a small parallel volume change ΔV of the cylinder is shown by dashed region

Later Kubicek *et al* (1966), Kubicek (1968) and Patterson (1989) made some assumption concerning the relationship between stroke volume and net change in the thorax blood volume as evaluated in eq. (28) (Malmivuo and Plonsey 1995).

Kubicek *et al* and Patterson had not used directly the cardiac impedance variation ΔZ_{C} in evaluating of the volume of blood in (28). The approximated value $\Delta\tilde{Z}_{\mathrm{C}}$ is used, which can be estimated if the slope of the ICGm, reflecting the systolic phase of the heart process, is continued (in imagination) until the end of the left ventricle ejection time interval, see Figure 9. The height of the continued slope is the value of $\Delta\tilde{Z}_{\mathrm{C}}$, which can be expressed as

$$\Delta\tilde{Z}_{\mathrm{C}} = T_{\mathrm{LVE}}\left(\frac{dZ}{dt}\right)_{\max} \tag{30}$$

Consequently substituting $\Delta\tilde{Z}_{\mathrm{C}}$ from (30) into (28) instead of ΔZ, the expression for the SV evaluating by Kubicek *et al* and Patterson can be presented:

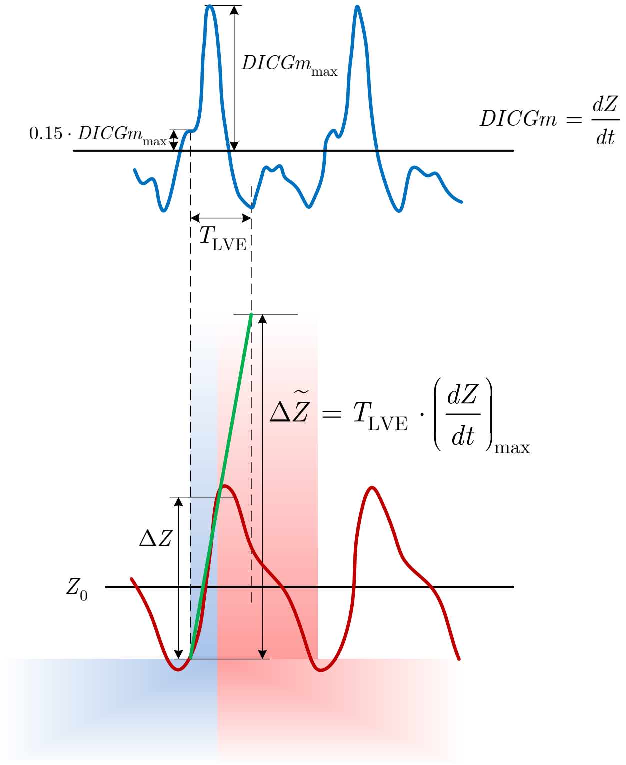
$DICGm_{\max}$
$0.15 \cdot DICGm_{\max}$
$DICGm = \frac{dZ}{dt}$
T_{LVE}
$\Delta\tilde{Z} = T_{\mathrm{LVE}} \cdot \left(\frac{dZ}{dt}\right)_{\max}$
ΔZ
Z_0

Figure 9 Evaluating the stroke volume (SV) by impedance change

$$SV = \rho \left(\frac{L}{Z_0} \right)^2 \Delta \tilde{Z}_{\mathrm{C}} \tag{31}$$

$$SV = \rho \left(\frac{L}{Z_0} \right)^2 T_{\mathrm{LVE}} \left(\frac{dZ}{dt} \right)_{\max} \quad \left[m^3 \right] \text{ (Kubicek and Patterson)} \tag{32}$$

B. The conductivity-dependent effect

It is clear that the equations (19) - (20), and consequently eqs. (21) - (22), show the dependency of the volume on the impedance (admittance) and on the geometry as well. But the volume estimation depends also on the conductivity of the tissue under examination. For example, by Salo (2001, p. 29) the resistivity of blood, like most electrolytes, depends on temperature with a resistivity decrease of $2\%/\mathrm{C}^\circ$. Moreover, by Grimnes and Martinsen (2008, Chapter 9) the conductivity of blood varies with the blood flow variation. The latter dependence is named as Sigman effect (Sigman *et al* 1937).

The conductivity σ (resistivity ρ) of the tissue (blood), is usually taken as a constant value. Thus in the real life observed conductivity variations are not reflected in the model (in the equations), they cause errors in the estimated values of the blood volume. However, by Salo with references to Geddes (1972) and Geddes and Baker (1975), different factors can be measured *in situ* and used for the stroke volume value estimation.

1.4.2 Difficulties in hemodynamic parameters analysis

One of the important troubles influencing the accuracy of hemodynamic parameters evaluation is the Sigman effect. The crux of the effect is the admittance of blood is flow dependant. Sigman *et al* (1937) were the first who had reported this. Since the “amount” of variation of the blood admittance due to the flow changes is not plethysmographic, this variation gives an error in blood volume estimations. The “amount” of variation can be several percents of the total blood impedance.

Another principle trouble, which influences the accuracy of the SV and other hemodynamic parameter estimation, is the over simplified model of torso and cardiovascular system in particular. Over simplification can be presented by ignoring of the tissue structure, thus for the hemodynamic parameter estimation the torso is assumed as homogenous and isotropic. The next simplification is geometrical. The torso is assumed to be cylindrical with a changing radius, which is surrounded by the air. Though such simplifications are very far from the reality, the models can, however, give satisfactory results. But, for example, taking into account at least the conductivity of the tissue surrounding the aorta and bolus effect in the aorta (see Figure 10), we can significantly increase accuracy of the estimated hemodynamic parameters.

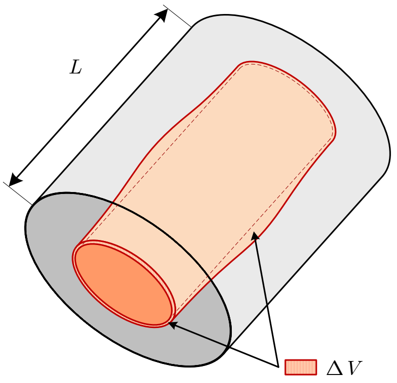

Figure 10 The effect of a bolus of blood passing the measured volume

Modern cardiac pacemakers are often equipped with EBI measurement tools for calculating the SV values from intracardiac impedance data. Using implantable catheter with multiple electrodes (more than one voltage sensing pair) gives possibility to segment the total volume of the blood inside the heart ventricle to several smaller volumes stacked together. For each smaller volume the cylindrical model with appropriate parameters should be used. Such a possibility was investigated by Salo (2001) in his PhD thesis.

1.5 Impedance Respirography (IRG)

Impedance respirography (IRG) is an EBI-based method for evaluating pneumodynamic parameters. The time variant part of EBI caused by breathing is a basis for the IRG (called also as impedance pneumography).

The IRG can reflect the state of lungs and the respiratory system in general. Estimation of pneumodynamic parameters is of great importance. The pneumodynamic parameters, especially minute ventilation (MV), reflect very closely the metabolic demand during physical exercises (Mond *et al* 1988, West 1988). The MV at rest is about $6\left[\mathrm{L}/\mathrm{min}\right]$, but during an exercise with moderate load the MV increases up to $60\left[\mathrm{L}/\mathrm{min}\right]$ (Webster 1995). Moreover, by Webster (1995), the heart rate and cardiac output are almost linearly related with MV. This property is effectively used in rate adaptive pacemakers (see Min *et al* (1999), Webster (1995) and Dell'Orto *et al* (2004)), where the pneumodynamic parameters are used to estimate the human workload by metabolic demand reflected in impedance respirogram (IRGm)[3], and consequently, to adapt the heart pacing rate to an adequate value.

---

[3] Terms, related to the impedance respirography (IRG) are defined using the same abbreviating scheme as for ICG, described in the section 1.4 (p. 26).

1.5.1 Pneumodynamic parameters

The pneumodynamic parameters, which are the most of interest, are the tidal volume (TV) and minute ventilation (MV). The TV is measured in litres [L] and is defined as the volume of air inspired into lungs during a single inspiration. The MV [L/min] is the average volume of air inspired into lungs in one minute and can be evaluated using values of the TV and the ventilation rate (VR [1/min]) as

$$MV = TV \cdot VR \tag{33}$$

A. Tidal volume (TV)

By Webster (1995), the TV value can be estimated by rectifying the IRGm and smoothing the result by the low-pass filter (LPF):

$$TV = \mathrm{f}_{LPF}\left(\left|IRGm\right|\right) \tag{34}$$

Despite the fact that this is a value, which is only proportional to, but not even close to the TV real value, such an approach is widely used in pacemaker designs due to its simplicity.

B. Minute ventilation (MV)

As it was mentioned above, MV corresponds very well to the metabolic demand during exercises, but it does not reflect adequately the static physical efforts (Min *et al* 1999).

It is needed to be mentioned that for pacemaker designers, the MV sometimes is not an adequate data source for pacing control. For example, during heavy physical loads the inspiration is deep, but ventilation rate is low, reducing the MV value. And even more, breathing can temporarily stop. However during such loads the heart rate should be, in opposite, increased (Min *et al* 1999).

For the cardiac pacing applications Min *et al* (1999) have found a solution: to use both, the tidal volume and the ventilation rate separately, TV and VR respectively, as two independent input values for the fuzzy logic based pacing control unit. In such a way a potentially inadequate influence of the MV is fixed by appropriate fuzzy logic.

1.5.2 Troubles in pneumodynamic parameters analysis

The ventilation rate, which varies in a wide range, can be named as the main trouble in analysis of pneumodynamic parameters. In opposite to the heart rate, which is fully autonomous, the ventilation rate can be changed by a person consciously. Therefore, the ventilation rate can change rapidly and moreover, can temporarily stop. For the signal processing purposes such variations can be treated as non deterministic, tracking of which is very difficult.

1.6 Uncertainties in the ICG and IRG

Origin of the uncertainties in the impedance cardiography and respirography can be conceptually divided into three classes.

The first one is the class of common problems characteristic to the EBI measurement in general. These problems are related to the quality of the EBI estimation methods and systems, including the quality of the circuitry part – the quality of current sources, voltage measurement units, demodulators, analogue-to- digital converters (DAC) etc.

The second one is the conformity of a model of the human organism, or the torso in particular, with the real state and the accuracy of such a model. In turn, the evaluated model of torso has to be combined from three sublevel models to be useful. These are the electrical, mechanical (hydraulic and pneumatic), and geometrical models of the torso. In addition, the electrode placement scheme must be selected in accordance with the model of the torso. The accuracy of the torso model and the electrode placement scheme both influence the reliability, repeatability and accuracy of the evaluated hemodynamic parameters.

The third class of troubles is related conditioning of the EBI signal for ICG and IRG applications. The raw EBI signal can be assumed as a sum of the basal component and the cardiac and respiratory components. Often additive stochastic disturbances and motion artefacts are presented in the EBI. The EBI signal to be useful for monitoring and diagnosing purposes must be decomposed into its components simultaneously with separating these components from disturbances and motion artefacts. In the ICG applications the basal and cardiac components are used directly in the SV and CO evaluation. For the ICG applications, in particular, the respiratory component can be used as additional information about the load of the human organism (see section 1.5 of the thesis), or can be treated as unwanted artefact. The cardiac component for the IRG applications, in turn, is usually treated as unwanted artefact.

The first and the second classes of the described trouble sources are shortly overviewed in sections 1.2 and 1.4 respectively. The more deep and detailed description goes out of the scope of the present PhD research work.

The third one, the conditioning of the raw EBI signal, in opposite, will be described in detail in the following text of the thesis and the proposed solution of the problem will be presented.

2

Problem statement

In this section, the problem is stated, which is under discussion in the thesis. Assumptions about the EBI are made and complexities, which are characteristic to the problem, are described in the first subsection 2.1. In the second subsection 2.2, a review of the known solutions, including short descriptions of their advantages and disadvantages, is made. In accompaniment with the review of known solutions based on the publications, an analysis of a possible solution – the use of the independent component analysis (ICA) applied to the EBI decomposition problem, is discussed. Combining the formal problem statement and the review of known and potential solutions in the same chapter of the thesis allows emphasizing the attention on diverse nature of the problem under discussion.

2.1 The EBI decomposition – problem statement

To discuss the topic of the current section, let us shortly review the considerations about the EBI as a kind of signals, firstly mentioned in the section 1.3 (page 21) of the thesis.

The EBI is assumed to be a sum (35) of the basal S_0, cardiac $S_C(t)$ and respiratory $S_R(t)$ components and unwanted artefacts, such as stochastic disturbances $n_S(t)$ and motion artefact $n_M(t)$:

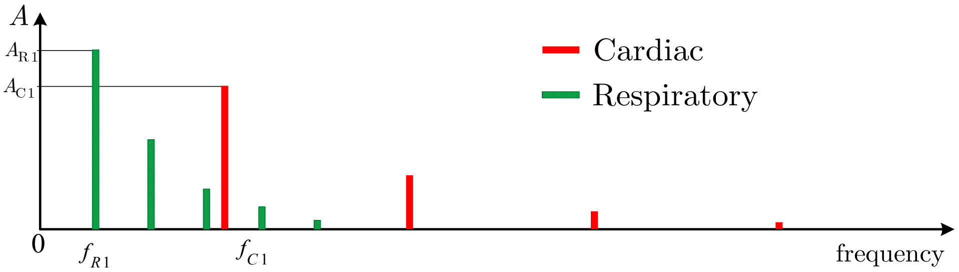

Figure 11 Sketch of a possible frequency domain harmonic spectrum of EBI signal, which consists of the cardiac and respiratory components

$$S(t) = S_0 + S_{\mathrm{C}}(t) + S_{\mathrm{R}}(t) + n_{\mathrm{S}}(t) + n_{\mathrm{M}}(t) \tag{35}$$

The main task of the EBI signal conditioning is to decompose the total EBI signal $S(t)$ into its useful components: basal, cardiac and respiratory ones selecting them at the same time from the disturbances and noise, which are often presented in the signal.

Since the author's research work and of the presented thesis is aimed to find a solution of the task defined above, let concentrate more attention on this problem.

Decomposition of the total EBI signal into its components: basal, cardiac and respiratory ones accompanied with simultaneous suppression of stochastic disturbances and motion artefacts, is not a trivial task. There are several complexities to overcome:

- harmonic frequency domain spectra of the cardiac and respiratory components can often be overlapped (Figure 11);
- the decomposition procedure assumes that the components as the output of the method must remain unchanged individually, however separated from each other;
- the EBI signal is non-stationary due to the variations of heart rate and lung ventilation rate in time domain, and moreover, due to the motion artefacts, if such are presented in the EBI signal;
- low frequency nature of the cardiac and respiratory signal components.

The latter makes difficult the real-time presentation of the results (the processing delay must be short). For example, the heart rate (HR) of a healthy person can vary from 60 bpm to 240 bpm, which corresponds to cardiac cycles $T_{\mathrm{C}} = 0.25$ to 1 s (frequencies $F_{\mathrm{C}} = 1$ to 4 Hz). Because the respiratory rate is about four times lower than HR, several higher harmonics of the respiratory signal lie in the frequency range of cardiac signal, i.e. the spectra are overlapping (see Figure 11).

Despite that the heart rate and ventilation rate of the estimated EBI on the upper plot in Figure 7 are different enough the respiratory component has rapid up- and down-fronts, which make the EBI decomposition problem more complex. In addition, on the bottom plot of the same figure, the EBI plot from another person shows that the ventilation rate changes from slower to faster rate in ten seconds and rapid fronts of the respiratory component remain. These two EBI examples give very well visual demonstration of the stated problem and show that usual filtering in the frequency domain cannot solve this problem. Therefore more application specific advanced methods and concepts are needed.

2.2 Decomposition the EBI signal – a review about known methods and potential solutions

Many papers and several books are written about EBI in general and about its measurement (estimation) techniques. Some of them are devoted to the specific topic, e.g., evaluation of hemodynamic or pneumodynamic parameters. However, only tens of the papers written over the past decades are discussing the problem of EBI conditioning by separating its components, cardiac and respiratory ones, in details. More often the cardiology application of the EBI is discussed, and in this context, the most of these papers report that the baseline drift caused by respiration is the great problem. This is due to the extremely complicated nature of the task.

In the current subsection, the literature review related with the stated problem, is given. Trivial frequency domain filtering cases are not discussed here, because they are suitable only for several stationary conditions, i.e. for the healthy human in the resting state. These cases are out of scope of the stated problem, in which the human is not obligatory resting. Moreover, the pathological cases are taken into account and respiratory component is included as an arbitrary function.

The selected range of papers can be divided into three different approaches: ensemble averaging, (classical) adaptive filtering, and several spectral analysis methods, which are presented in the following text. In addition, the independent component analysis (ICA) method, as a potential solution, is analyzed as well.

2.2.1 Ensemble averaging

The ensemble averaging technique uses multiple periods of the DICGm signal to suppress the disturbances, which are not correlated with the DICGm signal. Such approach is used by Muzi *et al* (1986), Zhang *et al* (1986) and Wang *et al* (1995). Woltjer *et al* (1996) referenced to Kim *et al* (1992) and declared that averaging has been shown to be effective in eliminating the effect of respiration. However, it is clear that the disturbing components must have a zero mean value to be effectively suppressed by averaging. But it becomes possible only, when averaging is done during a long time interval. Such averaging can suffer from the variability of the DICGm signal shape and event latencies that can cause less distinct events in the signal to disappear in the averaged signal (Hu *et al* 1997). As a result, this approach cannot be used in on-line monitoring of the cardiac parameters.

2.2.2 Adaptive filtering (classical)

Adaptive filtering is used by Yamamoto *et al* (1988) for suppression of the disturbances in the DICGm signal. This solution is based on the digital infinite impulse response (IIR) band-pass filter, which moves around the centre frequency (heart rate). Similarly, Min *et al* (2000) and Min *et al* (2002) proposed to use frequency adaptive finite impulse response (FIR) filters. Unfortunately, these solutions suppress also high-frequency components of the DICGm signal and introduce non-linear phase distortion. Another application of the adaptive filtering for reducing the respiration and motion artefacts in electrogastrogram was described by Chen *et al* (1993). In the latter work, the usage of three types of adaptive filters was studied: the time-domain, transform-domain and frequency-domain ones. Disadvantage of these filters appears in the need for a reference disturbance signal. The same disadvantage appears in a system for adaptive cancellation of the respiratory artefact investigated by Pandey and Pandey (2005). The scaled Fourier linear combiner (SFLC) by Barros *et al* (1995), reconstruct the DICGm signal from harmonic spectral components found by using an adaptive least mean square (LMS) filter, with reference inputs related to the R-R intervals of ECG.

2.2.3 Spectral methods

The third approach is based on the spectral analysis methods. In particular, the wavelet based time-frequency analysis is used by Ouyang *et al* (1998) and Pandy and Pandy (2007) to select the disturbance free DICGm signal from the noisy input. However, the spectral analysis, and using of wavelets in particular, require a great number of spectral components (levels in the wavelet case) to represent the input signal accurately. Another difficulty can arise in selection of the threshold, at which the separation of the useful component from noises is performed. Pandy and Pandy (2007) use the hard threshold, which has a similar disadvantage as the filtering with a constant cut-off frequency. The method by Ouyang *et al* (1998) uses the soft threshold, but the breath holding during 8 seconds is needed to construct the auto-regressive (AR) model of the cardiac BI signal. Moreover, the pre-whitening of the input EBI signal and spline based model construction of the respiratory component are required.

2.2.4 Independent component analysis (ICA) methods

Taking into account the assumption made in the section 1.3.2 (page 24) that the EBI signal can be expressed as a sum of the independent components, the following question arises: can the signal $S\left(t\right)$ be decomposed into its components using some well known method of independent components analysis[4] (ICA)? An answer to this question is presented below with explanations of two cases.

A. Multiple electrodes based ICA

Imagine that to separate all the components of EBI signal (35) using the ICA method, five voltage measurement electrode pairs are needed. In this case, the electrodes are placed separately and thus the EBI values estimated from measured voltage are different: these impedances are different.

---

[4] An explanations presented in the following text about the use of the ICA for the EBI applications are based on the author's understanding of the ICA method described in works of Hyvärinen and Oja (2000) and Hyvärinen *et al* (2001).

It must be remembered that the EBI is only assumed to be a signal, in reality it is the parameter of the tissue region (at whole) taken into account, which is placed between voltage measuring electrodes. These estimates can be similar in some cases in their values, but principally they are different impedances of different tissue regions. Moreover, each of such estimates can be described using expression (35) with its own content – similar, but different in value.

In opposite, let compare it with array of antennas. In such arrays, each antenna detects the *same* complicated signal(s), but in different spatial places, forming in such a way, different spatial "views" to the same complicated signal (only measurement disturbances are the "position specific").

However measuring the voltages for the EBI estimation using multiple electrodes is not just identical to different views to the same signal, because the signals are different (different impedances). And it is not possible to define, which of the EBI estimates is an "actual value", and which are just other estimates (if this sentence is right, in general).

Consequently, it is clear that it is conceptually wrong to use multiple electrodes based ICA for decomposition of the EBI into its components.

B. Multifrequency based ICA

Similar situation exists with multifrequency EBI estimation approach. Despite that in this case the EBI values are estimated at one electrode position, the values of this estimates at different frequencies are different.

Again it becomes clear that it is conceptually wrong to use the multi-frequency based ICA for decomposition of the EBI into its components.

However, Rossel *et al* (1995) have used a two frequency EBI estimator to suppress the motion artefacts in EBI to obtain the motion-free signal. The method proposed by Rossel *et al* (1995) is a kind of independent component analysis (ICA) method combined with adaptive filtering (AF) methods. Despite that some results were obtained by Rossel *et al*, interpretation of them, I think, is not conceptually right.

2.2.5 Concluding the review

In regard to the need of on-line monitoring of the hemodynamic and pneumodynamic parameters during exercises and especially in the ambulatory conditions, the ensemble averaging approach is not suitable. The adaptive filtering and spectral analysis are more promising approaches despite the fact that some of these require a reference disturbance signal. Moreover, all the above described noise cancellation methods and systems are based either on the ensemble averaging or adaptive filter by Yamamoto *et al* (1988) and Fourier linear combiner SFLC by Barros *et al* (1995), require the heart rate estimates obtained from the electrocardiogram (ECG). The availability and accuracy of the ECG based heart rate estimates are the mandatory prerequisites for the reliability of such methods. An exception to this rule is the coherent ensemble averaging method investigated by Hurwitz *et al*

(1990). However, as that method do not use the ECG signal, it has a common disadvantage of the ensemble averaging - a long time interval is needed for collecting a great number of ICG periods sufficient to perform the effective suppression of disturbances.

3

Proposed method – Model based EBI decomposition

A fast method for separation of the cardiac and respiration components is proposed, which uses only the initial EBI signal. In addition, the heart rate estimations derived from other signals like ECG can be used for supporting the procedure, if available, but this is certainly not obligatory. This approach eliminates the direct dependence on availability of the ECG signal, but allows using additional data to increase the speed and reliability of the separation process. Moreover, the proposed method is oriented to applications requiring the on-line monitoring of both, the cardiac and respiratory components. At the current stage, this method produces only a two-second constant delay of the separated cardiac and respiratory components with regard to the initial EBI signal. In opposite to the ensemble averaging technique reviewed in the previous section, the proposed method is on-line method decomposing the EBI signal into the cardiac and respiratory components in time domain using the cardiac EBI signal model and continuous tracking the heart rate (in contrast to the spectral analysis approach). No additional reference signal is required.

3.1 The method basics

The signal model based decomposition of the EBI into its components is proposed by the author and explained during the rest of the thesis.

Since the expression (35) is only the single "view" to the EBI of the tissue region between the selected electrodes, thus the task can be described as follows: we have five unknowns, which are needed to be found (separated), and only one known component – the sum of these unknown components, thus their linear combination.

The explanation of the proposed method is done with simplification of the EBI signal representation – only cardiac and respiratory components are taken into account:

$$S(t) = S_{\mathrm{C}}(t) + S_{\mathrm{R}}(t) \tag{36}$$

This allows concentrating an attention on the method conception by excluding extra complexities caused by the other EBI components, such as basal component, stochastic disturbances and motion artefact. Notes about these, excluded components will be given where they are needed in the text.

After simplification of the EBI signal representation in eq. (36), the main problem remains – now there are two unknowns and one known components, which are interrelated by a single expression. How can the signals be found (separated)?

Due to the possibility that the spectra of cardiac and respiratory signals are overlapping, typical filtering approach in frequency domain and other methods reviewed in the section 2.2 are not reasonable.

Therefore the method based on models of the cardiac and respiratory EBI components is proposed as a solution of the defined task.

The idea of proposed solution is laying in replacing of $S_{\mathrm{C}}\left(t\right)$ and $S_{\mathrm{R}}\left(t\right)$ by their models $S_{\mathrm{CM}}\left(t\right)$ and $S_{\mathrm{RM}}\left(t\right)$ respectively, whereas the EBI signal $S\left(t\right)$ can be expressed as system of equation (37). The functions $\mathrm{f}_{\mathrm{CM}}\left(\tilde{S}_{\mathrm{C}}\left(t_n\right)\right)$ and $\mathrm{f}_{\mathrm{RM}}\left(\tilde{S}_{\mathrm{R}}\left(t_n\right)\right)$ define the models for construction functions, which are based on the current values estimates $\tilde{S}_{\mathrm{R}}\left(t_n\right)$ and $\tilde{S}_{\mathrm{R}}\left(t_n\right)$ respectively –

$$\begin{cases} S\left(t\right) = S_{\mathrm{CM}}\left(t\right) + S_{\mathrm{R}}\left(t\right) \\ S\left(t\right) = S_{\mathrm{C}}\left(t\right) + S_{\mathrm{RM}}\left(t\right) \\ S_{\mathrm{CM}}\left(t\right) = \mathrm{f}_{\mathrm{CM}}\left(\tilde{S}_{\mathrm{C}}\left(t\right)\right) \\ S_{\mathrm{RM}}\left(t\right) = \mathrm{f}_{\mathrm{RM}}\left(\tilde{S}_{\mathrm{R}}\left(t\right)\right) \end{cases} \tag{37}$$

Now the estimations of cardiac and respiratory components can be obtained:

$$\begin{cases} \tilde{S}_{\mathrm{R}}\left(t\right) = S\left(t\right) - S_{\mathrm{CM}}\left(t\right) \\ \tilde{S}_{\mathrm{C}}\left(t\right) = S\left(t\right) - S_{\mathrm{RM}}\left(t\right) \\ S_{\mathrm{CM}}\left(t\right) = \mathrm{f}_{\mathrm{CM}}\left(\tilde{S}_{\mathrm{C}}\left(t\right)\right) \\ S_{\mathrm{RM}}\left(t\right) = \mathrm{f}_{\mathrm{RM}}\left(\tilde{S}_{\mathrm{R}}\left(t\right)\right) \end{cases} \tag{38}$$

The model construction is the most significant part of the proposed method. The functions $\mathrm{f}_{\mathrm{CM}}\left(\tilde{S}_{\mathrm{C}}\left(t_n\right)\right)$ and $\mathrm{f}_{\mathrm{RM}}\left(\tilde{S}_{\mathrm{R}}\left(t_n\right)\right)$ are more abstract representations, than real mathematical functions. The cardiac and respiratory model constructions will be described in details in sections 3.2 and 3.3 respectively.

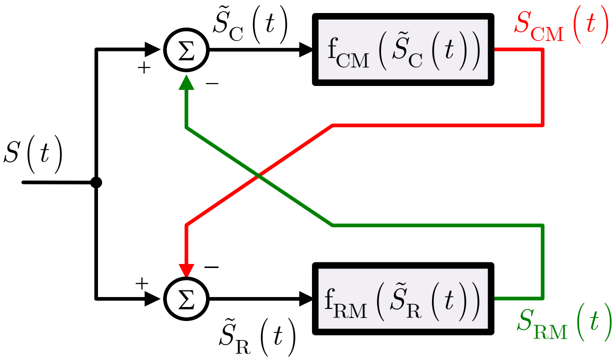

$\tilde{S}_{\mathrm{C}}(t)$
$\mathrm{f}_{\mathrm{CM}}(\tilde{S}_{\mathrm{C}}(t))$
$S_{\mathrm{CM}}(t)$
$S(t)$
Σ
+
−
$\mathrm{f}_{\mathrm{RM}}(\tilde{S}_{\mathrm{R}}(t))$
$\tilde{S}_{\mathrm{R}}(t)$
$S_{\mathrm{RM}}(t)$

Figure 12 The conceptual block-diagram of the bio-impedance signal decomposer (BISD) into its cardiac and respiratory components

A practical realization of the equation system (38) should be performed in parallel, as shown graphically in Figure 12 – both subtraction operations and signals model constructions should be performed simultaneously. Such the configuration can be realized as parallel signal processing algorithm, i.e. embedded into the FPGA module. However, at the current stage this algorithm is implemented as serialized software variant. The sequence of operations, in this realization, during single discrete time instance (t_n - the current discrete time instance) is presented below in the sequence of expressions:

$$\begin{aligned}
a)\quad & S_{\mathrm{CM}}(t_n) = \mathrm{f}_{\mathrm{CM}}(\tilde{S}_{\mathrm{C}}(t_{n-1})) \\
& \Downarrow \\
b)\quad & S(t_n) = S_{\mathrm{CM}}(t_n) + S_{\mathrm{R}}(t_n) \\
& \Downarrow \\
c)\quad & \tilde{S}_{\mathrm{R}}(t_n) = S(t_n) - S_{\mathrm{CM}}(t_n) \\
& \Downarrow \\
d)\quad & S_{\mathrm{RM}}(t_n) = \mathrm{f}_{\mathrm{RM}}(\tilde{S}_{\mathrm{R}}(t_n)) \\
& \Downarrow \\
e)\quad & S(t_n) = S_{\mathrm{C}}(t_n) + S_{\mathrm{RM}}(t_n) \\
& \Downarrow \\
f)\quad & \tilde{S}_{\mathrm{C}}(t_n) = S(t_n) - S_{\mathrm{RM}}(t_n) \\
& \Downarrow \\
g)\quad & S_{\mathrm{CM}}(t_{n+1}) = \mathrm{f}_{\mathrm{CM}}(\tilde{S}_{\mathrm{C}}(t_n))
\end{aligned} \tag{39}$$

It becomes clear, that the models of the EBI components, cardiac and respiratory ones, play the most significant role in the decomposition method. They define not only the accuracy of the method, but the possibility of this method at all. Any error between the real cardiac component and its model will be presented in the estimate of the respiratory component. Moreover, if the functions constructing the models are not immune enough to the errors between the models and original components, both cardiac and respiratory ones, the algorithm will be unstable due to the feedback loop (Figure 12), or if even the loop remains stable, the significant errors can propagate in the loop.

3.2 The cardiac EBI signal model

In this section the cardiac EBI model will be discussed briefly and the detailed description can be found in the applied published papers in the appendices A – F of the thesis.

In general, the constructing function of the cardiac signal[5] model consists of two stages: analysis and synthesis. Parameters of the cardiac signal, which are based on the currently available cardiac signal estimate $\tilde{S}_{\mathrm{C}}(t)$ are detected during the analysis stage. As a result, the model which is based on the detected and conditioned parameters can be synthesized.

$\tilde{S}_{\mathrm{C}}(t)$
$S_{\mathrm{CM}}(t)$

Figure 13 The block-diagram describing the construction of the cardiac EBI signal model

3.2.1 Cardiac signal parameters – an overview

Two kinds of signal parameters can be defined. The first kind parameters are based on signal nature and they are not model type specific. The second kind parameters are characteristic to the user defined model type[6], which particularly can take into account the signal nature too.

It should be noted that signal nature based and model type specific parameters can be estimated using different model types. However, such approach can potentially cause significant errors in the estimation of signal nature based values. The reasonable solution is to use the same model type for all kinds of parameter detection.

---

[5] For the simplicity in the following text the cardiac component of the EBI, viewed as a signal, will be called *the cardiac signal*, if no ambiguity will occur.

[6] In this case it is the model designed (selected) by the author of the thesis.

A. *Signal nature based parameters*

The cardiac signal is cyclic with varying period, thus frequency[7] (heart rate). Due to the cyclic nature, the cardiac signal can be parameterized using the frequency and amplitude notations.

Usually the frequency value of the cardiac signal can vary from $0.8\,\mathrm{Hz}$ to $\sim 2\,\mathrm{Hz}$ and up to $\sim 3\,\mathrm{Hz}$ for sportsmen during exercises. However, in extreme cases the cardiac frequency variations may be in a range from $\sim 0.5\,\mathrm{Hz}$ up to $\sim 4\,\mathrm{Hz}$.

An amplitude as a parameter can be applied to all kinds of signals, and its value depends on the selected basis. Moreover, its value depends on the selected measurement configuration.

B. *Model type based parameters*

In the case of cyclic signals the cyclic model for supporting the frequency and amplitude parameters should be used. For example, using the harmonic functions, the final model of a signal can be constructed using only the frequency and amplitude values defined as a signal nature based parameters, i.e. for a single component model $S_{\mathrm{CM}}\left(t\right) = A_{\mathrm{C}} \sin\left(\omega_{\mathrm{C}} t\right)$.

The real cardiac signal has a complicated waveform (Figure 14, upper plot) and consequently several harmonic spectral components are needed to model this signal accurately (Figure 14, bottom plot).

Despite the fact that orthonormal basis (OB) formed from the harmonic functions,

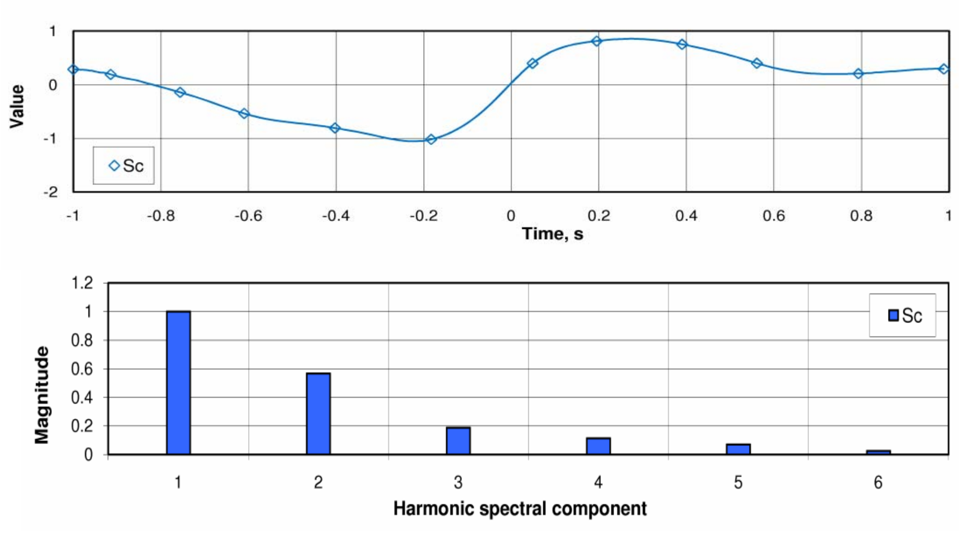

Figure 14 An averaged through multiples periods and scaled cardiac EBI signal $S_{\mathrm{C}}\left(t\right)$ (*upper plot*); for illustration, scaled harmonic power spectrum of an averaged through multiples periods cardiac EBI signal (*bottom plot*)

$$\left\{\mathrm{H}_k\left(t\right)\right\} = \left\{\cos_k\left(t\right), \sin_k\left(t\right)\right\}, \tag{40}$$

is powerful and widely used versatile signal processing tool, some application-specific orthonormal basis (ASOB) may give more appropriate and compact spectral representation of signals in some practical situations.

In some cases the one-period signal-shape of a cardiac EBI signal can be approximated by a non symmetrical triangular shape (Krivoshei 2006). However, the computationally effective triangular signal is not suitable for building an accurate cardiac EBI signal model in practice.

It is essential to use application-specific functions representing characteristics of the signals to be processed. There are some more conditions to be considered for flexibility and computational efficiency:

- using orthogonal system of functions makes possible independent detection of the components;
- using functions based on orthogonal polynomials enables simple recursive computational schemes;
- simple integration formulas can be derived from orthogonal polynomials;
- as BI signals are varying the weighting function should have one or two parameters that could be used for adaptation to waveform.

From classical othogonal polynomials the proper choice would be Jacobi poly-

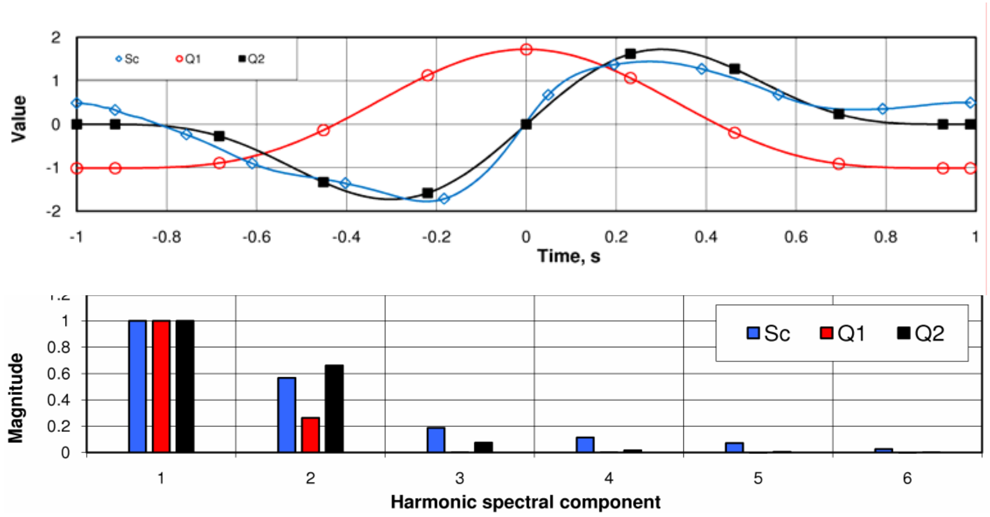

Figure 15 The first and the second components of the designed ASOB and an averaged through multiples periods and scaled cardiac BI signal $S_C(t)$, which is synchronous with the odd component $Q_2(t)$ of ASOB (*upper plot*): $A = B = 5$ (see eq. (41)) ; scaled harmonic power spectra of the same signals (*bottom plot*)

nomials which are defined on interval [-1,1] with the following weighting function

$$\mathrm{W}^{\mathrm{A,B}}\left(t\right) = \left(1 - t\right)^{\mathrm{A}} \left(1 + t\right)^{\mathrm{B}},\ t \in \left[-1,\,1\right]. \tag{41}$$

The parameters A and B of the Jacobi weight function (41) are *the model type based parameters* in the context of the task. Use of the Jacobi weight function for the cardiac signal modeling allows adapting the model shape to the signal shape by changing the values of parameters. Moreover, non equal values of the parameters give non symmetrical shape to the model. Such flexibility can be very useful for modeling the cardiac signal with a complicated shape.

The application-specific orthonormal basis (ASOB) has been designed applying the N^{th} order Gram-Schmidt process, called also as standard N^{th} order Gram-Schmidt orthogonalization process.

This process is applied to the matrix:

$$\left[\mathbf{1}\quad \mathbf{W}^{\mathrm{A,B}}\left(\mathbf{t}\right)\quad \mathbf{t}\cdot\mathbf{W}^{\mathrm{A,B}}\left(\mathbf{t}\right)\quad \mathbf{t}^{2}\cdot\mathbf{W}^{\mathrm{A,B}}\left(\mathbf{t}\right)\right], \tag{42}$$

each columns of which are mutually independent. In the eq. (42) $\mathbf{t}$ is the vector of discrete time instances t_i, the values of which are in the range $\left[-1,\,1\right]$, the operator $\left(\cdot\right)$ means element-wise multiplication of two column-vectors.

Thus the result of such process is a set of orthogonal vectors $\mathbf{Q}_k\left(\mathbf{t}\right)$:

$$\mathbf{Q}_k(\mathbf{t}) = \frac{\mathbf{q}_k(\mathbf{t})}{\parallel \mathbf{q}_k(\mathbf{t}) \parallel},\ k = 0,1,\ldots N \in \mathbb{Z}, \tag{43}$$

where

$$\begin{cases} \mathbf{q}_0(\mathbf{t}) = r_{00}\mathbf{W}^{0,0}(\mathbf{t}) \\ \mathbf{q}_1(\mathbf{t}) = r_{10}\mathbf{q}_0(\mathbf{t}) + \mathbf{W}^{\mathrm{A,B}}(\mathbf{t}) \\ \mathbf{q}_2(\mathbf{t}) = r_{20}\mathbf{q}_0(\mathbf{t}) + r_{21}\mathbf{q}_1(t) + \mathbf{t}\cdot\mathbf{W}^{\mathrm{A,B}}(\mathbf{t}) \\ \ldots \\ \mathbf{q}_N(\mathbf{t}) = r_{N0}\mathbf{q}_0(\mathbf{t}) + r_{N1}\mathbf{q}_1(\mathbf{t}) + \ldots + r_{N(N-1)}\mathbf{q}_N(\mathbf{t}) + \mathbf{t}^{N}\cdot\mathbf{W}^{\mathrm{A,B}}(\mathbf{t}) \end{cases} \tag{44}$$

In practical realization, the values of $\mathbf{W}^{\mathrm{A,B}}(\mathbf{t})$ in the time interval $t_i \in [-1,1]$, r_{km}, and the norms $\parallel \mathbf{q}_k(\mathbf{t}) \parallel$, $k = 0\,..\,N$, $m = 0\,..\,N-1$ are stored in a memory and used for synthesis of the bases functions $\mathbf{Q}_k(\mathbf{t})$ at each time instant during the whole processing time interval.

The cardiac EBI signal model (45) constructed from the second $\mathrm{Q}_2\left(t\right)$ component of the proposed ASOB:

$$S_{\mathrm{CM}}\left(t\right) = A_{\mathrm{C}}\left(t\right)\mathrm{Q}_2\left(\frac{\varphi_{\mathrm{C}}\left(t\right)}{\pi}\right) \tag{45}$$

where A_{C} is the detected amplitude and φ_{C} is the detected phase of the cardiac EBI component. It needs to be noted, that detected cardiac signal phase φ_{C} must be wrapped into the range $\left[-\pi, \pi\right]$.

The first component $\mathbf{Q}_1(\mathbf{t})$ is used to synchronize the second component $\mathbf{Q}_2(\mathbf{t})$ of the ASOB against the input signal $\mathrm{S}_{\mathrm{C}}(t)$, detecting, in this case, the phase of the cardiac component. For the time-frequency synchronization the 'signal-shape locked loop' (SSLL) is used (Krivoshei *et al* 2007a).

In such a manner the model can approximate the most significant features of the one-period signal-shape of the cardiac EBI signal.

The designed Jacobi weight function based ASOB is shown in Figure 15, where one can see that the cardiac signal can be modelled much more accurately using only the second component of the ASOB synchronous with the cardiac signal, than using the harmonic basis.

In detail the design of the ASOB and its use for cardiac signal modelling are described in the author's papers "Decomposition method of electrical bio-impedance signal into cardiac and respiratory components" (Krivoshei *et al* 2008b) and "An Adaptively Tunable Model of the Cardiac Signal for the Bio-Impedance Signal Decomposer (BISD)" (Krivoshei *et al* 2008a).

3.3 The respiratory EBI signal model

The main problem with modelling the respiratory signal is the significant variation of ventilation rate, which can occur unexpectedly and rapidly, whereas breathing can even stop for several seconds.

Therefore, the frequency domain model is used in the proposed method to model the respiratory EBI signal. This is a simple and reliable solution for such kind of signals.

After subtracting the cardiac signal model $S_{\mathrm{CM}}\left(t\right)$, shown in Figure 12, the respiratory estimate is mixed with a remainder of the cardiac signal – the error between the cardiac signal $S_{\mathrm{C}}\left(t\right)$ and its model $S_{\mathrm{CM}}\left(t\right)$. The cardiac remainder part usually does not contain the first harmonic component of the initial cardiac signal, but certainly consists the higher frequency harmonic components (Figure

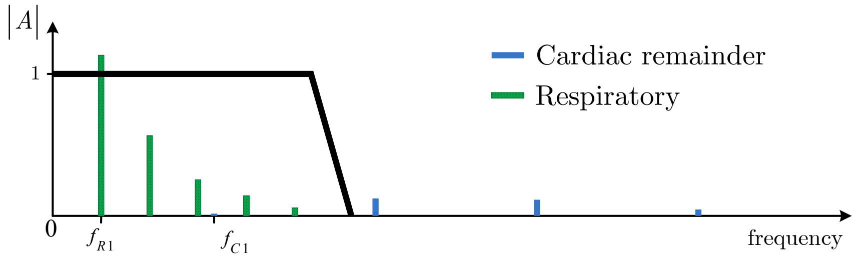

Figure 16 The sketch of the frequency domain respiratory EBI signal model – the low-pass finite impulse response (FIR) filter

16). Consequently, applying a low-pass filter, which works as a frequency domain mask passing the respiratory signal spectral content without changes and suppressing the remainder of cardiac signal. The finite impulse response (FIR) type filter with linear phase-frequency response is used to preserve the respiratory signal shape without distortions (Krivoshei *et al* 2007a, Krivoshei *et al* 2007b, Krivoshei *et al* 2008a, Krivoshei *et al* 2008b).

3.4 Practical realization of the electrical BI signal decomposer (BISD)

In the previous sections of the chapter 3 the introduction into the method and cardiac and respiratory signal models are given. The method description given in section 3.1 is more general – it is conceptual where the specifics of signal model are not taken into account. The main cause of difference between the configurations of conceptual decomposing method and its practical realization is the respiratory BI signal model, which is selected to be a low-pass FIR filter. Of course, such a filter delays the signal. Consequently, synchronization between the cardiac and respiratory components is needed in two subtraction units in Figure 12 (also in Figure 17 and Figure 18).

As a result, two practical realizations of the proposed method, where the signal models specifics are taken into account, are presented in the current section.

The first one is the BI signal decomposer, which is based on the semi-adaptive model of the cardiac BI signal.

The second one is the BI signal decomposer, based on fully adaptable model of the cardiac BI signal.

3.4.1 BISD with a semi-adaptive cardiac model

In this release of the EBI signal decomposer the semi-adaptive cardiac component model is used. The term semi-adaptive cardiac model means that the values of the model-type based parameters (see section 3.2.1) are constant for the current realization. In the proposed case these are the Jacobi weight function parameters A and B in the eq. (41). In opposite, values of the signal nature based parameters, such as signal frequency and amplitude (signal scale), are tuneable during the whole signal processing time interval.

In the proposed method the module, which constructs the cardiac signal model by tracking its parameters synchronously with the estimated cardiac signal, is named signal-shape locked loop (SSLL). The proposed SSLL is described in the publications of the author: the main description is published by Krivoshei *et al* (2007a) and additions to it by Krivoshei *et al* (2008a) and (2008b).

As it was said above, the respiratory BI signal model is realized as a low-pass FIR filter with a constant cut-off frequency $f_{\mathrm{cut}} = 1.6$ Hz ($\mathrm{LPF_R}$ in Figure 17 and Figure 18), which suppresses the remainder part of the cardiac signal. As all causal filters, the $\mathrm{LPF_R}$ delays the signal. Consequently, the respiratory signal model

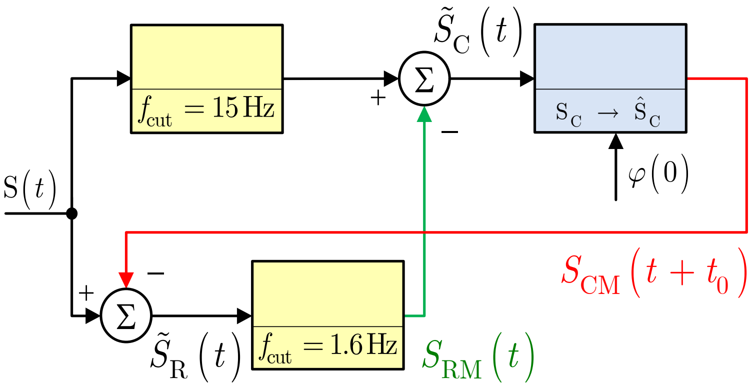
$f_{cut} = 15\,\text{Hz}$
$\tilde{S}_C(t)$
$S_C \rightarrow \hat{S}_C$
$\varphi(0)$
$S(t)$
+
−
$S_{CM}(t+t_0)$
$f_{cut} = 1.6\,\text{Hz}$
$\tilde{S}_R(t)$
$S_{RM}(t)$

Figure 17 The block-diagram of the proposed BISD with semiadaptive cardiac BI model

$S_{RM}(t)$ is delayed with respect to the estimated respiratory signal $\tilde{S}_R(t)$. The delay time in the current release is 2 seconds.

As a result, the signals must be synchronized in the practical realization of the proposed method. Therefore the second low-pass filter LPF_C with equal delay time is added before the subtraction unit into the upper branch of the proposed BISD, which is shown in Figure 17 and Figure 18. Use of this filter allows not only synchronize the signals between the upper and bottom branches, but also suppresses the stochastic disturbances with frequencies higher than 15 Hz.

Moreover, an additional time or phase shift (t_0 or $\varphi(0)$, respectively) of the cardiac BI signal model $S_{CM}(t)$ towards the 'future' (Figure 17 and Figure 18) is required to compensate the delay of the signal in the filter LPF_C and synchronize the cardiac signal model $S_{CM}(t)$ with the input BI signal $S(t)$ in Figure 17.

3.4.2 BISD with fully adaptable cardiac model

Though the proposed method and its practical realization using semi-adaptive cardiac signal model separates the cardiac and respiratory components effectively in different conditions (Krivoshei *et al* 2007b and Krivoshei *et al* 2008b), the use of fully adaptable cardiac model (Krivoshei *et al* 2008a) can significantly increase accuracy of the method together with decreasing of its computation load.

It is clear that, if the shape of the first component of designed ASOB can be adapted to the shape of the cardiac signal period by tuning the model type based parameters of this signal model, then, in the most cases the cardiac BI signal can be modelled by using only the first component of the designed ASOB. As a result, the use of more accurate cardiac signal model accompanied by non significant cardiac remainder part in the respiratory estimate $\tilde{S}_R(t)$, will allow to use 'shorter' FIR filters LPF_R and LPF_C. This, in turn, enables to lower computational load and gives a shorter delay of the signals.

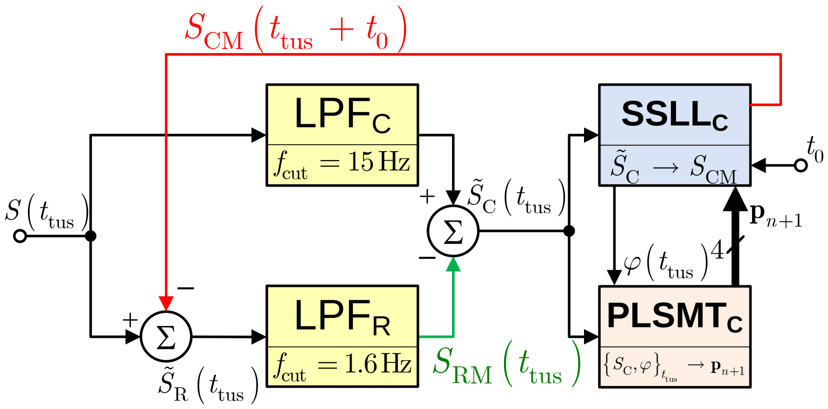
$S_{\mathrm{CM}}(t_{\mathrm{tus}}+t_0)$
LPF$_\mathrm{C}$
$f_{\mathrm{cut}}=15\,\mathrm{Hz}$
SSLL$_\mathrm{C}$
$\tilde{S}_\mathrm{C} \to S_{\mathrm{CM}}$
t_0
$S(t_{\mathrm{tus}})$
$\tilde{S}_\mathrm{C}(t_{\mathrm{tus}})$
$\mathbf{p}_{n+1}$
$\varphi(t_{\mathrm{tus}})$
4
LPF$_\mathrm{R}$
$f_{\mathrm{cut}}=1.6\,\mathrm{Hz}$
PLSMT$_\mathrm{C}$
$\{S_\mathrm{C},\varphi\}_{t_{\mathrm{tus}}} \to \mathbf{p}_{n+1}$
$\tilde{S}_\mathrm{R}(t_{\mathrm{tus}})$
$S_{\mathrm{RM}}(t_{\mathrm{tus}})$

Figure 18 The block-diagram of the proposed BISD with fully adaptable cardiac BI model

Such a proposed solution is presented in Figure 18, where the base configuration from Figure 17 is complemented by the tuner of cardiac signal model, which is named as ‘period locked signal model tuner’ (PLSMT). The input signals for this module are the estimate of the cardiac BI signal and its phase. At the output of this module is the vector of parameters of the model, which is adapted to the cardiac BI signal at the current time instance.

Both inputs of the PLSMT$_\mathrm{C}$ are sampled uniformly in time domain, which is reflected in the time symbol index – t_{tus}.

However, in the PLSMT$_\mathrm{C}$ the input signal $\tilde{S}_\mathrm{C}(t_{\mathrm{tus}})$ is resampled uniformly in the phase domain[8] – $\tilde{S}_\mathrm{C}(t_{\mathrm{pus}})$ to fix the number of samples per signal period. This operation is realized in the sub-module PLS (see Figure 19). After that the resampled signal $\tilde{S}_\mathrm{C}(t_{\mathrm{pus}})$ is averaged over several periods by the averaging module AVG. The ensemble averaged signal $\overline{\mathrm{s}}$ is used as a cardiac signal template to tune the model parameters in the signal model tuner (SMT) module.

As a result, the model tuner (SMT) itself and the signal model parameters (SMP) as parts of the module PLSMT$_\mathrm{C}$ (see Figure 18 and Figure 19) are realized

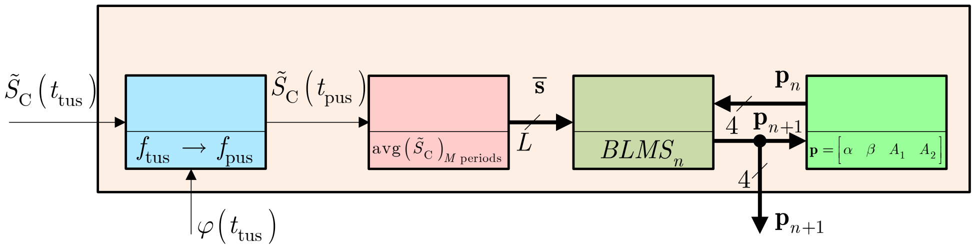
$\tilde{S}_\mathrm{C}(t_{\mathrm{tus}})$
$f_{\mathrm{tus}} \to f_{\mathrm{pus}}$
$\tilde{S}_\mathrm{C}(t_{\mathrm{pus}})$
$\mathrm{avg}(\tilde{S}_\mathrm{C})_{M\ \mathrm{periods}}$
$\overline{\mathrm{s}}$
L
$BLMS_n$
$\mathbf{p}_n$
4
$\mathbf{p}_{n+1}$
$\mathbf{p}=[\alpha\ \ \beta\ \ A_1\ \ A_2]$
4
$\mathbf{p}_{n+1}$
$\varphi(t_{\mathrm{tus}})$

Figure 19 The block-diagram of the period locked signal model tuner (PLSMT) as a part of the proposed BISD with fully adaptable cardiac BI model

using the MatLAB[9] programming environment separately from the main algorithm, which is, in turn, developed using C++ programming language.

The full description of this release can be found in the paper of Krivoshei *et al* (2008a).

---

[9] MatLAB® is the product of the MathWorks Inc.

4

Discussion

In this section, certain questions related to the stated problem and the developed signal decomposition method will be discussed and perspectives for the future development will be presented as well.

The decomposition of dynamic electrical bioimpedance (EBI) signal into cardiac and respiratory components in the presence of noise is very complicated, in general. In the section 2.2 has been shown that this task cannot be solved effectively when using and developing the known methods as ensemble averaging, frequency domain filtering with either constant or moving cut-off frequency, and spectrum analysis. New advanced methods are required for obtaining satisfactory results.

On the background of general complexities, an additional complication is originated from varying conditions (different patients, different kind pathologies, etc.). Thus, the method for solving the sophisticated task must be as flexible as possible for successful operating in such varying situations. Moreover, the flexibility of the method must be achieved without significant losses in accuracy to be usefully implemented in clinical and especially in ambulatory conditions.

In the thesis is presented an adaptive method of the EBI decomposition into its components – cardiac and respiratory ones – which is based on the models of these components. The cardiac component model is parametric and uses the specially designed orthogonal and normalized signals called as application specific orthonormal basis (ASOB). The parametric cardiac model has the signal nature based parameters – the frequency and the amplitude, plus the specific model type based parameters. The respiratory model is designed in the frequency domain. This is just a low-pass filter, which suppresses the remainder part of the cardiac component – the difference between the EBI cardiac component and its parametric model. The LPF with finite impulse response is used to preserve the waveform of the respiratory component unchanged.

Though the proposed method shows acceptable and sometimes even near to perfect results, there is still much space for future developments. First, the integration of the proposed fully adaptive model of cardiac component into the main signal decomposition algorithm should find the final solution.

Second, the model of respiratory component should be developed also in time domain, if possible, instead of the frequency domain model as proposed in the thesis. This task is extremely complicated due to the almost arbitrary varying ventilation rate, which can be even stopped for a while. However, if such the model could be developed, the accuracy of the proposed signal decomposition method will be significantly increased at whole, especially in the case of strongly overlapped spectra of the cardiac and respiratory components. Moreover, the use of an adaptable parametric time domain model of the respiratory component – in addition to the cardiac one – makes possible also effective suppression of motion and other artefacts.

Special attention should be paid to the further development of frequency detection method. Fast detection of such very low frequencies as the cardiac component and especially the respiratory one have, is a very complicated task.

The use of spectral analysis method for frequency detection is almost not suitable in the case of cardiac signal, and especially not applicable when analysing the respiratory component. There is a fundamental constraint: the better resolution in frequency domain takes longer time interval. For the frequency values less than one hertz, the process takes several seconds, e.g. about ten and even more.

The phase-locked loop (PLL) based frequency detector in combination with level crossing detector is used in the proposed method and described in detail by Krivoshei *et al* (2007a, 2007b and 2008b). This approach allows continuously track the frequency of the signal. The level crossing frequency detector estimates the frequency roughly and then the PLL based frequency detector in turn elaborates the more exact estimate.

The frequency estimator, which is described in the papers mentioned in the previous paragraph, is designed for estimation of the cardiac signal frequency only and is fast and accurate enough for this purpose. However, for developing of the respiratory parametric model, the design of above described frequency estimator must be revised to be fast and accurate enough in the conditions of rapidly and unexpectedly varying ventilation rate.

5

Conclusions

In the beginning of PhD studies became clear that further development of known methods was not suitable for solving the task of effective separation the cardiac and respiratory components of electrical bioimpedance (EBI) signal. Therefore, already in the early stadium of his work the author stated the aim of his research in a manner that new advanced methods are required to develop.

Taking into account the possibility of overlapping the spectra of cardiac and respiratory components and non-stationary variations of these components, it became clear that time domain parametric models are needed. It became evident that at least the parametric time domain model of the cardiac component can be developed. The respiratory component is less deterministic due to its arbitrary and widely varying ventilation rate and it cannot be modelled exactly in time domain.

Finally, following author's viewpoints have been featured and the next results achieved:

- the known methods, such as ensemble averaging, classical adaptive filtering and spectral methods were reviewed and it is shown that these are not effective enough for solving the stated decomposition problem;
- the possible solutions, which are based on the independent component analysis (ICA) were analyzed, too, and it is concluded that the ICA is conceptually not suitable to solve the stated problem;

  the developed solution for the stated problem – decomposition of thoracic EBI variations into its cardiac and respiratory components – overcomes the known methods in flexibility of applications, shortness of the output signal delay, and operation reliability;
- the developed method allows to decompose the EBI signal on-line in non-stationary conditions. Delay of the resulting decomposed signals with respect to the input is only two seconds, which is the shortest nowadays;

- moreover, the novel method allows decompose the EBI signal into its components also in the case when the harmonic spectra of these components are partially overlapped;
- only the proposed method uses solely raw EBI data to solve the stated problem without any obligatory reference information, i.e. the electrocardiogram (ECG) signal;
- the distinctive feature of the developed method is that it is based on the parametric time domain model of the cardiac EBI component and frequency domain model of the respiratory EBI component;
- the model of cardiac component is based on the functions of application specific orthonormal basis (ASOB). In turn, the ASOB is developed using the Jacobi weight function. Peculiarity of this function enables to get a flexible shape for the time domain model of cardiac signal. Therefore the model is so well suitable for representation of the cardiac EBI component;
- the model of respiratory component is designed in the frequency domain using the finite impulse response filter for the implementation of model. The filter suppresses the remainder part of the cardiac signal model;
- the method will be implemented in the combined electrical signal (ECG) and impedance signal (ICG) cardiograph (ECG/ICG monitor), which enables to widen the established ECG techniques for making both cardiac and vascular system diagnosing simultaneously taking into account also respiration parameters;
- the developed novel solution promises significant increase in accuracy and diagnosing value of the EBI based cardiologic devices, which in turn, enables to enhance the reliability of diagnosing the cardiovascular diseases worldwide.

A appendix

“A Bio-Impedance Signal Synthesiser (BISS) for Testing of an Adaptive Filtering System”

KRIVOSHEI A

Proc. Int. Biennial Baltic Electronics Conf.
BEC 2006
pp 225–8 (4 pages)

© 2006 IEEE. Reprinted, with permission, from Proc. Int. Biennial Baltic Electronics Conf.BEC 2006, A Bio-Impedance Signal Synthesiser (BISS) for Testing of an Adaptive Filtering System, Krivoshei A.

A Bio-Impedance Signal Synthesiser (BISS) for Testing of an Adaptive Filtering System

A. Krivoshei

Department of Electronics, TTU, Ehitajate tee 5, 19086 Tallinn, Estonia, E-mail: andreik@elin.ttu.ee

ABSTRACT: This paper presents a design of the bio-impedance signal synthesiser (BISS), based on a model of the waveform of the electrical bio-impedance (BI) signal. To get a simple BI signal model, the shapes of the BI signal components, cardiac and respiratory, are approximated by piece-wise linear functions, which are constructed, taking into account the human physiology.

1 Introduction

Measurement and following analysis of electrical bio-impedance (BI) as a parameter of the living tissue, is a topical research and development area nowadays [1].

From point of view of research, medical diagnosis and signal processing, the time variation of the BI can be used as a signal source. Relatively rapid variations on the BI, caused by cardiac and respiratory activities, may be discussed as a kind of biological signal – the bio-impedance signal.

2 Bio-impedance Signal

Phasor of the bio-impedance (Fig. 1) can be presented as a sum of time non-variant $\dot{Z}_0$ and time variant $\Delta\dot{Z}(t)$ parts:

$$\dot{Z}(t) = \dot{Z}_0 + \Delta\dot{Z}(t) \qquad (1)$$

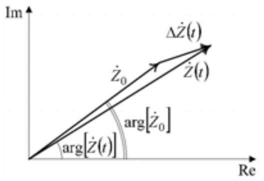

Fig. 1 The diagram of the bio-impedance (BI) phasor $\dot{Z}(t)$, and its parts Z_0 and $\Delta\dot{Z}(t)$.

The part of the BI, which varies in time $\Delta\dot{Z}(t)$, again can be presented as a sum of its in-phase and quadrature components:

$$\Delta\dot{Z}(t) = \Delta Z_{\mathrm{Re}}(t) + j\Delta Z_{\mathrm{Im}}(t) \qquad (2)$$

The time non-variant part (or mean value) of the BI phasor is the main component of organism's impedance in its quantitative sense.

However, despite the fact that the amplitude of the time variant part is several decimal orders lower, than the value of the non-variant one, it is of an essential interest from the point of the biological processes monitoring and diagnostics systems design.

The time variant part of the BI phasor reflects processes in patient's normal physiological state, e.g. breathing, heart beating and muscular activities. But some changes in the BI can be caused by pathological reasons.

Since the attention in the current paper is paid to the changes caused by breathing and cardiac activity, the time variant part of the BI phasor $\Delta\dot{Z}(t)$ is assumed to be expressible as a sum of cardiac and respiratory signals, stochastic disturbance (noise) $n_S(t)$ and deterministic disturbance $n_D(t)$, caused by muscular activity, i.e.

$$\Delta\dot{Z}(\mathrm{t}) = \Delta\dot{Z}_{\mathrm{C}}(\mathrm{t}) + \Delta\dot{Z}_{\mathrm{R}}(\mathrm{t}) + \dot{n}_S(t) + \dot{n}_D(t) \qquad (3)$$

At the output of the BI measurement systems [4] there are often presented demodulated real and imaginary components. So, separate signal processing of real $\Delta Z_{\mathrm{Re}}(t)$ and imaginary $\Delta Z_{\mathrm{Im}}(t)$ parts can be needed.

Assuming, that real and imaginary impedance signals may have different magnitudes of harmonics, but consist of the same spectral components, only one part of the complex signal is discussed in this paper. Consequently Eq. 3 can be rewritten in a scalar form[1]:

$$\Delta Z(\mathrm{t}) = \Delta Z_{\mathrm{C}}(\mathrm{t}) + \Delta Z_{\mathrm{R}}(\mathrm{t}) + n_S(t) + n_D(t) \qquad (4)$$

Direct analysis of the total BI signal $\Delta Z(t)$ may be restricted by several causes. So, in general, it needs to be preconditioned firstly.

Separation of the cardiac and respiratory components, with suppression of the stochastic and deterministic disturbances, seems to be a natural way of such processing.

But it is not a trivial filtering due to the variations of the cardiac and respiratory signal's periods, in a relatively wide range. Not talking about the higher harmonics of the respiratory signal, which lay in the frequency range of the cardiac signal.

---

[1] All relations written for the scalar signal can be used for the real part and imaginary part as well as for the module of the complex signal

An adaptive filtering system (AFS) proposed in [2] is a trial to solve the problem of separation of the two signals. This filtering system has been checked with several real BI signals, and has been tested using very simple model of the BI signal: a symmetrical triangular waveform for the cardiac signal model and a sinusoidal signal as the respiratory component model.

However, so simple model of the BI signal, especially for the respiratory component, does not allow testing of the AFS in conditions, which are more realistic ones.

Therefore a bio-impedance signal synthesiser (BISS), based on the piece-wise linear modelling of the BI signal components, has been designed for the AFS testing purpose (Fig. 2).

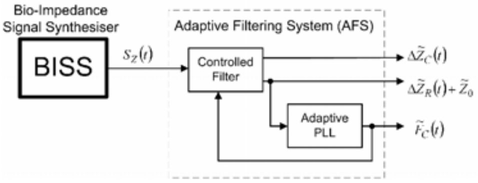

Fig. 2 The block-diagram of the testing system.

3 Bio-impedance Signal Synthesiser

According to the said above, the bio-impedance signal synthesiser, or BISS (Fig. 3), consists of three synthesisers ($S_{\Delta Z_C}$, $S_{\Delta Z_R}$ and S_{Z_0}) and of the summing element. The 1st order low-pass filter (LPF) is added to smooth the synthesised respiratory signal.

The synthesiser S_{Z_0} of the mean value Z_0 is a source of constant signal.

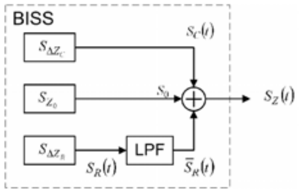

Fig. 3 The block-diagram of the bio-impedance signal synthesiser (BISS).

$S_{\Delta Z_C}$, $S_{\Delta Z_R}$ are the synthesisers of periodic signals, cardiac and respiratory respectively, which are based on the templates (models) of one cycle, approximated by piece-wise linear functions.

4 Model of the Bio-impedance Signal

The models of the BI signal components are based on the approximation of the waveform of the real measured signals, cardiac and respiratory, by piece-wise linear functions. Design of these models will be described in details in the following two subsections (*a* and *b*).

As model for the mean value of the BI signal Z_0 is a constant value it is not of the interest from the point of dynamic signal analysis.

a) The model of the cardiac component

The waveforms of the simultaneously measured BI (a) and ECG (b) signals of one person are shown in the Fig. 4 and 5. One can see that the cardiac BI waveform can be approximated by a triangular signal (a piece-wise linear function) quite well.

Analysis of the signal waveforms (Fig. 4 and Fig. 5) shows that there is a strong relation between the time duration of the BI signal front and the S-T interval of the ECG signal. This time interval corresponds to the systole phase of the cardiac cycle, which is related to the isovolumetric ventricular contraction and to the ventricular ejection processes [3].

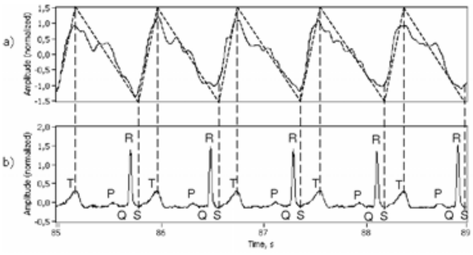

Fig. 4 The waveforms of simultaneously measured BI (a) and ECG (b) signals (the solid lines), in the case of the uniform heart rate with proposed piece-wise linear model of the cardiac BI signal (a), the dashed triangle).

Duration of the systolic phase of the cardiac cycle depends on the properties of the heart, and just slightly changes with the heart rate variations.

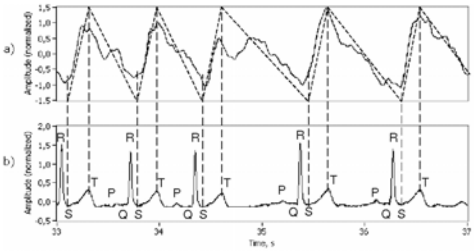

Fig. 5 The waveforms of simultaneously measured BI (a) and ECG (b) signals, in case of the non uniform heart rate (cardiac signal frequency).

Another example in the Fig. 5 clearly demonstrates that the BI signal front duration (S-T time interval of the ECG) does not depend on the heart rate.

The resultant cardiac BI signal model is shown in the Fig. 6 where T_C is a period and A_C is a peak to peak amplitude of the cardiac signal. In this model:

$$T_C = T_{C1} + T_{C2}\,. \tag{5}$$

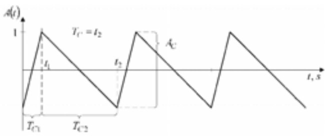

Fig. 6 The waveform of the cardiac component of the BI signal model, $F_C = 1$ Hz.

The time intervals T_{C1} and T_{C2} depend on the cardiac signal frequency F_C :

$$\begin{cases} T_{C1} = g(F_C) \\ T_{C2} = g'(F_C) \end{cases} \tag{6}$$

The dependency of time intervals T_{C1} and T_{C2} on the heart rate is described by the empirical equation (7) and illustrated in the Fig. 7.

$$\begin{cases} T_{C1}(f) = -0.0165 \cdot F_C + 0.2165 \\ T_{C2}(f) = 1/F_C - T_{C1}(f) \end{cases} \tag{7}$$

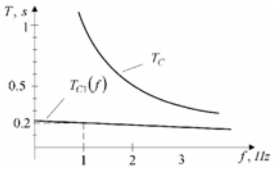

Fig. 7 Dependency of T_{C1} and T_{C1} on the cardiac signal frequency.

However, working at different rates (e.g. 60 and 180 bpm) the heart can not pump out the same volume of the blood in one cardiac cycle. Therefore the peak to peak amplitude of the cardiac signal, which is related to volume of pumped blood, is lower at the higher heart rate.

Such behaviour can be empirically modelled, applying a constant slew rate (SR_f) of the front of the cardiac BI signal. Assuming that the amplitude of the cardiac signal $A_C = 1$ (normalized value) at the frequency $F_C = 1$ Hz, the value of the SR_f can be determined as follows:

$$SR_f = \frac{A_C}{T_{C1}} = 5\left[s^{-1}\right], \quad \text{if} \;\; F_C = 1Hz \;\; \text{and} \;\; A_C = 1 \tag{8}$$

Now the rule of the amplitude variation can be presented in the next form:

$$A_C = SR_f \cdot T_{C1} \tag{9}$$

As an example, the cardiac BI signal model at the cardiac frequency $F_C = 3$ Hz is shown in the Fig. 8:

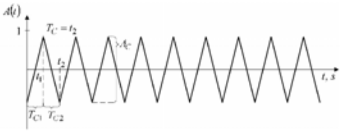

Fig. 8 The waveform of the cardiac component of the BI signal model, $F_C = 3$ Hz.

To summarize this subsection, the system of piece-wise linear functions of the cardiac BI signal model has the form

$$S_C(t) = \begin{cases} \dfrac{A_C}{T_{C1}(f)} \cdot t + S_C(0), & t \in [0;\, t_1] \\ -\dfrac{A_C}{T_{C2}(f)} \cdot t + S_C(t_1), & t \in [t_1;\, t_2] \end{cases}, \tag{10}$$

which is oriented on use of (7 - 9).

b) *The model of the respiratory component*

Design of the model of the respiratory BI signal is more complicated, than of the cardiac one. The frequency and the depth of the respiration (amplitude of the signal) as parameters of the signal vary in time and these variations can not be introduced into the piece-wise model.

In the Fig. 9 is shown an example of the measured respiratory BI signal of a person and the proposed model of this signal. The trapezium signal shape seems to be a quite good approximation of the respiratory BI waveform.

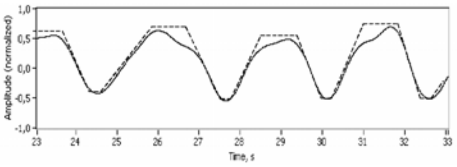

Fig. 9 The respiratory component waveform of the measured respiratory BI signal (the solid line) and proposed piece-wise linear model of this signal (the dashed line).

Assuming the uniformity of the respiration (its frequency and amplitude), the one cycle model of the respiratory BI signal can be presented as in the Fig. 10.

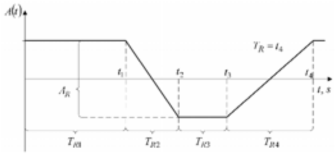

Fig. 10 The waveform of the respiratory component of the BI signal model.

The model of this signal is expressed as a system of piece-wise linear functions:

$$S_R(t)=\begin{cases}\frac{A_R}{2}, & t\in[t0;\,t_1]\\ -\frac{A_R}{T_{R2}}\cdot t+S_R(t_1), & t\in[t_1;\,t_2]\\ -\frac{A_R}{2}, & t\in[t_2;\,t_3]\\ \frac{A_R}{T_{R4}}\cdot t+S_R(t_3), & t\in[t_3;\,t_4]\end{cases} \qquad (11)$$

5 Results

The proposed BISS is realized as a digital software system (a DLL module, programmed in C++ language).

Comparison of the Fig. 11 and 12 shows a relatively good correspondence between the spectra of the synthesized BI signal and the real measured BI signal.

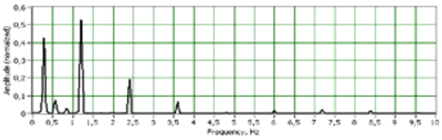

Fig. 11 The magnitude spectrum of the BI signal model.

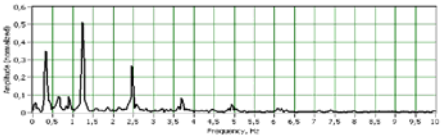

Fig. 12 The magnitude spectrum of the real BI signal.

The cardiac and respiratory signals, generated by BISS, are shown in the Fig. 13.

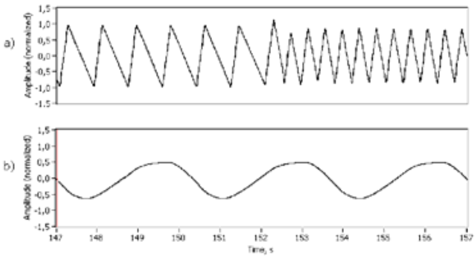

Fig. 13 The time diagram of the synthesised BI signals, cardiac (a) and respiratory (b). The frequency of the cardiac signal is doubled since 152.5s.

The Fig. 14 demonstrates the total BI signal at the output of the BISS (a) and the measured BI (b). One can see that the generated signal corresponds to the measured one quite well.

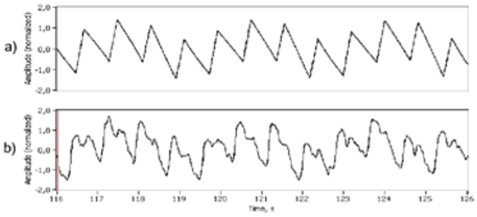

Fig. 14 The waveforms example of the synthesised (a) and measured BI signals (b).

6 Conclusions

The experimental version of the BI signal synthesizer (BISS), is realized as a DLL module, programmed in C++ language.

The synthesised signal does not model all aspects of the real measured BI, due to the model simplicity, however it reflects the main features of the cardiac and respiratory parts of the BI. The piece-wise linear function, with minimum number of points, was used to model the BI impedance signal taking into account the human physiology elements [3]. Partially the empirical expressions were introduced.

BISS is destined for the adaptive filtering system testing [2], but it can be also used in other research areas, where the BI signal source is necessary.

Future development of the BISS will be oriented on design of a more accurate model of the BI signal and use of it for testing purposes and for complex BI signal processing.

7 Acknowledgment

This work was supported by Estonian Science Foundation (the grants no. 5614, 5892, 5897 and 5902) and Enterprise Estonia through the Competence Centre ELIKO.

References

[1] S. Grimnes and Ø. G. Martinsen, "Bioimpedance & Bioelectricity Basics". Academic Press, London, 2000.

[2] A. Krivoshei, M. Min, T. Parve and A. Ronk, "An Adaptive Filtering System for Separation of Cardiac and Respiratory Components of Bioimpedance Signal". To be published in Proc. of MeMeA2006, Italy, April 2006.

[3] A. J. Vander, J. H. Sherman and D. S. Luciano, "Human Physiology". McGraw-Hill, New York, 1990.

[4] M. Min, T. Parve, V. Kukk, A. Kuhlberg, "An Implantable Analyzer of Bio-Impedance Dynamics: Mixed Signal Approach". IEEE Trans. Instrum. Meas., Vol. 51, No. 4, pp. 674-678, Aug. 2002.

B appendix

“An Adaptive Filtering System for Separation of Cardiac and Respiratory Components of Bioimpedance Signal”

KRIVOSHEI A, MIN M, PARVE T AND RONK A

Proc. Int. Workshop on Medical Measurements and Applications
MeMeA 2006
pp 10–5 (6 pages)

© 2006 IEEE. Reprinted, with permission, from Proc. Int. Workshop on Medical Measurements and Applications MeMeA 2006, An Adaptive Filtering System for Separation of Cardiac and Respiratory Components of Bioimpedance Signal, Krivoshei A, Min M, Parve T and Ronk A.

MeMeA 2006 – International Workshop on
Medical Measurement and Applications
Benevento, Italy, 20-21 April 2006

An Adaptive Filtering System for Separation of Cardiac and Respiratory Components of Bioimpedance Signal

Andrei Krivoshei, Mart Min, Toomas Parve, Ants Ronk
Department of Electronics, Tallinn University of Technology
Ehitajate tee 5, 19086 Tallinn, Estonia
Phone: +372 6202 150, Fax: +372 6202 151, Email: andrei.krivoshei@ttu.ee

Abstract *– This paper presents an adaptive filtering system for separation of two bio-impedance signal components: cardiac and respiratory signals. The proposed filtering system is adaptive to the parameters of the input signal's cardiac component (the reference signal), which is corrupted by the respiratory component and also by additive stochastic disturbances. The adaptation is achieved applying estimation and continuous tracking of the heart rate using a time-optimal Adaptive Phase-Locked Loop (APLL). Technical solutions of the filtering system are oriented on applications in portable and implantable medical devices.*

Keywords *– Adaptive control, parameter estimation, phase-locked loop, gain control, digital filters, digital signal processing, bio-impedance, heart rate estimation, heart monitoring, cardiac pacing.*

I. INTRODUCTION

Measurement and following analysis of electrical bio-impedance (EBI) enables to get information about physiological performance of a living tissue, to get diagnostic images, to find hemodynamical parameters, etc. Bioimpedance based information is used in cardiac pacemakers for solving several tasks [1, 2].

Analysis of heart activity has been of interest from several points of view. Heart rate variability [3] has been one of the investigation objects of cardiologists for a longer period. Another related field of interest is sleep-disordered breathing and obstructive sleep apnea [3].

In this paper, the main attention is paid to two application areas of the bio-impedance signal analysis.

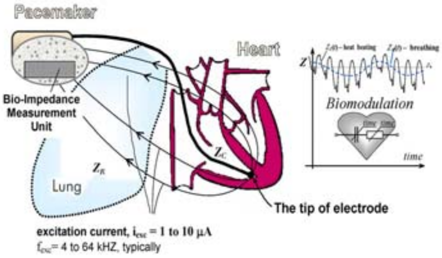

Fig. 1 Explanation of biomodulation of the impedance between the tip electrode and pacemaker case.

The first of them is cardiac pacing monitoring and control, where the best known application is a rate adaptive pacemaker (Fig. 1) [1], and the second is body activity analysis, performed e.g. by means of portable devices. Separation and subsequent analysis of the bio-impedance signal's cardiac and respiratory components is necessary in both application areas.

II. BIO-IMPEDANCE SIGNAL

The varying component of EBI can be considered as a bio-impedance signal. In general, it is assumed to be a sum of cardiac and respiratory signals, and of a stochastic disturbance (noise) $n_s(t)$:

$$\Delta Z(t) \approx \Delta Z_C(t) + \Delta Z_R(t) + n_S(t). \tag{2.1}$$

In the bio-impedance signal analysis the shape of the signal is of interest, especially the shape of the cardiac component. But the control system of a tunable filter is based only on parameters of the fundamental harmonics of cardiac and respiratory components. The sum of other spectral components of the signal can be considered as a deterministic disturbance $n_d(t)$.

Therefore, taking into account only fundamental harmonics of the bio-impedance signal, one can rewrite the equation 2.1 for the control system in a more convenient (simplified) form:

$$\Delta Z(t) = A_C \sin[\omega_C t + \phi_C(0)] + A_R \sin[\omega_R t + \phi_R(0)] + n_S(t) + n_d(t) \tag{2.2}$$

Ratios of the parameter values are of significant importance. In a case of non-invasive bio-impedance measurement, the amplitude A_R of the respiratory signal may be 10 times (or even more) greater than the cardiac signal's amplitude A_C and therefore one has to use rather complicated signal processing. Moreover, the cardiac signal component can be modulated by the respiratory signal.

In stationary situation, the parameters A_C and ω_C, which are of interest in cardiac pacing applications (monitoring of pacing), can be estimated without serious problems.

But in real life this estimation is complicated because the cardiac parameters A_C and ω_C change in time due to several reasons. Some of these changes reflect normal variations of patient's physiological state. But some changes can be caused by pathological reasons. So, a solution of this problem becomes not trivial and it is important to estimate A_C and ω_C as exactly and fast as possible, especially when only limited technical means can be applied as in implanted devices.

III. FILTERING APPROACH

Filtering seems to be a natural way for separating the cardiac component from the other signal components. The heart rate ω_C of a healthy person can vary from 60 bpm, to 240 bpm (from 1 to 4 Hz). Unfortunately, muscular activities cause disturbances within nearly the same frequency range. Respiratory rate is about four times lower than heart rate, therefore, the higher harmonics of the respiratory signal lay in this frequency range too. Besides, synchronization between the cardiac and respiratory activity has been noticed under some conditions.

Thus, the cardiac signal has to be identified/filtered in a selective way. The best approach is to use a phase-locked loop (PLL) for finding the cardiac component (its frequency) from the total impedance signal (Eq. 2.1).

The found ω_C can be used to tune a filtering system towards separation of the cardiac signal in the best way. Evidently, a narrow-band filter is not the best basis for the filtering system: in this filter most of the information carried by the shape of the signal can be lost. Fortunately, the cardiac signal's waveform is quite smooth and thus only a few higher harmonics are essential.

The first harmonic of the cardiac component together with the nearest higher harmonics can be selected out by means of a high-pass filter (HPF). In order to suppress the respiratory component, the cut-off frequency f_T of the HPF must be close to the first harmonic of the cardiac signal. It is not possible to use a fixed f_T value, e.g. 0.8 Hz, for the range of f_C from 1 to 4 Hz because the higher values of f_C are usually accompanied with higher respiratory rate. So ω_R can reach the pass-band of the filter, not talking about the higher harmonics of the respiratory signal.

Holding f_T close to the f_C one can make the described undesired situation less troubling, substantially, but can not avoid it fully.

IV. THE CONTROLLED FILTER

Accomplishment of the controlled filter (CF) is not a very easy task, especially in the case of portable and implantable medical devices, where real-time signal processing is required. The problems of design of high-pass filters for low frequency range are not very well established yet. But many of these problems, especially tunability problem, can be overcome when the HPF is formed on the basis of LPF, delay and subtracting.

Block diagram of the controlled filter is shown in Fig. 2. The filter consists of a low pass filter LPF, with finite impulse response (FIR), to preserve shape of the signal, for filtering the respiratory component. The high pass filter for separation of the cardiac component is realized by subtracting the filtered respiratory signal from the delayed impedance signal ΔZ .

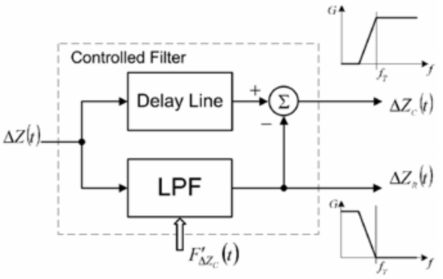

Fig. 2 Block diagram of the controlled filter.

To realize the high pass filter, the length of the delay line must be chosen equal to

$$N_{DL} = \frac{N_{LPF} - 1}{2}, \qquad (3.1)$$

where N_{LPF} , the length of the LPF is an odd number.

V. PLL BASED FILTERING SYSTEM

The proposed adaptive system for separation of the useful bioimpedance signal components: cardiac and respiratory ones, can be considered as a non-linear feedback control system in Fig. 3, where the feedback signal is a frequency of the cardiac component (the heart rate). This frequency can be detected by time-optimal adaptive PLL (APLL) [4-6] and used to tune the parameters of the controlled filter, which extracts the cardiac and respiratory components of the EBI signal.

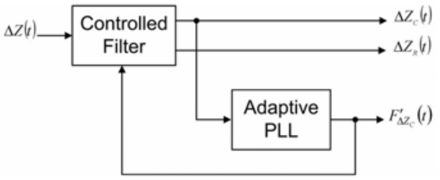

Fig. 3 Block diagram of the adaptive filtering system.

VI. THE ADAPTIVE PLL

The idea of an adaptive PLL has been proposed for applications in the lock-in measurement [5-6], but here it is modified for tracking the cardiac signal frequency (see Fig. 4). In general, APLL's operation can be carried out in two modes: a searching mode and a tracking mode. In the tracking mode APLL operates as a classical phase-locked loop without any control from an introduced supervisor, but the supervisor continues to follow the process. If APLL is not locked, the supervisor, using an estimation of the cardiac signal frequency $\hat{F}_{\Delta Z_c}$, tries to speed up the searching process by tuning the pass band of the controlled filter in accordance with a predefined algorithm.

As several parts of the APLL are conventional for typical PLL systems, only some specific blocks (APD, FE) are described in detail.

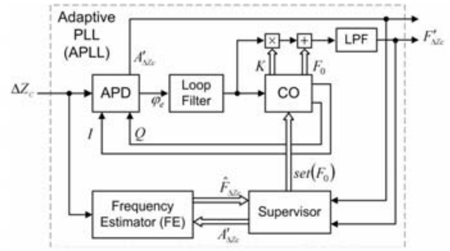

Fig. 4 Block diagram of the Adaptive PLL.

A. Amplitude Phase Detector

It has been stated that the amplitude of the cardiac signal can vary in time. Thus, the gain of the multiplying phase detector (PD) together with the gain of the whole phase-locked loop can change too. Such conditions make it impossible to use the PD effectively without applying any signal-conditioning algorithm.

One possible solution of tracking the periodic signal with varying amplitude has been proposed in [8, 9] and [10]. Using such a method, not the original signal is sent to the input of the correlator (multiplying PD), but the difference between this signal and the in-phase component (I) of the controlled oscillator (CO) output. So this solution is not suitable for tracking of the cardiac signal, the amplitude of which can vary in a wide range, and especially in cases when this amplitude can have high values.

This paper proposes to use an amplitude-phase detector APD (Fig. 5), which allows to find not only the phase error estimate, but an estimate of the amplitude of the fundamental cardiac signal component too.

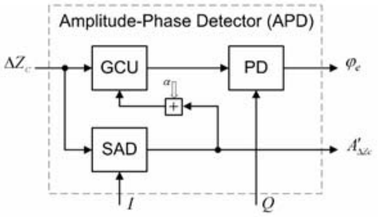

Fig. 5 Block diagram of the Amplitude-Phase Detector (APD), where α is a predefined minimum value of the input signal amplitude, which determine the maximum allowed gain of the GCU.

For this purpose, a synchronous amplitude detector SAD (Fig. 6 and Fig. 7) is provided. The estimate of the $A'_{\Delta Z_c}$ amplitude is used in APD to normalize the input signal of PD by tuning the gain of the gain controllable unit (GCU).

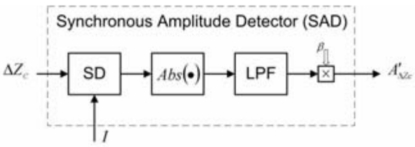

Fig. 6 Block diagram of the Synchronous Amplitude Detector (SAD).
SD – synchronous detector (multiplier),
LPF – low pass filter,
β - proportionality coefficient (in case of the sinusoidal in-phase signal I, $\beta = 2$).

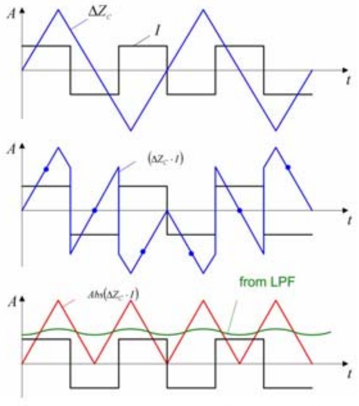

Fig. 7 Waveforms in the Synchronous Amplitude Detector (SAD) in the case of unlocked system.
The simplified cardiac signal has triangular waveform and the in-phase output I of the APLL controlled oscillator has rectangular waveform.

B. Frequency Estimator

The frequency estimator FE is based on a level crossing method proposed in [7] and adopted for the current task. The cardiac signal is selected out by a controlled filter (see Fig. 2). After that the signal is triggered and the rectangular waveform *P(t)*

$$P(t)=\begin{cases} 1, & if \;\; A'_{\Delta Zc} \geq L_P \\ -1, & if \;\; A'_{\Delta Zc} \leq L_N \end{cases} \tag{6.1}$$

is obtained (Fig. 8 and Fig. 9) using triggering levels

$$\begin{cases} L_P = \gamma \cdot A'_{\Delta Zc} \\ L_N = -\gamma \cdot A'_{\Delta Zc} \end{cases}, \text{ where } 0 \leq \gamma \leq 1 \tag{6.2}$$

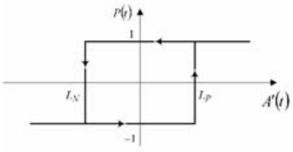

Fig. 8 The hysteresis diagram of the frequency estimator trigger

Intervals between positive and negative edges of the signal *P(t)* are counted by counters C_N and C_P, respectively. So the counted time intervals represent estimations of the cardiac signal periods

$$T_P = C_P T_S, \; [s] \tag{6.3}$$

$$T_N = C_N T_S, \; [s] \tag{6.4}$$

where T_S is a sampling period.

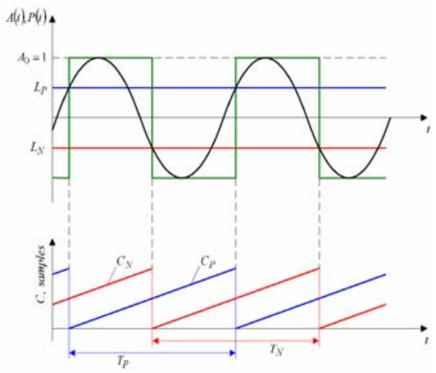

Fig. 9 Time response diagram of the frequency estimator (FE), $\gamma = 0.5$.

Therefore periods of the cardiac signal and the frequency estimates can be calculated using the next equations

$$\hat{T}_{\Delta Z_C} = \frac{T_P + T_N}{2}, \; [s] \tag{6.5}$$

$$\hat{F}_{\Delta Z_C} = 1/\hat{T}_C, \; [Hz] \tag{6.6}$$

As a result, the first frequency estimate can be got after 1.5 signal periods, and a group delay of FE is one signal period.

VII. FILTERING SYSTEM: BEHAVIOR DESCRIPTION

The filtering system works under control of supervisor block and has two working modes: tracking and searching.

A. Tracking mode

Tracking mode is the main operation mode of the proposed adaptive filtering system, when APLL is tuned on the cardiac component of the bio-impedance signal and tracks it continuously. The frequency of the cardiac signal, detected by APLL, is used to correct the cut-off frequency of HPF, formed by the controlled filter CF.

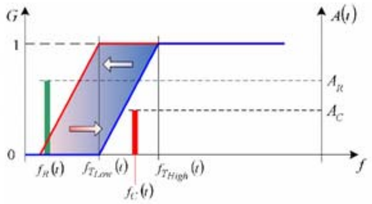

Fig. 10 Time-frequency domain behavior of the adaptive filtering system in the tracking mode.

B. Searching mode

Searching mode will be activated in case of unlocked state of APLL. The situations, in which the searching mode is used, are the following: 1) the system responses to the initial start or to the system reset, 2) the system loses the signal in result of some manipulations with electrodes in the bio-impedance measurement process. It is important to "find" the cardiac signal as fast as possible and to begin or continue tracking it.

The following rules have been formulated for achieving the desired result:

$$\text{if}\quad \begin{cases} F'_{\Delta Z_C} - \hat{F}_{\Delta Z_C} < 0.2 \\ APLL\ \ is\ \ NOT\ \ Locked \end{cases},$$

$$\text{then}\quad \begin{cases} F_0 = \hat{F}_{\Delta Z_C} \\ f_T(n) = f_T(n-1) + (-1)^n \vartheta_f \cdot Ts, \qquad n = 0, 1 \end{cases} \tag{7.1}$$

where $\vartheta_f\ [Hz/s]$ is a speed of changing of the CF cut-off frequency $f_T(n)$ in the current sampling period, and F_0 is a free run frequency of the controlled oscillator (CO) of the APLL.

A graphical representation of the CF amplitude and frequency response "sliding" is shown in Fig. 11.

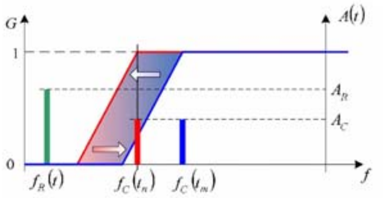

Fig. 11 Time-frequency domain behavior of the adaptive filtering system in the searching mode.

VIII. RESULTS

The proposed method of signal separation is realized as a digital software system (PC version, programmed in C++, the LabView user interface).

The system has been tested using models of the cardiac and respiratory signals: triangle and sinusoidal signals, respectively, the amplitudes of which are normalized by the amplitude of the cardiac component.

Moreover, the frequency of the cardiac signal has been modulated by a waveform of the frequency 0.1Hz so that 10% modulation depth is obtained.

The results of tests are shown in Fig. 12–14, which present changes of the input signal and corresponding time responses of the filtering system. Fig. 15 presents the system response to the real invasive bio-impedance signal.

Each figure consists of four plots:

a) The input signal ΔZ (delayed by 3.5 seconds);

b) The obtained cardiac component ΔZ_C (high-pass output of the CF);

c) The obtained respiratory component ΔZ_R (low-pass output of the CF);

d) The estimates ($F'_{\Delta Z_C}$ and $\hat{F}_{\Delta Z_C}$) of the cardiac signal's frequency and the current cut-off frequency f_T of the controlled filter (CF).

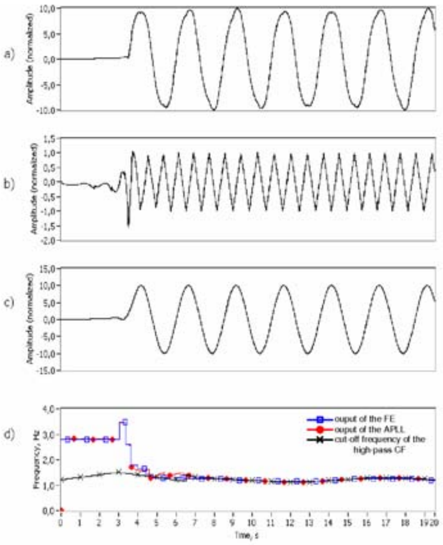

Fig. 12 Time responses just after the start of the filtering system.

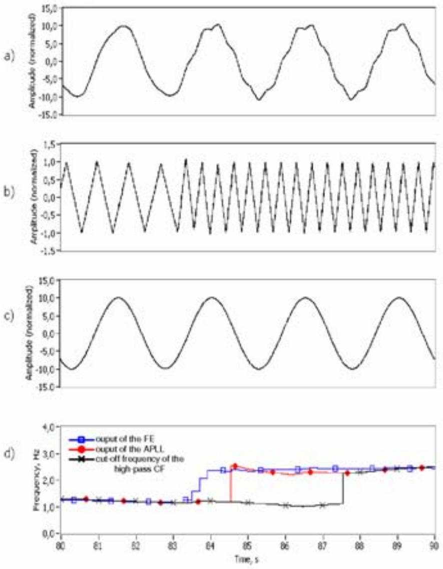

Fig. 13 Time responses of the filtering system just after the frequency step of the cardiac signal model from 1.2 Hz to 2.4 Hz.

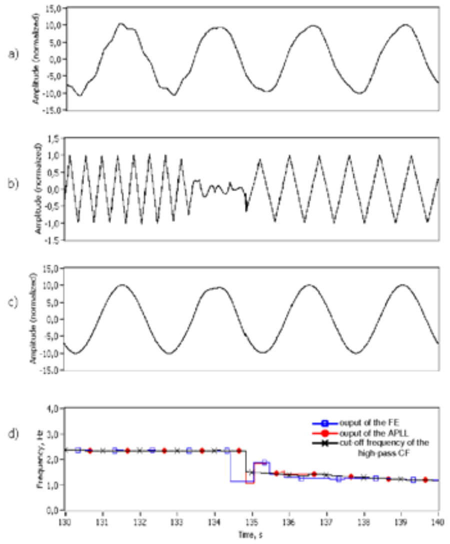

Fig. 14 Time responses of the filtering system just after the frequency step of the cardiac signal model from 2.4 Hz to 1.2 Hz.

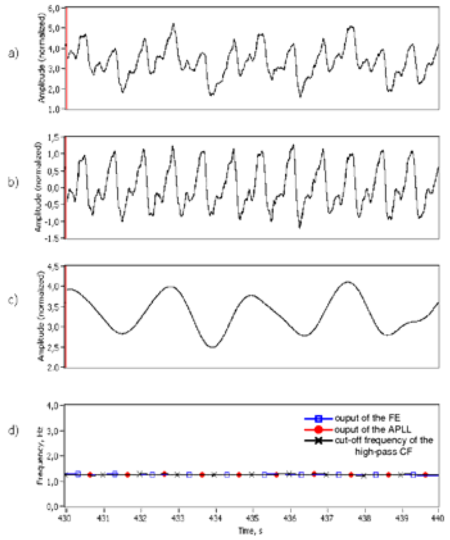

Fig. 15 Time response of the filtering system in case of the real measured bio-impedance signal at the input.

SUMMARY AND FUTURE DEVELOPMENT

The proposed solution of an adaptive filtering system for separation of bio-impedance signal components (cardiac and respiratory) has shown several promising features, which make it useful for cardiac pacing and monitoring applications.

The results have been achieved using developed software system (C++, the LabView user interface).

This system can be used in portable and implantable devices for monitoring cardiac and respiratory activities.

The proposed solution is relatively simple and suits for applications in embedded systems, where microcontrollers, digital signal processor (DSP), or FPGA based solutions are used.

Further development of the filtering system is targeted to application in much more complex analysis of cardiac processes.

ACKNOWLEDGMENT

This work was supported by Estonian Science Foundation (the grants no. 5892, 5897 and 5902) and Enterprise Estonia through the competence center ELIKO.

REFERENCES

[1] Rate adaptive pacemaker. US Patent 6,885,892. Authors: M.Min, A.Kink, T.Parve. Applicant: St.Jude Medical AB, USA/Sweden, issued on 26th of April, 2005.

[2] M. Min, T. Parve, V. Kukk, A. Kuhlberg, "An Implantable Analyzer of Bio-Impedance Dynamics: Mixed Signal Approach [Telemetric Monitors]". *IEEE Trans. Instrum. Meas.*, Vol. 51, No. 4, pp. 674-678, Aug. 2002.

[3] S. Chatlapalli, H. Nazeran, V. Melarkod, R. Krishnam, E. Estrada, Y. Pamula and S. Cabrera, "Accurate Derivation of Heart Rate Variability Signal for Detection of Sleep Disordered Breathing in Children". *Proc. Of the 26th Annual Intern. Conf. of the IEEE EMBS,* Vol. , No. , pp. 538-541, Sept. 1-5, 2004.

[4] M. Min, "Minimization of Transient Time in the Third Order Phase-Locked Loop". *Proc. ECCTD 87*, Part 2, pp. 835-840, Sept. 1987, Paris.

[5] M. Min, A. Ronk, E. Rüstern and H. Sillamaa, "Adaptive Frequency Control in the Phase Synchronization Measurement System". *IFAC Tallinn 90*, Vol. 4, pp. 161-167, 1990.

[6] M. Min, T. Parve and A. Ronk, "Design Concepts of Instruments for Vector Parameter Identification". *IEEE Trans. Instrum. Meas.*, Vol. 41, pp. 50-53, Feb. 1992.

[7] A. Ronk, "Spectral Analysis by Crossing with Properly Chosen Signals". *Baltic Electronics Conf. BEC 96, Tallinn*, pp. 205-208, Oct. 7-11, 1996.

[8] M. Karimi-Ghartemani and M. R. Iravani, "A New Phase-Locked Loop (PLL) System". *Proc. Of the 44th IEEE MWSCAS 2001*, Vol. 1, pp. 421-424, Aug. 14-17, 2001

[9] M. Karimi-Ghartemani and M. R. Iravani, "A nonlinear Adaptive Filter for Online Signal Analysis in Power Systems: Applications". *IEEE Trans. Of Power Delivery*, Vol. 17, No. 2, April 2002.

[10] H. L. Van Trees, "Detection, Estimation and Modulation Theory", *John Wiley & Sons*, Part II, 1968.

C appendix

"Signal-Shape Locked Loop (SSLL) as an Adaptive Separator of Cardiac and Respiratory Components of Bio-Impedance Signal"

KRIVOSHEI A, MIN M AND KUKK V

Proc. Int. Workshop on Medic. Meas. and Applic.
MeMeA 2007
pp 47–52 (6 pages)

© 2007 IEEE. Reprinted, with permission, from Proc. Int. Workshop on Medical Measurements and Applications MeMeA 2007, Signal-Shape Locked Loop (SSLL) as an Adaptive Separator of Cardiac and Respiratory Components of Bio-Impedance Signal, Krivoshei A, Min M and Kukk V.

International Workshop on Medical
Measurement and Applications - MeMeA 2007
Warsaw, Poland, 4-5 May 2007

Signal-Shape Locked Loop (SSLL) as an Adaptive Separator of Cardiac and Respiratory Components of Bio-Impedance Signal

Andrei Krivoshei, Mart Min, Vello Kukk
Department of Electronics, Tallinn University of Technology, Ehitajate tee 5, 19086 Tallinn, Estonia
Phone: +372 6202 150, Fax: +372 6202 151, Email: andrei.krivoshei@ttu.ee

Abstract *– The paper presents an on-line signal processing system for adaptive separation of two infra-low frequency signals: cardiac and respiratory bio-impedance (BI) signals, which are the time varying components of the total BI signal. The separation process of such signals as cardiac and respiratory BI components, is not a trivial filtering due to overlapping of spectra and non stationarity of these signals, and moreover, due to the infra-low frequency range. Therefore, advanced signal processing concepts and methods are needed to achieve the goal. The Signal-Shape Locked Loop (SSLL) concept was introduced to solve the task. Using this concept, it is possible to separate two (or more) independent signal components from the total input signal. Technical solution of the system is intended for applications in portable and implantable cardiac devices.*

Keywords *– Adaptive parameter estimation, independent components separation, digital model-based signal processing, heart rate monitoring, cardiac pacing*

I. INTRODUCTION

Measurement of the electrical bio-impedance (BI) as a parameter of the tissue gives not only information about the performance of living tissue, but also makes possible to analyse the dynamics of physiological processes in organs [1], such as respiration and heart activity. Estimation of hemodynamical parameters and respiration monitoring are very important for both, stationary devices in clinical conditions and portable devices. In the latter case, the design of the implantable devices, as rate adaptive pacemakers (Fig. 1), is considered in the works [1, 2].

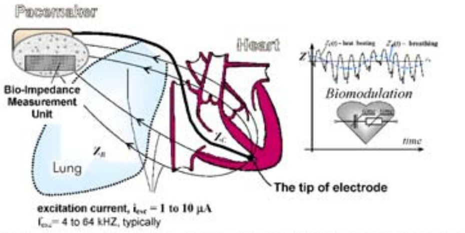

Fig. 1 Explanation of biomodulation of the impedance between the tip electrode and pacemaker case.

Unfortunately, direct analysis of the total BI signal without separation of the cardiac and respiratory components may be restricted and estimation of dynamical parameters is complicated or not possible at all. Therefore, the main attention is paid to separation of cardiac and respiratory components as accurate and fast as possible to be useful for on-line dynamical parameters monitoring.

II. BIO-IMPEDANCE SIGNAL

Since we assume that bio-impedance as a parameter of living tissue is measured using sine wave excitation at some fixed frequencies and levels, the phasor models can be used. Moreover, such an assumption makes possible to present the time variation of BI as a signal, which is more appropriate representation for engineering research, medical diagnosing, and handling of signal processing.

The phasor of the bio-impedance, for a fixed frequency of the sine wave excitation (Fig. 2), can be presented as a sum of time invariant $\overline{Z}_0$ and variant $\Delta\overline{Z}(t)$ parts:

$$\overline{Z}(t)=\overline{Z}_0+\Delta\overline{Z}(t) \tag{1}$$

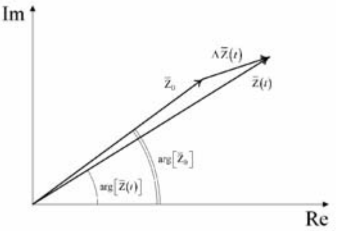

Fig. 2 Diagram of the bio-impedance (BI) phasor $\overline{Z}(t)$ and its parts $\overline{Z}_0$ and $\Delta\overline{Z}(t)$.

The time invariant part (or mean value) of the BI phasor is the basal component of organism's impedance in its quantitative sense.

However, despite the fact that amplitude of the time variant part is much lower than the value of the in-variant one, it is of an essential interest for monitoring of biological processes, and also for designers of diagnostics systems, since the time variant part carries information about dynamics of physiological processes and organs, such as respiration and heart activity.

The time variant part of the BI phasor[1] $\overline{s}(t)$ is assumed to be expressed as a sum of cardiac and respiratory signals, stochastic disturbance $n_S(t)$ and deterministic disturbance $n_D(t)$, caused i.e. by muscular activity:

---

[1] As the BI is assumed to be a signal, the symbol ΔZ is replaced with S in the text.

$$\overline{S}(t) = \overline{S}_C(t) + \overline{S}_R(t) + n_S(t) + n_D(t) \qquad (2)$$

Output of the BI measurement systems is often presented by the signal's real and imaginary components. So, separate processing of real $S_{Re}(t)$ and imaginary $S_{Im}(t)$ parts can be used.

As the real and imaginary parts of BI signals may have different magnitudes, but consist of the same spectral components, only one part of the complex signal is discussed in this paper. Consequently Eq. (2) can be rewritten in a scalar form[2]:

$$S(t) = S_C(t) + S_R(t) + n_S(t) + n_D(t) \qquad (3)$$

Separation of the cardiac and respiratory components together with suppression of the stochastic and deterministic disturbances, is a complex task due to the overlapped spectra of signals (Fig. 3), non-stationarity, and moreover, due to the infra-low frequency range.

The heart rate (HR) of a healthy person can vary from 60 bpm to 240 bpm (F_C varies from 1 to 4 Hz). Respiratory rate is about four times lower than HR, therefore the higher harmonics of the respiratory signal lay in the frequency range of cardiac signal, too (Fig. 3).

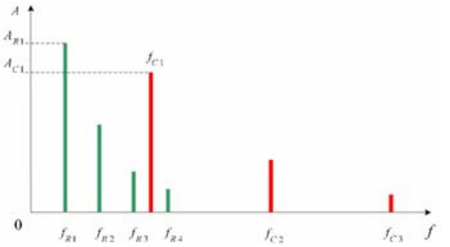

Fig. 3 An example of the spectrum of a BI signal, which consists of combination of the cardiac $\{A_C; f_C\}$ and respiratory $\{A_R; f_R\}$ spectral components.

Expressing the time variant part of the BI signal $S(t)$ as a sum of the cardiac $S_C(t)$ and respiratory $S_R(t)$ components in the Eqs (2) and (3), we assume that these components are received from independent signal sources.

A blind separation of independent components using ICA (Independent Component Analysis) method is described in various articles and books, i.e. in [10]. However, taking into account *à priori* knowledge about the spectral components of quasi-periodic signal can give much more effective solution of the task.

The SSLL concept, described in the next section, is intended to solve the problem.

III. SIGNAL-SHAPE LOCKED LOOP (SSLL)

In this section the SSLL concept, based on the one-period signal model, is discussed. The explanation is done on the example of the cardiac BI signal, $S_C(t)$ for both, a single-component SSLL, and a two-component one, going through the following subsections, including a short description of the model of cardiac BI signal.

A. Cardiac BI signal model

The variation of cardiac BI signal $S_C(t)$ is assumed to be caused by cardiac activity of mammals. Quasi-periodical nature of this signal and approximate knowledge about its spectrum and shape allow us to design the one-period signal-shape model.

The design of the cardiac BI signal model based on the real part of measured BI, is described in detail in [4]. This model is shown below in Fig. 4, for the case, when the signal amplitude is normalised, and the signal frequency $F_C = 1Hz$.

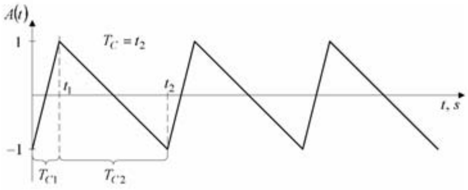

Fig. 4 Waveform of the cardiac BI signal model, $F_C = 1Hz$.

Mathematical description of this model is given by Eqs (4) and (5).

$$S_C(t) = \begin{cases} \dfrac{2}{T_{C1}(f)} \cdot t + S_C(0), & t \in [0; t_1] \\[2ex] -\dfrac{2}{T_{C2}(f)} \cdot t + S_C(t_1), & t \in [t_1; t_2] \end{cases} \qquad (4)$$

where the $T_{C1}(t)$ and $T_{C2}(t)$ are

$$\begin{cases} T_{C1}(f) = -0.0165 \cdot F_C + 0.2165 \\[1ex] T_{C2}(f) = 1/F_C - T_{C1}(f) \end{cases} \qquad (5)$$

The triangular waveform of the real part of cardiac BI signal is taken for the basis. Of course, it does not cover all the possible variants of signal-shapes. However, this approximation is suitable for some set of the cardiac signals, and it can be used for testing systems, which are related to BI hemodynamics. And what is more important, this is the key element in the SSLL concept at the current stage of research, applied to the adaptive separation of the cardiac and respiratory components of bio-impedance signal.

---

[2] All the relations written for the scalar signal can be used for the real and imaginary parts and magnitude of the complex signal.

B. Single-component tracking loop

Previous knowledge about the one-period signal-shape gives us a possibility to estimate the difference $e(t)$ between the input signal $S_C(t)$ and its approximate model $\hat{S}_C(t)$, see (Fig. 5).

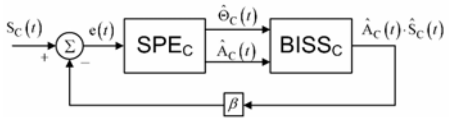

Fig. 5 Block-diagram of the single-component SSLL, implemented as an estimator of cardiac BI signal model.

An algorithm implemented in the estimator (SPE$_C$) of cardiac signal parameters, is intended to minimise the square of distance (7) between the input signal and the reference approximation $\hat{S}_C(t)$, generated by the cardiac BI signal synthesizer (BISS$_C$) [4], adjusting so values of reference signal amplitude $\hat{A}_C(t)$ and integral phase $\hat{\Theta}_C(t)$.

The difference between the signals is

$$e(t) = S_C(t) - \beta\cdot\hat{A}_C(t)\cdot\hat{S}_C(t)\,. \tag{6}$$

Therefore the square of distance between the two signals in L_2 functional space is

$$d^2(t) = \int_0^t e^2(\tau)d\tau = \int_0^t \left[S_C(\tau) - \beta\cdot\hat{A}_C(\tau)\cdot\hat{S}_C(\tau)\right]^2 d\tau\,. \tag{7}$$

The minimisation of square of distance can be achieved using the gradient descent method,

$$\frac{d\zeta(t)}{dt} = -\mu_\zeta \frac{d\left[J(t,\zeta(t))\right]}{d\zeta(t)}\,, \tag{8}$$

where $\zeta(t)$ is a parameter of the signal, and μ_ζ is a real positive number, which determines for each parameter $\zeta(t)$ of signal the speed of minimisation process.

The cost function is

$$J(t,\zeta(t)) = e^2(t)\,. \tag{9}$$

For the proposed system, two signal parameters are to be controlled – the amplitude $\hat{A}_C(t)$, and the frequency $\hat{\omega}_C(t)$. The integral phase $\hat{\Theta}_C(t)$ is calculated from $\hat{\omega}_C(t)$.

$$\begin{cases} \dfrac{d\hat{A}_C(t)}{dt} = 2\mu_{\hat{A}}\cdot\left[S_C(t) - \beta\cdot\hat{A}_C(t)\cdot\hat{S}_C(t)\right]\cdot\hat{S}_C(t) \\[2ex] \dfrac{d\hat{\omega}_C(t)}{dt} = 2\mu_{\hat{\omega}}\cdot\left[S_C(t) - \beta\cdot\hat{A}_C(t)\cdot\hat{S}_C(t)\right]\cdot\hat{A}_C(t)\cdot\dfrac{d\hat{S}_C(t)}{d\hat{\omega}_C(t)} \\[2ex] \dfrac{d\hat{\Theta}_C(t)}{dt} = \displaystyle\int_0^t \hat{\omega}_C(\tau)d\tau \end{cases} \tag{10}$$

Since the control of angular frequency $\hat{\omega}_C$ of only the fundamental spectral component is needed to minimise the cost function (except the amplitude control), the cardiac signal model can be represented using only the inphase fundamental harmonic component, for this case, with the fundamental frequency $\hat{\omega}_C$:

$$\hat{S}_C(t) = \cos\left(\int_0^t \hat{\omega}_C(\tau)d\tau\right) \tag{11}$$

Derivative of which with respect to angular frequency is

$$\frac{d\hat{S}_C(t)}{d\hat{\omega}_C(t)} = -\hat{\omega}_C(t)\sin\left(\int_0^t \hat{\omega}_C(\tau)d\tau\right) = -\hat{\omega}_C(t)\sin\left(\hat{\Theta}_C(t)\right) \tag{12}$$

The feedback coefficient β can have one of two discrete values $\{0,1\}$. If $\beta = 0$, the SSLL becomes to the classical PLL configuration, described by the second and third equations in the set (10), and to the synchronous amplitude detector configuration, described by the first equation in the set (10). In the latter case, of course, the low-pass filter (LPF) should be used for amplitude detection instead of an integrator.

However, despite of the fact that the similar system configurations (without β, i.e. $\beta = 1$) were discussed before, only the sinusoidal signal models were used in such systems, still [6 - 9].

In contrast, the current paper presents the concept of SSLL – the tracking closed loop system, based not only on the sinusoidal, but more complicate signal models.

C. Two-component tracking loop

We call a feedback system in Fig. 6 as the two-component Signal-Shape Locked Loop (SSLL). This system is intended for separation of two independent signals and is based on cross-compensation method, whereas at least one of the two Signal Analysis (SA) subsystems in it is the single-component SSLL.

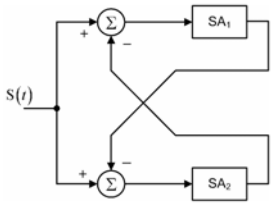

Fig. 6 The block-diagram of the two-component Signal-Shape Locked Loop (SSLL).

IV. BI SIGNAL SEPARATOR

The system for adaptive separation of the cardiac and respiratory components of the BI signal is described above in section III-C. The block-diagram of current realisation of the system is shown in Fig. 7.

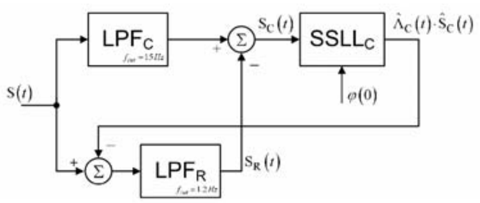

Fig. 7 Block-diagram of a realisation of the Signal-Shape Locked Loop (SSLL) as the separator of cardiac and respiratory BI signal components.

The cardiac BI signal $S_C(t)$ is tracked by the SSLL$_C$, which is described in the section III-B. This configuration contains, in addition, the level crossing based frequency estimator (FE) [3, 5] to detect fast and large changes of cardiac frequency, and to correct the free run frequency of the PLL (SSLL, $\beta=0$ and $d\hat{A}_C(t)/dt=0$). The Adaptive PLL (APLL) [3] tracks the small changes of the cardiac frequency.

For amplitude detection of the cardiac BI signal, two independent subsystems are used – one (SSLL, $\beta=0$ and $d\hat{\omega}_C(t)/dt=0$, [3]) for the PLL input signal normalisation, and the other (SSLL, $\beta=1$ and $d\hat{\omega}_C(t)/dt=0$) for precise amplitude $\hat{A}_C(t)$ control.

Despite of the fact that the SSLL with $\beta=1$, described in the section III-B, works perfectly at sufficiently higher frequencies [6 - 8], the SSLL$_C$ with the more complicate configuration (contains APLL with $\beta=0$, $d\hat{A}_C(t)/dt=0$ and FE; two amplitude detection subsystems with $d\hat{\omega}_C(t)/dt=0$ and $\beta=0$ for first detector and $\beta=1$ for second one) is found to be more reliable for handling infra low frequency signals.

Since the respiratory BI signal is less deterministic than the cardiac one, the signal modelling procedure is more complicated. The current version of the system uses the FIR (finite impulse response) low-pass filter LPF$_R$ with $f_{cut}=1.2\,Hz$ to suppress the remainder part of the cardiac signal, subtracted from the input BI signal $S(t)$.

The second low-pass filter LPF$_C$ is used in the upper branch of the two-component SSLL to compensate the delay of the respiratory signal in the LPF$_R$, and to suppress the high frequency noise. Moreover, an additional phase shift $\varphi(0)$ of the cardiac signal into the 'future' (Fig. 8) is required to compensate the same delay of the cardiac signal in the LPF$_C$.

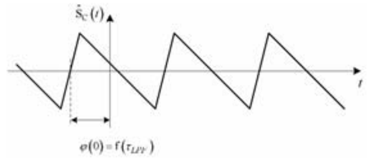

Fig. 8 The simplified time domain diagram of the cardiac BI signal model.

V. RESULTS

The proposed adaptive system is realised as a digital software system, which operates on clock frequency $200\,Hz$ (PC version, programmed in C++, the LabView user interface and communication interface with BI measuring device (in plans) as well).

The system has been tested using models of the cardiac and respiratory signals, generated by external BISS [4], the amplitudes of which are normalized by the amplitude of the cardiac component. The results of tests are shown in Fig. 9 - 12, which present the input signal and corresponding time domain responses of the separating system.

Fig. 13 presents the system response to the real component of the measured BI signal. Each figure consists of four plots:

a) The input signal $S(t)$, delayed by 2 seconds;

b) The obtained cardiac component S_C a red line, and its model - a gray line;

c) The obtained respiratory component S_R ;

d) The estimates of the cardiac frequency $F_C(t)$ - a black line, and its amplitude $\hat{A}_C(t)$ - a red line.

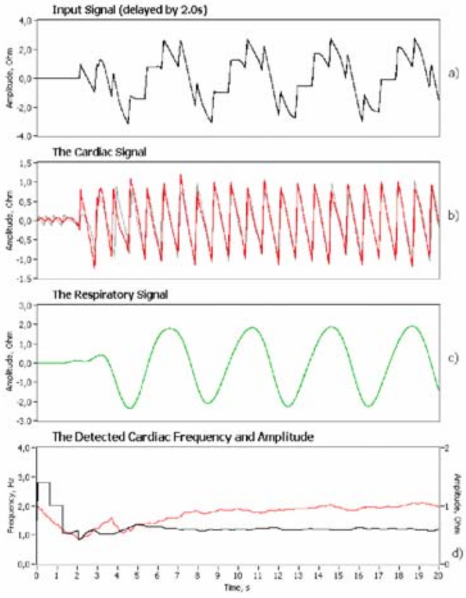

Fig. 9 Time responses of the proposed separating system to the test BI signal, generated by the external BISS, just after the system start.

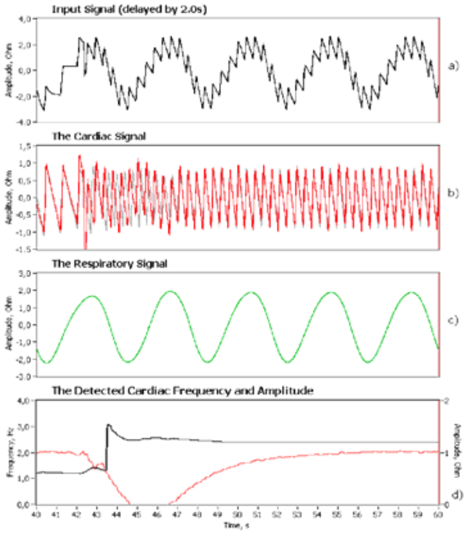

Fig. 10 Time responses of the proposed separating system to the frequency step of the test cardiac BI signal from 1.2 *Hz* to 2.4 *Hz*.

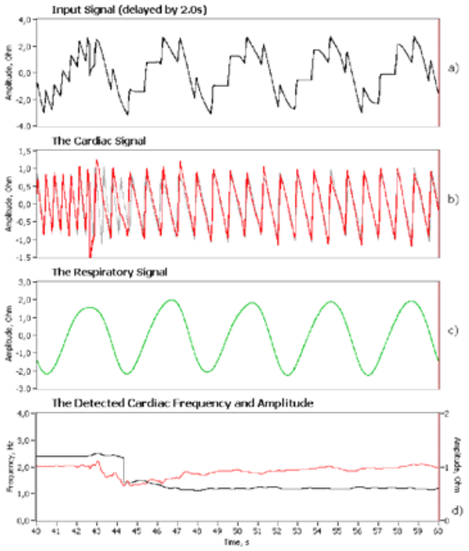

Fig. 11 Time responses of the proposed separating system to the frequency step of the test cardiac BI signal from 2.4 *Hz* to 1.2 *Hz*.

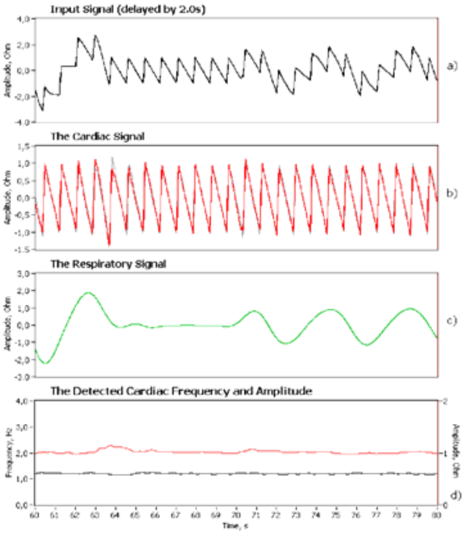

Fig. 12 Time responses of the proposed separating system to the amplitude step of the test respiratory BI signal from 2.0 *Ohm* to 0.0 *Ohm* and back to 1.0 *Ohm*.

VI. SUMMARY AND FUTURE DEVELOPMENT

The proposed system for adaptive separation of two infra-low frequency signals: the cardiac and respiratory components of BI signal, has shown several promising features. The Signal-Shape Locked Loop (SSLL) concept was introduced to solve the task.

The results have been achieved using developed software system (C++, the LabView user interface).

The proposed solution is relatively simple and suits for applications in embedded systems, where microcontrollers, digital signal processor (DSP), or FPGA based solutions are used.

Further development of the separating system is targeted to the design of more accurate and more tuneable model of the cardiac BI signal, since this model is the key element in the synthesis of the SSLL. Also, a more reliable respiratory BI signal model should be developed on the bases of accumulated knowledge.

ACKNOWLEDGMENT

This work was supported by Estonian Science Foundation (grants no. G7212, G7243 and G5614), Enterprise Estonia through the Competence Centre ELIKO and EITSA. The authors express their thanks to Dr. Jürgen Lamp from JR Medical Ltd for providing practical information and giving valuable advice.

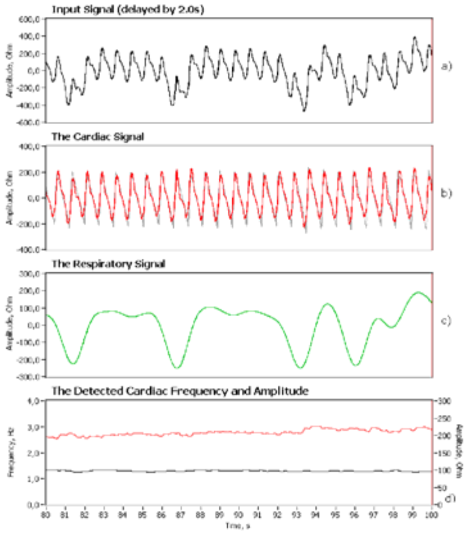

Fig. 13 Time responses of the proposed separating system to the measured BI signal.

REFERENCES

[1] M. Min, T. Parve, V. Kukk, A. Kuhlberg, "An Implantable Analyzer of Bio-Impedance Dynamics: Mixed Signal Approach [Telemetric Monitors]". *IEEE Trans. Instrum. Meas.*, Vol. 51, No. 4, pp. 674-678, Aug. 2002.

[2] Rate adaptive pacemaker. US Patent 6,885,892. Authors: M.Min, A.Kink, T.Parve. Applicant: St.Jude Medical AB, USA/Sweden, issued on 26th of April, 2005.

[3] A. Krivoshei, M. Min, T. Parve and A. Ronk, "An Adaptive Filtering System for Separation of Cardiac and Respiratory Components of Bioimpedance Signal". *Proc. of MeMeA2006.* pp. 10-15, Italy, April 2006. (CD)

[4] A. Krivoshei, "A Bio-Impedance Signal Synthesiser (BISS) for Testing of an Adaptive Filtering System". *Proc. of Baltic Electronics Conference BEC2006.* pp. 225-228, Estonia, October 2006.

[5] A. Ronk, "Spectral Analysis by Crossing with Properly Chosen Signals". *Baltic Electronics Conf. BEC 96, Tallinn*, pp. 205-208, Oct. 7-11, 1996.

[6] M. Karimi-Ghartemani and A. K. Ziarani, "Periodic orbit analysis of two dynamical systems for electrical engineering applications," *J. Eng. Math.*, Vol. 45, No. 2, pp. 135–154, Feb. 2003.

[7] M. Karimi-Ghartemani and A. K. Ziarani, "A Nonlinear Time-Frequency Analysis Method". *IEEE Trans. on Signal Processing.* Vol. 52, No. 6, pp. 1585-1595, June 2004

[8] M. Karimi-Ghartemani and M. R. Iravani, "A nonlinear Adaptive Filter for Online Signal Analysis in Power Systems: Applications". *IEEE Trans. Power Delivery*, Vol. 17, No. 2, pp. 617-622, April 2002.

[9] H. L. Van Trees, "Detection, Estimation and Modulation Theory". *John Wiley & Sons*, Part II, 1968.

[10] A. Hyvärinen, J. Karhunen, E. Oja, "Independent Component Analysis". *John Wiley & Sons*, 2001.

D appendix

“Bio-Impedance Signal Decomposer (BISD) as an Adaptive Signal Model Based Separator of Cardiac and Respiratory Components”

KRIVOSHEI A, KUKK V AND BIRJUKOV A

Proc. Int. Conf. On Electr. Bio-Impedance
ICEBI 2007, IFMBE Proc. **17**
pp 209–12 (4 pages)

Bio-Impedance Signal Decomposer (BISD) as an Adaptive Signal Model Based Separator of Cardiac and Respiratory Components

Andrei Krivoshei[1], Vello Kukk[2] and Andrei Birjukov[1]

[1] Department of Electronics, Tallinn University of Technology, Tallinn, Estonia
[2] Department of Computer Control, Tallinn University of Technology, Tallinn, Estonia

Abstract — **The paper presents the Bio-Impedance Signal Decomposer (BISD) for adaptive separation of two infra-low frequency signals: cardiac and respiratory bio-impedance (BI) signals, which are the time varying components of the total BI signal. The adaptively tuneable cardiac BI signal model (CBISM), constructed from components of a specially designed orthonormal basis is the key element of the proposed BISD. If combined with the signal-shape locked loop (SSLL) concept, this allows an on-line decomposition of a BI signal into its cardiac and respiratory components with partially overlapping spectra. The proposed BISD is currently designed and realised as a digital (PC software) system. The solution is also oriented to be used for portable and implantable cardiac devices, such as rate adaptive pacemakers as well as for stationary devices in clinical conditions.**

Keywords — **Electrical Bio-Impedance, components separation, model-based signal processing, heart rate monitoring, cardiac pacing.**

I. INTRODUCTION

Measurement of the electrical bio-impedance (BI) as a parameter of living tissue gives not only some information about physiological performance of the tissue, but it also makes possible an analysis of some physiological processes or organs dynamics, such as respiration and heart activity. However, the direct analysis and extraction (estimation) of dynamical parameters from the BI signal without decomposing it to the cardiac and respiratory components may be very complicated or impossible.

However the decomposition of the total BI signal into its components is not a trivial filtering due to partially overlapping of spectra and non-stationarity of these components, and also because of infra-low frequency range. Therefore, advanced signal processing methods and/or concepts are needed to achieve our goal: to make the separate analysis of heart and respiration activities possible.

The Signal-Shape Locked Loop (SSLL) concept, based on the cross-compensation method and on the one-period cardiac BI signal model (CBISM), has been introduced in [1] and an advanced development is proposed in the current paper to solve the task – the decomposition of the total input BI signal into the cardiac and respiratory components.

II. BIO-IMPEDANCE SIGNAL - CONSIDERATIONS

Since we assume that bio-impedance as a parameter of living tissue is measured using sine wave excitation at some fixed frequencies and levels, the phasor models can be used. Moreover, such an assumption makes possible to present the time variation of BI as a signal, which is more appropriate representation for an engineering research, medical diagnosing, and signal processing.

The phasor of the bio-impedance for a fixed frequency of the sine wave excitation (Fig. 1) can be presented as a sum of time invariant $\overline{Z}_0$ and variant $\Delta\overline{Z}(t)$ parts.

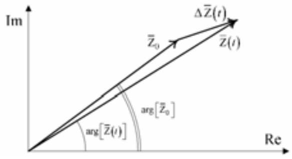

Fig. 1 Diagram of the bio-impedance (BI) phasor.

The time variant part of the BI phasor[1] $\overline{S}(t)$ is assumed to be expressed as a sum of cardiac and respiratory signals, stochastic disturbance (noise) $n_S(t)$ and deterministic disturbance $n_D(t)$, caused i.e. by muscular activity:

$$\overline{S}(t)=\overline{S}_C(t)+\overline{S}_R(t)+n_S(t)+n_D(t) \tag{1}$$

Output of the BI measurement systems is often presented by the signal's inphase and quadrature components, which may have different magnitudes, but consist of the same harmonic spectral components. Therefore only one part of the complex signal is discussed in this paper. Consequently Eq. (1) can be rewritten in a scalar form[2]

$$S(t)=S_C(t)+S_R(t)+n_S(t)+n_D(t) \tag{2}$$

---

[1] As the BI is assumed to be a signal, the symbol ΔZ is replaced with S in the text.

[2] All the relations written for the scalar signal can be used for the real and imaginary parts and magnitude of the complex signal.

Expressing the time variant part of the BI signal $s(t)$ as a sum of the cardiac $S_C(t)$ and respiratory $S_R(t)$ components in the Eqs (1) and (2), we assume that these components are received from independent signal sources.

Separation of such nearly independent components as the cardiac and respiratory ones together with suppression of the stochastic and deterministic disturbances, is a complex task due to the overlapping spectra of signals (Fig. 2), non-stationarity, and moreover, due to the infra-low frequency range, i.e. the heart rate (HR) of a healthy person can vary from 60 bpm to 240 bpm (F_C varies from 1 to 4 Hz). Respiratory rate is about four times lower than HR, therefore the higher harmonic spectral components of the respiratory signal lay in the frequency range of cardiac signal, too.

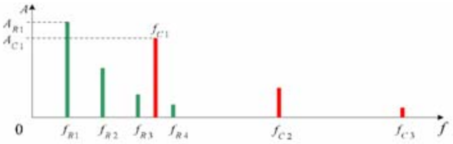

Fig. 2 The sketch of possible harmonic magnitude spectrum of a BI signal, which consists of the combination of the cardiac $\{A_C;\ f_C\}$ and respiratory $\{A_R;\ f_R\}$ components.

A blind separation of independent components using ICA (Independent Component Analysis) method is described in various articles and books, i.e. in [2]. However, taking into account *à priori* estimate of the harmonic spectrum content of quasi-periodic signal, such as the cardiac BI signal one, can give much more effective solution of the task.

III. APPLICATION SPECIFIC ORTHONORMAL BASIS

Despite the fact that orthonormal basis (OB) formed from the harmonic functions, i.e. (3), is a powerful, widely used and versatile signal processing tool, an application specific orthonormal basis (ASOB) may give more appropriate and compact spectral representation of an analysing signal in some practical situations.

$$\{H_k(k\omega t)\} = \{\cos_k(k\omega t),\ \sin_k(k\omega t)\} \tag{3}$$

In many cases the one-period signal-shape of a cardiac BI signal can be approximated by a non symmetrical triangular shape [3]. However the computationally efficient triangular signal is not suitable for appropriate adaptively tuneable CBISM.

The application specific OB, to be a useful tool in cardiac BI signal processing, should be designed in such manner that the first spectral component (k=0) of the formal basis (4) approximates the most significant features of the one-period signal-shape of the cardiac BI signal.

$$\{Q_k(t)\} = \left\{0.5\left[a_{2k}\, q_{2k}(t) + a_{2k+1}\, q_{2k+1}(t)\right]\right\} \tag{4}$$

To satisfy such criterion the triangular weight function in power of four (5) is used with the Classical Gram-Schmidt (CGS) process applied to the function set $\mathcal{F} = \{1,\ t^1, \ldots, t^m\}$, in the time interval $[-1,\ 1)$.

$$W_{trng}(t) = \left[1 - |t|\right]^4, \quad t \in [-1,\ 1) \tag{5}$$

The resulting ASOB is formed from the functions (6) and its first four components are presented in Fig. 3.

$$q_m(t) = \frac{h_m(t)}{\left\| h_m(t) \right\|}, \text{ where} \tag{6}$$

$$\begin{cases} h_0(t) = R_0(t) \\ h_1(t) = g_{10}\, h_0(t) + R_1(t) \\ \\ h_N(t) = g_{N0}\, h_0(t) + g_{N1}\, h_1(t) + \ldots + g_{N,N-1}\, h_{N-1}(t) + R_N(t) \end{cases} \tag{7}$$

The coefficients g_{nm} found during CGS process and $R_m(t)$ are weighted functions from the set $\mathcal{F} = \{1,\ t^1, \ldots, t^m\}$.

$$R_m(t) = \sqrt{W_{trng}(t)} \cdot t^m = W_{S\_trng}(t) \cdot t^m, \quad t \in [-1, 1),\ m = 0 \ldots N \tag{8}$$

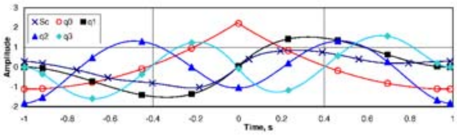

Fig. 3 The first four components of the designed ASOB and an averaged through multiples periods cardiac BI signal $S_C(t)$, which is synchronous with the odd component $q_1(t)$ of ASOB.

Harmonic power spectra of the first two components of ASOB and an averaged through multiples periods cardiac BI signal are presented in Fig. 4.

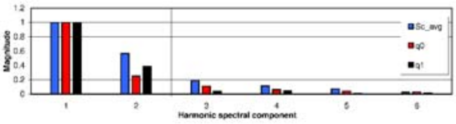

Fig. 4 Scaled Harmonic power spectra of the first two components of ASOB and an averaged through multiples periods cardiac BI signal.

The values of $\mathrm{w}_{S\_trng}(t)$ in the time interval $t \in [-1, 1)$, g_{nm} and the norm values $\left\|\mathrm{h}_m(t)\right\|$, $m = 0 \,..\, N$ are stored in memory and used for synthesis of the basis functions $\mathrm{q}_m(t)$ at each time instant during whole processing time interval.

IV. CARDIAC BIO-IMPEDANCE SIGNAL MODEL (CBISM)

In the current section the construction procedure of the cardiac BI signal model $\hat{\mathrm{S}}_{\mathrm{C}}(t)$ is described. Since the on-line signal processing is required, the given procedure may be divided into three logical parts, which are explained in the following subsections.

A. Time-frequency synchronisation

Since the frequency (period) of the cardiac BI signal $\mathrm{S}_{\mathrm{C}}(t)$ is the time variant parameter, the time-frequency synchronisation between basis and cardiac BI signal should be done to guarantee an adequate estimates of amplitude values during the following processing step IV-B.

At the current stage of the work only the even component $\mathrm{q}_0(t)$ is used to synchronise the odd component $\mathrm{q}_1(t)$ of the application specific OB with the input signal of the SSLL$_C$ $\mathrm{S}_{\mathrm{C}}(t)$ (see Fig. 5 and [1]). For such synchronisation the adaptive PLL [1, 4] is intended.

B. Cardiac BI signal decomposition in ASOB

For estimation of amplitudes of the spectral components of cardiac BI signal in the ASOB, adaptive linear adder (ALA) [5] is used. The instantaneous estimates $a_k(t)$ of the amplitude values of spectral components (the weight values of ALA) are being found using LMS algorithm (11) with the cost function (9), when $N = 5$.

$$\mathrm{J}(t) = \mathrm{e}^2(t), \text{ where} \tag{9}$$

$$\mathrm{e}(t) = \mathrm{S}_{\mathrm{C}}(t) - \hat{\mathrm{S}}_{\mathrm{C}}(t) = \mathrm{S}_{\mathrm{C}}(t) - \sum_{k=0}^{N} a_k(t) \cdot \mathrm{q}_k(t) \tag{10}$$

$$a_k(t) = 2\mu_{a_k} \int_0^t \mathrm{e}(\tau)\mathrm{q}_k(\tau)\,d\tau \tag{11}$$

where μ_{a_k} is a real positive number, which determines the speed of the cost function (9) minimisation process. In practical cases the process minimisation speed can be increased using serial connection of the integrator in (11) and a high-pass filter with the transfer function (12).

$$\mathrm{TF}_k(s) = \frac{\tau_z s + 1}{\tau_p s + 1}, \text{ where i.e. } \tau_z > \tau_i > \tau_p \text{ and } \tau_i = 1/2\mu_k \tag{12}$$

C. Synthesis of the CBISM

As a result of the above subsections, the cardiac BI signal model (the output signal of the SSLL$_C$) is expressed as

$$\hat{\mathrm{S}}_{\mathrm{C}}(t) = \sum_{k=0}^{N} a_k(t) \cdot \mathrm{q}_k(t) \tag{13}$$

V. BIO-IMPEDANCE SIGNAL DECOMPOSER (BISD)

The adaptive BISD, intended for the separation of two infra-low frequency signals: cardiac and respiratory BI signals, is designed as two-component SSLL operating in the ASOB to achieve better results than in [1], where the non-symmetrical triangular signal is used as a CBISM. The block-diagram of the proposed BISD is shown in Fig. 5.

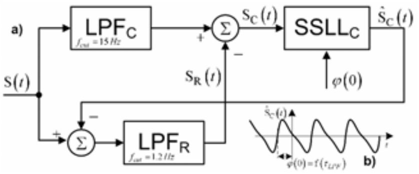
a)
LPF$_C$
$f_{cut} = 15\,Hz$
$\mathrm{S}_{\mathrm{C}}(t)$
SSLL$_C$
$\hat{\mathrm{S}}_{\mathrm{C}}(t)$
+
−
$\mathrm{S}(t)$
$\mathrm{S}_{\mathrm{R}}(t)$
$\varphi(0)$
−
+
LPF$_R$
$f_{cut} = 1.2\,Hz$
$\hat{\mathrm{S}}_{\mathrm{C}}(t)$
t
$\varphi(0) = f(\tau_{LPF})$
b)

Fig. 5 Block-diagram of the BISD realisation (a) and the sketch of the CBISM (b).

The cardiac BI signal $\mathrm{S}_{\mathrm{C}}(t)$ is tracked by the SSLL$_C$, which is described in [1] and in the previous section for the case of using it with the proposed ASOB.

Since the respiratory BI signal is less deterministic than the cardiac one, the signal modelling procedure is more complicated. The current version of the BISD uses the FIR (finite impulse response) low-pass filter LPF$_R$ with $f_{cut} = 1.2\,Hz$ to suppress the remainder part of the CBISM $\hat{\mathrm{S}}_{\mathrm{C}}(t)$, subtracted from the input BI signal $\mathrm{S}(t)$.

The second low-pass filter LPF$_C$ is used in the upper branch of the two-component SSLL to compensate the delay of the respiratory signal in the LPF$_R$, and to suppress the high frequency noise. Moreover, an additional phase (time) shift $\varphi(0)$ of the CBISM into the 'future' (Fig. 5b) is required to compensate the same delay of the cardiac signal $\mathrm{S}_{\mathrm{C}}(t)$ in the LPF$_C$.

VI. RESULTS

The proposed BISD is realised as a digital software system, which operates at clock frequency $200\,Hz$ (PC version, programmed in C++, the LabView user interface and communication interface with BI measuring device (in plans) as well).

The system has been tested using the synphase component of the measured BI signal.

Fig. 6-7 present time responses of the BISD to the input signals obtained from two persons. Each of the figures consists of four plots:

1. The input signal $s(t)$, delayed by 2 seconds;
2. The obtained cardiac component $s_C(t)$ - a red line, and its model $\hat{s}_C(t)$ - a green line;
3. The obtained respiratory component $s_R(t)$;
4. The estimates of the cardiac BI signal instantaneous frequency $\hat{F}_C(t)$ - a black line, and its instantaneous amplitude value $\hat{A}_C(t)=\sqrt{a_0^2(t)+a_1^2(t)}$ - a red line.

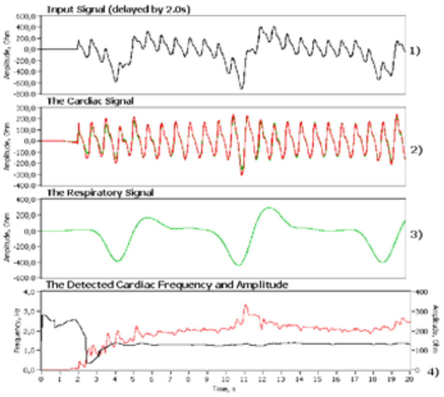

Fig. 6 Time responses of the proposed BISD to the input BI signal from a person nr.1, just after the system start.

VII. CONCLUSIONS

The proposed BISD is designed as an adaptive one-period cardiac BI signal model based signal processing system. Promising results were achieved using an application specific orthonormal basis, designed to model and track the cardiac BI component in a mode near to the real-time operation. The pre-recorded BI signals were used to test the BISD. However, the proposed solution is suits for on-line processing of measured BI.

Despite that the promising results are achieved, the future development is required to get more robust, precise and fast BISD, including pathological cases as well.

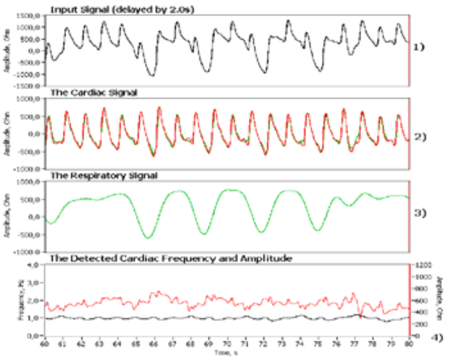

Fig. 7 Time responses of the proposed BISD to the input BI signal from a person nr.2.

ACKNOWLEDGMENT

This work was supported by Estonian Science Foundation (grants no. G7212, G7243 and G5614), Enterprise Estonia through the Competence Centre ELIKO and EITSA. The authors express their thanks to Dr. Jürgen Lamp from JR Medical Ltd for providing practical information and giving valuable advice.

REFERENCES

1. Krivoshei A, Min M, Kukk V (2007) Signal-Shape Locked Loop (SSLL) as an Adaptive Separator of Cardiac and Respiratory Components of Bio-Impedance Signal, MeMeA07 Proc., Warsaw, Poland, 2007, "In press"
2. Hyvärinen A, Karhunen J, Oja E (2001) Independent Component Analysis. John Wiley & Sons
3. Krivoshei A (2006) A Bio-Impedance Signal Synthesiser (BISS) for Testing of an Adaptive Filtering System, BEC2006 Proc., Baltic Electronics Conf., Tallinn, Estonia, 2006, pp. 225-228
4. Krivoshei A, Min M, Parve T, Ronk A (2006) An Adaptive Filtering System for Separation of Cardiac and Respiratory Components of Bioimpedance Signal, MeMeA06 Proc., Benevento, Italy, 2006, pp. 10-15
5. Widrow B, Stearns S.D (1985) Adaptive Signal Processing. Prentice Hall, N.J.

Address of the corresponding author:

Author: Andrei Krivoshei
Institute: Department of Electronics
Street: Ehitajate tee 5
City: Tallinn
Country: Estonia
Email: andreik@elin.ttu.ee

E appendix

“An Adaptively Tunable Model of the Cardiac Signal for the Bio-Impedance Signal Decomposer (BISD)”

KRIVOSHEI A, KUKK V AND MIN M

Proc. Int. Workshop on Medic. Meas. and Applic.
MeMeA 2008
pp 49–52 (4 pages)

© 2008 IEEE. Reprinted, with permission, from Proc. Int. Workshop on Medical Measurements and Applications MeMeA 2008, An Adaptively Tunable Model of the Cardiac Signal for the Bio-Impedance Signal Decomposer (BISD), Krivoshei A, Kukk V and Min M.

MeMeA 2008 – IEEE International
Workshop on Medical Measurements and Applications
Ottawa, Ontario, Canada - May 9-10, 2008

An Adaptively Tunable Model of the Cardiac Signal for the Bio-Impedance Signal Decomposer (BISD)

Andrei Krivoshei[1], Vello Kukk[2], Mart Min[1]
[1]Department of Electronics
[2]Department of Computer Control
Tallinn University of Technology, Ehitajate tee 5, 19086 Tallinn, Estonia
Phone: +372 6202 158, Email: andrei.krivoshei@ttu.ee

Abstract *– The paper presents the further development of the bio-impedance signal decomposer (BISD) of the total bio-impedance (BI) signal to its cardiac and respiratory components. The Jacobi orthonormal polynomials based adaptively tunable model of the cardiac BI signal is proposed in the paper, which plays very important role in the decomposition task. The importance arises from the fact, that the BISD must be reliable and have to correct operate with signals taken from different persons, and in such cases, when the cardiac BI signal of a person is changing in time. For the proposed system the reliability significantly depends on the difference between the model of the cardiac signal and the real cardiac signal (the reference signal). The averaged through several periods version of the already separated cardiac BI signal is used as reference signal in the proposed algorithm for tuning the parameters of the cardiac BI signal model using a modified Newton adaptation algorithm. After the model is elaborated, the system separates the cardiac and the respiratory components more accurately by tracking the cardiac BI signal.*

Keywords *– Adaptive signal processing, adaptive parameter estimation, bio-impedance, model-based signal processing, heart rate monitoring*

I. INTRODUCTION

Measurement and following analysis of the electrical bio-impedance (BI) is the topical research area in biomedical engineering nowadays. It can play significant role in such applications as the living tissue parameters extraction (estimation), and in monitoring of the dynamical processes in the tissue and organs, such as respiration and heart activity, which are very important for the medical diagnostics.

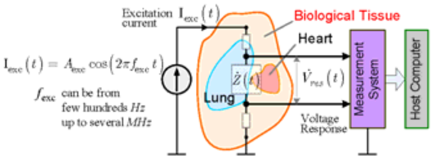
Excitation current $I_{exc}(t)$
Biological Tissue
Heart
$I_{exc}(t) = A_{exc}\cos(2\pi f_{exc}t)$
f_{exc} can be from few hundreds Hz up to several MHz
$\dot{Z}(t)$
$\dot{V}_{res}(t)$
Lung
Voltage Response
Measurement System
Host Computer

Fig. 1 The block-diagram of a typical measurement configuration for estimation of the bio-impedance value $\dot{Z}(t)$

The generalized scheme for measurement of the BI using single frequency cosine excitation current $I_{exc}(t)$ generator is shown in the Fig. 1. More detailed description of the BI itself as a parameter characterizing living tissue, and its measurement techniques can be found, for example in [1]

As it was mentioned above, using the BI as a parameter of the living tissue, which varies in time, makes possible to analyze the dynamics of physiological processes in organs, i.e. respiration and heart activity, and to get the information about the performance of living tissue as well.

Unfortunately, possibility of direct analysis of the total BI signal without decomposing it to the cardiac and respiratory components may be restricted, and estimation of the dynamical parameters is complicated or impossible.

Therefore, the main attention in this work is paid to separation of cardiac and respiratory components as accurately and fast as possible to be useful for on-line (or even real-time) monitoring of dynamical parameters.

However, the task of decomposition of the total BI signal to its components is complicated due to partial overlapping of their spectra and non-stationarity of these components, and also because of infra-low frequencies of the signals. The heart rate (HR) of a healthy person can vary from 60 bpm to 240 bpm, and consequently, the frequency $F_C = 1 / T_C$ (here T_C is the period of repetition of the cardiac BI signal in time) varies from 1 to 4 Hz. Respiratory rate is about four or more times lower than HR, therefore the higher harmonic spectral components of the respiratory signal lay in the frequency range of cardiac signal, too.

As a result, advanced signal processing methods and/or concepts are needed to achieve the goal: to make possible the separate analysis of heart and respiration activities.

The current paper proposes further development of the BISD, which is based on the previously developed method [3, 4] and the system of the cardiac and respiratory BI signals separation, called the Bio-Impedance Signal Decomposer (BISD) [5].

II. GENERAL STRUCTURE OF THE BISD

Assuming that the cardiac and respiratory components of the total BI signal are practically independent [3],

$$S(t) = S_C(t) + S_R(t) \tag{1}$$

allows the use of two-component Signal-Shape Locked Loop (SSLL, proposed in [3]) as BI signal decomposer (Fig. 2).

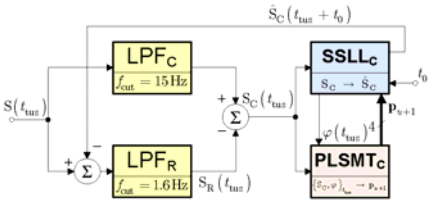

Fig. 2 The block-diagram of the bio-impedance signal decomposer (BISD) with block of period-locked signal model tuner (PLSMT), which works with the cardiac BI signal model; t_{tus} are the time instances distributed uniformly in the time domain (tus - time uniform sampling).

In addition to the BISD configuration, which is shortly described in the following paragraphs and in more detail in [2-4], the Period-Locked Signal Model Tuner (PLSMT) is intended to tune the parameters of the cardiac BI signal model.

The cardiac BI signal $S_C(t_{tus})$, where t_{tus} are the time instances distributed uniformly in the time domain (tus - *time uniform sampling*), is tracked by the single-component SSLL$_C$, which operates in the application specific orthonormal basis (ASOB), proposed in [4] and further modified by use of the Jacobi function as a weighting function in [5].

Since the respiratory BI signal is less deterministic than the cardiac one, the signal modeling procedure is more complicated. The current version of the BISD uses the finite impulse response (FIR) low-pass filter LPF$_R$ with cut-off frequency $f_{cut}=1.6\,Hz$ to suppress the remainder part after subtracting of the Cardiac Bio-Impedance Signal Model (CBISM) $\hat{S}_C(t_{tus}+t_0)$ from the input signal $S(t_{tus})$.

The second low-pass filter LPF$_C$ is used in the upper branch of the two-component SSLL to form delay for the cardiac signal with the same duration as delay for the respiratory signal in the LPF$_R$, and to suppress the high frequency noise.

An additional time (phase) shift t_0 of the CBISM into the 'future' (Fig. 2) is required to compensate the same delay of the cardiac signal $S_C(t_{tus})$ in the LPF$_C$:

$$t_0 = 0.5T_{tus}\left(N_{LPF}-1\right) \tag{2}$$

where T_{tus} is the period of sampling and N_{LPF} is the length (odd number) of the low-pass filter LPF$_C$.

Reliable and correct operation of the proposed BISD with signals taken from different persons, and in such cases, when the cardiac BI signal of a person is changing in time, significantly depends on the difference between the model of the cardiac signal and the real cardiac signal. Therefore a mechanism (algorithm) for adaptive tuning of the cardiac BI signal model is required.

The PLSMT, which is intended to solve this task, is described in details in the following section.

The interaction between the SSLL$_C$ and PLSMT$_C$ in the proposed BISD is shown in the Fig. 2. The input signals for PLSMT$_C$ are the separated cardiac BI signal $S_C(t_{tus})$ and the estimated value of its phase $\varphi(t_{tus})$, both are uniformly sampled in time with period T_{tus}. The vector of parameters of the signal model $\mathbf{p}_{u+1}$ with updated values just after the tuning process in the SSLL$_C$ is done. These values are used until the vector of parameters with updated values will be available.

III. THE PERIOD-LOCKED SIGNAL MODEL TUNER

The block-diagram of a subsystem called the Period-Locked Signal Model Tuner (PLSMT) is shown in Fig. 3, and description of it is given in the following subsections.

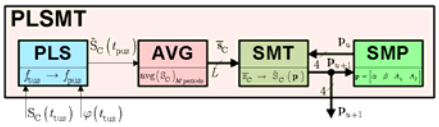
PLSMT
PLS
$f_{tus} \rightarrow f_{pus}$
$\tilde{S}_C(t_{pus})$
AVG
$\mathrm{avg}(S_C)_{M\ periods}$
$\overline{s}_C$
L
SMT
$\overline{s}_C \rightarrow \hat{s}_C(\mathbf{p})$
$\mathbf{p}_u$
4
$\mathbf{p}_{u+1}$
SMP
$\mathbf{p}=[\alpha\ \beta\ A_1\ A_2]$
4
$S_C(t_{tus})$
$\varphi(t_{tus})$
$\mathbf{p}_{u+1}$

Fig. 3 The block-diagram of the Period-Locked Signal Model Tuner (PLSMT); t_{pus} are the time instances distributed uniformly in the phase domain (pus - phase uniform sampling).

A. Reference signal preconditioning

The Period-Locked Sampler (PLS) resamples the input signal $S_C(t_{tus})$, which has been already sampled uniformly in time. The result of this operation is the signal $\tilde{S}_C(t_{pus})$, which is sampled uniformly in the phase domain, where t_{pus} are the time instances distributed uniformly in the phase domain (pus - *phase uniform sampling*). The number of samples per period of the cardiac BI signal is L (for the current design $L=20$). Therefore the period of sampling in the phase domain is

$$P_{pus} = 2\pi\,/\,L\ \left[rad\right]. \tag{3}$$

The reference signal is presented by a vector $\overline{s}_C$ of length L, which is the averaged (through M periods, in the block AVG in the Fig. 3) version of the separated cardiac BI signal.

B. Signal model tuner (SMT)

The model of the cardiac BI signal (CBIS) $\hat{s}(\mathbf{p})$, used in the Signal Model Tuner (SMT) in the Fig. 3, is formed from components of the application specific orthonormal basis (ASOB). Where $\hat{s}(\mathbf{p})$ is the vector of length L, which is at the same time, the function of the vector $\mathbf{p}$. Elements of the vector (4) $\mathbf{p}$ are the parameters of the CBISM. The values of these parameters have to be adaptively tuned to minimize the square of distance between the model of the cardiac signal and the reference signal. The meaning of the parameters is described below.

$$\mathbf{p} = \left[\alpha \quad \beta \quad A_1 \quad A_2\right] \tag{4}$$

C. The cost function

To minimise the square of distance between the model of the cardiac signal and the reference signal, the cost function is defined as

$$\mathrm{C}(\mathbf{p}) = \sum_{l=0}^{L-1} e^2(t_l,\mathbf{p}) = \sum_{l=0}^{L-1}\left[\overline{s}_{\mathrm{C}}(t_l) - \hat{s}(t_l,\mathbf{p})\right]^2, \tag{5}$$

or in the vector (of length L) notation:

$$\mathrm{C}(\mathbf{p}) = \left[\mathbf{e}(\mathbf{t},\mathbf{p})\right]^{\mathbf{T}}\mathbf{e}(\mathbf{t},\mathbf{p}), \tag{6}$$

$$\mathrm{e}(\mathbf{t},\mathbf{p}) = \overline{\mathbf{s}}_{\mathrm{C}}(\mathbf{t}) - \hat{\mathbf{s}}(\mathbf{t},\mathbf{p}), \tag{7}$$

where $\mathbf{t} = \{t_l\}$ is the vector of phase uniformly sampled time values $\mathbf{t} \subset \{t_{\mathrm{pus}}\}$, $t_{\mathrm{pus}} \in [-1,1)$ and $l = 0,1,\ldots,(L-1)$.

D. The model of the cardiac BI signal

The model of cardiac BI signal $\hat{\mathbf{s}}(\mathbf{t},\mathbf{p})$ constructed from the first $\mathrm{Q}_1(\mathbf{t},\mathbf{p})$ and the second $\mathrm{Q}_2(\mathbf{t},\mathbf{p})$ components of the ASOB (10)(11) is

$$\hat{\mathbf{s}}(\mathbf{t},\mathbf{p}) = A_1\mathrm{Q}_1(\mathbf{t},\mathbf{p}) + A_2\mathrm{Q}_2(\mathbf{t},\mathbf{p}), \tag{8}$$

$$\begin{aligned} A_1 &= A_{1\exp} + \tilde{A}_1 \\ A_2 &= A_{2\exp} + \tilde{A}_2 \ , \end{aligned} \tag{9}$$

where A_1, A_2 are amplitude values of polynomials $\mathrm{Q}_1(\mathbf{t},\mathbf{p})$ and $\mathrm{Q}_2(\mathbf{t},\mathbf{p})$ respectively and $A_{1\exp}, A_{2\exp}$ are expected (or initial) values of these amplitudes; $\tilde{A}_1$ and $\tilde{A}_2$ are adaptive parts of the total amplitude values.

Components of the ASOB are expressed in (10) and (11).

$$\mathrm{Q}_i(\mathbf{t},\mathbf{p}) = k_i\,\mathrm{q}_i(\mathbf{t},\mathbf{p}), \tag{10}$$

where k_i are normalizing and scaling factors for polynomials[1] $\mathrm{q}_i(\mathbf{t},\mathbf{p})$, $i = 0,1,\ldots,(N-1) \in \mathbb{Z}$, which are defined in (11).

$$\begin{cases} \mathrm{q}_0(\mathbf{t},\mathbf{p}) = g_{00}\mathbf{w}^{0,0}(\mathbf{t}) \\ \mathrm{q}_1(\mathbf{t},\mathbf{p}) = g_{10}\,\mathrm{q}_0(\mathbf{t},\mathbf{p}) + \mathbf{w}^{\mathrm{A,B}}(\mathbf{t}) \\ \mathrm{q}_2(\mathbf{t},\mathbf{p}) = g_{20}\,\mathrm{q}_0(\mathbf{t},\mathbf{p}) + g_{21}\,\mathrm{q}_1(\mathbf{t},\mathbf{p}) + \mathbf{t}\circ\mathbf{w}^{\mathrm{A,B}}(\mathbf{t}) \\ \ldots \\ \mathrm{q}_{N-1}(\mathbf{t},\mathbf{p}) = g_{N-1,0}\,\mathrm{q}_0(\mathbf{t},\mathbf{p}) + \ldots + \mathbf{t}^{N-1}\circ\mathbf{w}^{\mathrm{A,B}}(\mathbf{t}). \end{cases} \tag{11}$$

The coefficients g_{ij} are calculated during the standard Gram-Schmidt Process (GSP).

In the third expression in (11) and in the text below the symbol "dot" ($\circ$) is used to show the element by element multiplication operation of two vectors of the same length.

In this paper the Jacobi function (12) is used as the weight function with GSP (10)(11).

$$\mathbf{w}^{\mathrm{A,B}}(\mathbf{t}) = \mathbf{w}(\mathbf{t};\mathrm{A,B}) = (\mathbf{1}-\mathbf{t})^{\mathrm{A}}(\mathbf{1}+\mathbf{t})^{\mathrm{B}}, \tag{12}$$

where

$$\mathrm{A} = \mathrm{A}_{\min} + c^{(1+\alpha)}, \quad \mathrm{B} = \mathrm{B}_{\min} + c^{(1+\beta)}. \tag{13}$$

The values of constants $\mathrm{A}_{\min}, \mathrm{B}_{\min}$ and c are predefined for the current adaptation procedure, but can be changed for the next one. The constant c can be defined using initial (or expected) values of A, B and its minimum values $\mathrm{A}_{\min}, \mathrm{B}_{\min}$, for the case, when $\alpha = \beta = 0$.

E. Adaptive process

The procedure of the cost function minimisation (by tuning the values of the elements of the $\mathbf{p}$) is realized using a quasi-Newton method (modified version will be described in the following paragraphs).

The expression for the original iterative Newton method [6] for the $(n+1)-\mathrm{th}$ iteration is

$$\mathbf{p}_{n+1} = \mathbf{p}_n + \upmu\cdot\frac{\mathbf{J}_n(\mathrm{C}_n(\mathbf{p}),\mathbf{p})}{\mathbf{H}_n(\mathrm{C}_n(\mathbf{p}),\mathbf{p}^{\mathbf{T}}\mathbf{p})}, \tag{14}$$

where the function[2] $\mathbf{J}_n(\mathrm{C}_n,\mathbf{p})$ is the Jacobian matrix of first order partial derivatives of function C_n with respect to the vector of parameters $\mathbf{p}$ and $\mathbf{H}_n(\mathrm{C}_n,\mathbf{p}^{\mathbf{T}}\mathbf{p})$ is the Hessian matrix of second order partial derivatives of C_n with respect to the matrix of the parameters products $\mathbf{p}^{\mathbf{T}}\mathbf{p}$.

The Jacobian and Hessian matrixes can be presented as

$$\mathbf{J}_n(\mathrm{C}_n,\mathbf{p}) = 2\mathbf{e}_n^{\mathbf{T}}\mathbf{J}_n(\mathbf{e}_n,\mathbf{p}), \tag{15}$$

$$\mathbf{H}_n(\mathrm{C}_n,\mathbf{p}^{\mathbf{T}}\mathbf{p}) = 2\left[\mathbf{J}_n^{\mathbf{T}}(\mathbf{e}_n,\mathbf{p})\mathbf{J}_n(\mathbf{e}_n,\mathbf{p}) + \mathbf{G}_n\right]. \tag{16}$$

For the modified Newton method we define

$$\mathbf{G}_n = \mathbf{0}. \tag{17}$$

And therefore

$$\mathbf{p}_{n+1} = \mathbf{p}_n + \upmu\circ\left(\mathbf{e}_n^{\mathbf{T}}\frac{\mathbf{J}_n(\mathbf{e}_n,\mathbf{p})}{\mathbf{J}_n^{\mathbf{T}}(\mathbf{e}_n,\mathbf{p})\mathbf{J}_n(\mathbf{e}_n,\mathbf{p})}\right). \tag{18}$$

The constant vector $\upmu$ defines the speed of the adaptation process (18) convergence.

It is needed to be mentioned, that no problems with convergence of modified Newton (16) - (18) algorithm were found for allowed range of parameters values in the vector $\mathbf{p}$.

---

[1] These polynomials is the result of the standard Gram-Schmidt Process (GSP) applied to the function set $\mathcal{F} = \{1, t^1, .., t^{N-1}\}$, in the time interval $[-1, 1)$ with the given weight function.

[2] For more compact presentation, the functions $\mathrm{C}_n,\mathbf{e}_n$ of vectors $\mathbf{t}$ and $\mathbf{p}$, are written here and below without mark of dependency on vectors $\mathbf{t}$ and $\mathbf{p}$.

IV. RESULTS

At the current stage the BISD is designed as a digital software system programmed in C++ (the user interface is programmed using the LabView), excluding the signal model tuner (SMT). The latter one has been tested separately in the MATLAB environment (in this case $L = 160$), and is in the stage of embedding into the main algorithm of the BISD now.

For the current realization the initial values of some variables and the values for constants are defined in (19).

$$\begin{array}{ll} \mathrm{A}_{\min} = 2.0 & A_{1\exp} = -0.1 \\ \mathrm{B}_{\min} = 1.8 & A_{2\exp} = 0.8 \\ c = 3.0 & \tilde{A}_1 = 0 \\ \alpha = \beta = 0 & \tilde{A}_2 = 0 \end{array} \tag{19}$$

The Fig. 4 shows the first $\mathrm{Q}_1(\mathbf{t})$ and the second $\mathrm{Q}_2(\mathbf{t})$ components of the ASOB, and the CBISM (8) based on it as well.

In the next figure (Fig. 5) the outcomes of the adaptation process is shown for the values of the vector $\mathbf{p}$ elements (the parameters of the CBISM) and for the cost function values.

DISCUSSION AND CONCLUSIONS

In this paper the adaptively tunable model of the cardiac bio-impedance signal is proposed. The model is constructed from the components $\mathrm{Q}_1(\mathbf{t})$ and $\mathrm{Q}_2(\mathbf{t})$ of the orthonormal basis (10)-(11). For this the Jacobi function is used as a weight function with the Gram-Schmidt Process (GSP). The adaptation is achieved using the modified Newton method.

The realization of this adaptive process is done in the so-called signal model tuner (SMT) module, which has been tested separately from the main decomposing system (BISD), at the moment.

The realization of the SMT, and the tests have been done in the MatLAB environment. The outcomes of these experiments are shown in Fig. 4 and Fig. 5.

Such a model is needed to reliably separate the cardiac and the respiratory components of the total bio-impedance signal. The authors think that this improves accuracy of the BISD proposed in their previous works significantly by tracking the cardiac component with the adaptive model.

In perspective, such a model can be the first step towards the automatic classification of the pathological cases in the impedance cardiology.

ACKNOWLEDGMENT

This work was supported by Estonian Science Foundation (grants no. G7212, G7243 and G5614), Enterprise Estonia through the Competence Centre ELIKO and Estonian Infotechnology Foundation EITSA. The authors express their thanks to Dr. Jürgen Lamp from JR Medical Ltd for providing practical information and giving valuable advice.

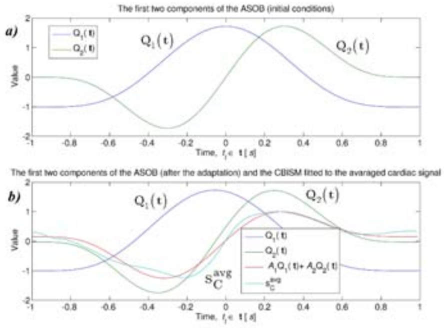

Fig. 4 The first $\mathrm{Q}_1(\mathbf{t})$ and the second $\mathrm{Q}_2(\mathbf{t})$ components of the ASOB, and the CBISM based on it; *a)* - before the adaptation process ($A_1 = 0$, $A_2 = 1$) and after it *b)*.

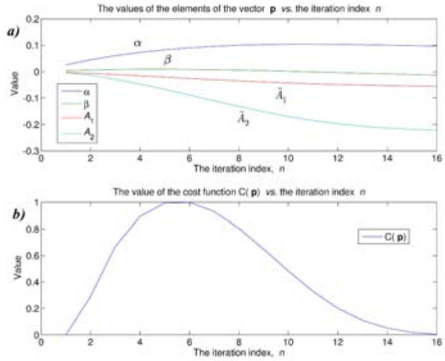

Fig. 5 The values of the elements of the vector $\mathbf{p}$ *a)* and the value of the cost function $\mathrm{C}(\mathbf{p})$ *b) vs.* the iteration index *n*.

REFERENCES

[1] S. Grimnes and Ø. G. Martinsen, "Bioimpedance & Bioelectricity Basics". *Academic Press*, London, 2000.

[2] A. Krivoshei, M. Min, T. Parve and A. Ronk, "An Adaptive Filtering System for Separation of Cardiac and Respiratory Components of Bioimpedance Signal". *Proc. of MeMeA2006.* pp. 10-15, Italy, April 2006. (CD)

[3] A. Krivoshei, M. Min and V. Kukk, "Signal-Shape Locked Loop (SSLL) as an Adaptive Separator of Cardiac and Respiratory Components of Bio-Impedance Signal". *Proc. of MeMeA2007.* pp. 47-52, Poland, May 2007. (CD).

[4] A. Krivoshei, V. Kukk and A. Birjukov, "Bio-Impedance Signal Decomposer (BISD) as an Adaptive Signal Model Based Separator of Cardiac and Respiratory Components". *Proc. of 13th Int. Conf. on the Electrical Bioimpedance (ICEBI) 2007*. vol. 17, pp. 209 – 212, Graz, Austria, August 2007.

[5] A. Krivoshei, V. Kukk and M. Min, "Decomposition method of electrical bio-impedance (BI) signal into cardiac and respiratory components". *Physiological Measurement.* Accepted for publication.

[6] Widrow B, Stearns S.D (1985) "Adaptive Signal Processing". Prentice Hall, N.J.

F appendix

“Decomposition method of electrical bio-impedance signal into cardiac and respiratory components”

KRIVOSHEI A, KUKK V AND MIN M

Physiological Measurement, 2008
***29**(6), S15 - S25 (11 pages)*

IOP PUBLISHING PHYSIOLOGICAL MEASUREMENT

Physiol. Meas. **29** (2008) S15–S25 doi:10.1088/0967-3334/29/6/S02

Decomposition method of an electrical bio-impedance signal into cardiac and respiratory components

A Krivoshei[1], V Kukk[2] and M Min[1]

[1] Department of Electronics, Tallinn University of Technology, Ehitajate tee 5, 19086 Tallinn, Estonia
[2] Department of Computer Control, Tallinn University of Technology, Ehitajate tee 5, 19086 Tallinn, Estonia

E-mail: andrei.krivoshei@ttu.ee

Received 30 November 2007, accepted for publication 6 May 2008
Published 10 June 2008
Online at stacks.iop.org/PM/29/S15

Abstract

The paper presents a method for adaptive decomposition of an electrical bio-impedance (BI) signal into two components: cardiac and respiratory. The decomposition of a BI signal is not a trivial process because of the non-stationarity of the signal components and overlapping of their harmonic spectra. An application specific orthonormal basis (ASOB) was designed to solve the decomposition task using the Jacobi weighting function in the standard Gram–Schmidt process. The key element of the bio-impedance signal decomposer (BISD) is a model of the cardiac BI signal, which is constructed from the components of the ASOB and is intended for use in the BISD for on-line tracking of the cardiac BI signal. It makes it possible to separate the cardiac and respiratory components of the total BI signal in non-stationary conditions. In combination with the signal-shape locked loop (SSLL), the BISD allows us to decompose the BI signals with partially overlapping spectra. The proposed BISD based method is accomplished as a PC software digital system, but it is oriented towards applications in portable and stationary cardiac devices and in clinical settings.

Keywords: bio-impedance, independent components separation, model-based signal processing, heart rate monitoring, cardiac pacing

(Some figures in this article are in colour only in the electronic version)

1. Introduction

Measurement of the electrical bio-impedance (BI) as a parameter of living tissue not only gives information about the physiological performance of the tissue, but also makes it possible to analyse some dynamic processes in organs, such as respiration and cardiac activity (Grimnes and Martinsen 2000).

Over the past few decades impedance cardiography[3] (ICG) has played an important role in the estimation of the stroke volume and other parameters of the cardiovascular system (Cotter *et al* 2006). The advantages of using BI, and ICG in particular, are non-invasiveness and cost-effectiveness, which makes continuous long-term monitoring possible.

However, the measured BI signal consists not only of its cardiac component, but also contains the respiration component, motion artefacts and stochastic disturbances. For ICG applications, all these three components are unwanted parts of the signal, which can be treated as noise[4]. The suppression of such noise is a very important signal processing task, whereas the known and used noise removal methods can be divided into three different approaches.

The first approach is an ensemble averaging technique which uses multiple periods of the ICG signal to suppress the disturbances, which are not correlated with the ICG signal. Such an approach is used by Muzi *et al* (1986), Zhang *et al* (1986) and Wang *et al* (1995). Woltjer *et al* (1996) referenced to Kim *et al* (1992) and declared that averaging has been shown to be effective in eliminating the effect of respiration. However, it is clear that the disturbing components must have a zero mean value to be effectively suppressed by averaging. But this becomes possible only when averaging is done over a long time interval. Such averaging can suffer from the variability of the ICG signal shape and event latencies that can cause less distinct events in the signal to disappear in the averaged signal (Hu *et al* 1997). As a result, this approach cannot be used in on-line monitoring of the cardiac parameters.

The second approach is an adaptive filtering used by Yamamoto *et al* (1988) for the suppression of the disturbances in the ICG signal. This solution is based on the digital infinite impulse response (IIR) band-pass filter, which moves around the centre frequency (heart rate). Unfortunately, this solution also suppresses the high-frequency components of the ICG signal and introduces non-linear phase distortion. Another application of adaptive filtering for reducing the respiration and motion artefacts in an electrogastrogram was described by Chen *et al* (1993). In the latter work, the use of three types of adaptive filters was studied, i.e., time-domain, transform-domain and frequency-domain filters. A disadvantage of these filters is the need for a reference disturbance signal. The same disadvantage appears in a system for adaptive cancellation of the respiratory artefact investigated by Pandey and Pandey (2005). The scaled Fourier linear combiner (SFLC) by Barros *et al* (1995) reconstructs the ICG signal from harmonic spectral components found by using an adaptive least mean square (LMS) filter, with reference inputs related to the R–R intervals of the ECG.

The third approach is based on spectral analysis methods. In particular, wavelet-based time–frequency analysis is used by Ouyang *et al* (1998) and Pandey and Pandey (2007) to select the disturbance free ICG signal from the noisy input. However, spectral analysis, and the use of wavelets in particular, require a great number of spectral components (levels in the wavelet case) to represent the input signal accurately. Another difficulty can arise in the selection of the threshold, at which the separation of a useful component from noises is performed. Pandey and Pandey (2007) use the hard threshold, which has a similar disadvantage to that of filtering with a constant cut-off frequency. The method by Ouyang *et al* (1998) uses the soft threshold, but breath holding for 8 s is needed to construct the auto-regressive (AR) model of the cardiac BI signal. Moreover, pre-whitening of the input BI signal and spline based model construction of the respiratory component are required.

With regard to the need for on-line monitoring of the cardiac parameters during exercises and especially in ambulatory conditions the ensemble averaging approach is not suitable.

---

[3] ICG is the first time derivative $\mathrm{d}\mathbf{Z}(t)/\mathrm{d}t$ of the BI signal $\mathbf{Z}(t)$.

[4] However, this does not mean that the respiration component of BI holds no interest for medical applications.

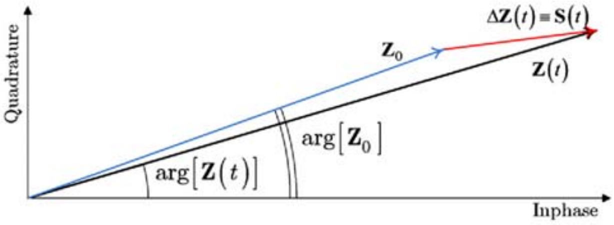

Figure 1. Phasor diagram of the bio-impedance (BI).

Adaptive filtering and spectral analysis are more promising approaches despite the fact that some of these require a reference disturbance signal. Moreover, all the above-described noise cancellation methods and systems, based either on the ensemble averaging, or adaptive filter by Yamamoto *et al* (1988) and Fourier linear combiner SFLC by Barros *et al* (1995), require heart rate estimates obtained from the electrocardiogram (ECG). The availability and accuracy of ECG-based heart rate estimates are the mandatory prerequisites for the reliability of such methods. An exception to this rule is the coherent ensemble averaging method investigated by Hurwitz *et al* (1990). However, although that method does not use the ECG signal, it has a common disadvantage of ensemble averaging—a long time interval is needed for collecting a great number of ICG periods sufficient to perform effective suppression of disturbances.

In this paper we propose a fast method for the separation of the cardiac and respiration components, which uses only the initial BI signal. In addition, heart rate estimations derived from other signals such as ECG can be used to support our method, if available, but this is certainly not obligatory. Our approach eliminates the direct dependence on the availability of the ECG signal, but allows us to use additional data to increase the speed and reliability of the separation process. Moreover, the proposed method is oriented to applications requiring on-line monitoring of both the cardiac and respiratory parameters. At the present stage, this method produces only a 2 s constant delay of the separated cardiac and respiratory components with regard to the initial BI signal. Contrary to the ensemble averaging technique we propose on-line decomposition into cardiac and respiratory components in the time domain using the cardiac BI signal model and continuous tracking of the heart rate (in contrast to the spectral analysis approach). Moreover, no additional reference signal is required. The proposed method is based on the previous works of the authors (Krivoshei *et al* 2006, 2007a, 2007b).

2. Bio-impedance signal considerations

Since we assume that bio-impedance as a parameter of living tissue is measured using sine wave excitation at some predetermined frequency and level, phasor models can be used. Moreover, such an assumption makes it possible to represent the variations of BI in the time domain as a signal. This is a more appropriate representation of BI based information for engineering, medical diagnosis and signal processing. Because only the time variant part of the BI signal is of interest, the symbol $\Delta\mathbf{Z}(t)$ is replaced with $\mathbf{S}(t)$ in the following.

The phasor of the bio-impedance for a fixed frequency of the sine wave excitation (figure 1) can be presented as a sum of the time invariant $\mathbf{Z_0}$ and variant $\Delta\mathbf{Z}(t) \equiv S(t)$ parts.

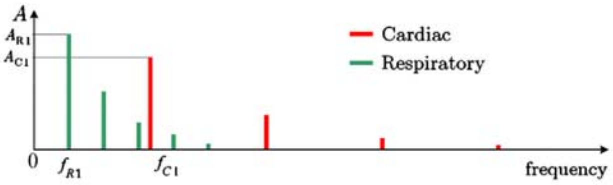

Figure 2. Sketch of a possible spectrum of a BI signal, which consists of cardiac and respiratory components.

The time variant part of the BI phasor $\mathbf{S}(t)$ is assumed to be expressed as a sum of cardiac $\mathbf{S}_\mathrm{C}(t)$ and respiratory $\mathbf{S}_\mathrm{R}(t)$ signals, stochastic disturbance (noise) $\mathbf{n}_\mathrm{S}(t)$ and deterministic disturbance $\mathbf{n}_\mathrm{D}(t)$, caused, e.g., by muscular activity:

$$\mathbf{S}(t) = \mathbf{S}_\mathrm{C}(t) + \mathbf{S}_\mathrm{R}(t) + \mathbf{n}_\mathrm{S}(t) + \mathbf{n}_\mathrm{D}(t). \tag{1}$$

The output of BI measurement systems is often presented by the signal's in-phase and quadrature components, which can be represented also by the magnitudes of vectors (see figure 1). Consequently, equation (1) can be rewritten in a scalar form:

$$S(t) = S_\mathrm{C}(t) + S_\mathrm{R}(t) + n_\mathrm{S}(t) + n_\mathrm{D}(t). \tag{2}$$

Expressing the time variant part of the BI signal $S(t)$ as a sum of the cardiac $S_\mathrm{C}(t)$ and respiratory $S_\mathrm{R}(t)$ components in equations (1) and (2), we assume that these components are received from independent signal sources.

The separation of such nearly independent cardiac and respiratory components accompanied with suppression of stochastic and deterministic disturbances is a complex task due to overlapping of the spectra (figure 2), non-stationary signal components, and moreover, due to the low frequency nature of these signals. The latter makes difficult the real-time presentation of the results (the processing delay must be short). For example, the heart rate (HR) of a healthy person can vary from 60 bpm to 240 bpm, which corresponds to cardiac cycles $T_\mathrm{C} = 0.25$ to 1 s, and to frequencies $F_\mathrm{C} = 1$ to 4 Hz. Because the respiratory rate is about four times lower than HR, the lowest harmonics of the respiratory signal lay in the frequency range of the cardiac signal, too (the spectra are overlapping; see figure 2).

A blind separation of independent components using the ICA (independent component analysis) method is described in various articles and books; see Hyvärinen *et al* (2001). However, taking into account an *a priori* estimate of the one-period signal-shape of a quasi-periodic signal (that is, the instantaneous spectrum content) can give a much more effective and faster solution of the task.

3. Application specific orthonormal basis

Despite the fact that the orthonormal basis formed from the harmonic functions, given in (3), is a powerful, widely used and versatile signal processing tool,

$$\{H_k(t)\} = \{\cos_k(t), \sin_k(t)\}, \tag{3}$$

application of a specific orthonormal basis (ASOB) may give a more appropriate and compact spectral representation of complicated signals in practical situations.

The one-period signal-shape of a cardiac BI signal can be approximated by a non-symmetrical triangular waveform (Krivoshei 2006). However, the computationally efficient triangular signal is not suitable for an accurate cardiac BI signal model in practice.

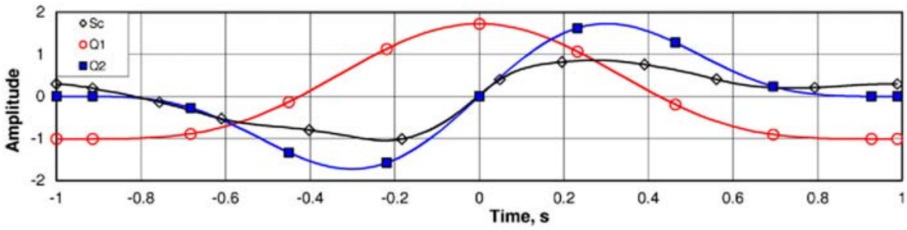

Figure 3. The first $Q_1(t)$ and second $Q_2(t)$ components of the designed ASOB, and the scaled cardiac signal $S_C(t)$ averaged through multiple periods synchronously to the odd component $Q_2(t)$.

The application specific orthonormal bases should be designed in a manner such that the cardiac BI signal model (4) constructed from the first $Q_1(t)$ and the second $Q_2(t)$ components of the created ASOB (5)–(7) could approximate the most significant features of the one-period signal-shape of the cardiac BI signal,

$$\hat{S}_C(t) = A_1 Q_1(t) + A_2 Q_2(t). \tag{4}$$

The variables A_1 and A_2 in (4) are the amplitudes of $Q_1(t)$ and $Q_2(t)$ in $\hat{S}_C(t)$, respectively. To satisfy such a criterion, the Jacobi weight function (5) can be used with the standard Nth order Gram–Schmidt process applied to the function set $\mathcal{F} = \{1, t^1, \ldots, t^{N-1}\}$ within the time interval $[-1, 1)$:

$$W^{A,B}(t) = (1-t)^A(1+t)^B, \qquad t \in [-1, 1). \tag{5}$$

The Jacobi function (5) is selected as a weight function for ASOB, since it has two parameters, A and B, that may help to adapt to specific waveforms. For example, the non-symmetrical waveform can be obtained if A and B have different values. Due to this performance of the Jacobi function, the shape of the second component $Q_2(t)$ of the designed ASOB can be adopted to the waveform of the cardiac BI signal.

The resulting ASOB is formed from the components expressed in (6). The first and second components are presented in figure 3:

$$Q_k(t) = \frac{q_k(t)}{\|q_k(t)\|}, \qquad \text{where} \tag{6}$$

$$\begin{cases} q_0(t) = g_{00} W^{0,0}(t) \\ q_1(t) = g_{10} q_0(t) + W^{A,B}(t) \\ q_2(t) = g_{20} q_0(t) + g_{21} q_1(t) + t \cdot W^{A,B}(t) \\ \ldots \\ q_N(t) = g_{N0} q_0(t) + g_{N1} q_1(t) + \cdots + g_{N(N-1)} q_N(t) + t^N \cdot W^{A,B}(t). \end{cases} \tag{7}$$

The variables g_{km} are found during the Gram–Schmidt process.

Harmonic power spectra of the first $Q_1(t)$ and second $Q_2(t)$ components of the ASOB, and of the cardiac BI signal $S_C(t)$ averaged through multiple periods, are presented in figure 4.

In practice, the values of $W^{A,B}(t)$ in the time interval $t \in [-1, 1)$, g_{km}, and the norms $\|q_k(t)\|, k = 0, \ldots, N, m = 0, \ldots, N-1$ are stored in a memory and used for synthesis of the bases functions $Q_k(t)$ at each time instant during the whole processing time interval.

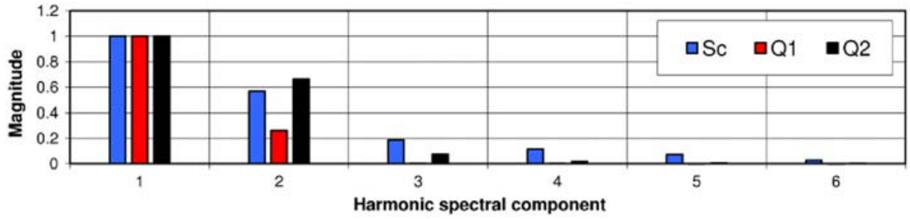

Figure 4. Scaled harmonic spectra of the first and second components $Q_1(t)$ and $Q_2(t)$ of the ASOB, and of the averaged cardiac signal $S_C(t)$.

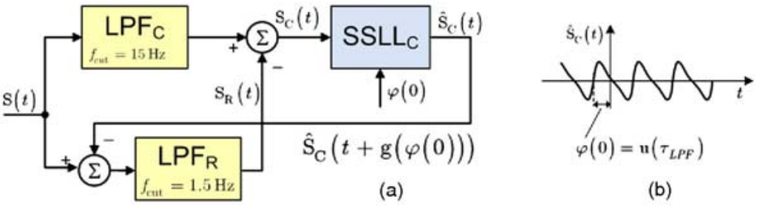

Figure 5. The developed bio-impedance signal decomposer BISD (a), and the cardiac bio-impedance signal model CBISM (b).

4. Cardiac bio-impedance signal model (CBISM)

In the present section the construction procedure of the cardiac BI signal model $\hat{S}_C(t)$ is described. The given procedure is divided into three logical parts, which are explained in the following subsections. The tasks of heart rate estimation, phase synchronization between the separated cardiac signal $S_C(t)$ and its model $\hat{S}_C(t)$, and the synthesis of this model are solved in the signal shape locked loop ($SSLL_C$) block of the proposed BI signal decomposer BISD (see figure 5(a)). The detailed explanation of the $SSLL_C$ with a triangular CBISM by Krivoshei (2006) is presented in Krivoshei *et al* (2007a).

4.1. Time–frequency synchronization

Since the frequency (or period) of the cardiac BI signal $S_C(t)$ is a time variant parameter, time–frequency synchronization between the basal and cardiac signals should be done to guarantee adequate estimates of amplitudes during the following processing steps described in section 4.2.

The odd component $Q_1(t)$ is used to synchronize the even component $Q_2(t)$ of the ASOB against the input signal $S_C(t)$ of the signal shape locked loop $SSLL_C$; see figure 5 and Krivoshei *et al* (2007a).

4.2. Cardiac BI signal decomposition in ASOB

For the estimation of amplitude values of the spectral components of the ASOB representing the cardiac BI signal, an adaptive linear combiner by Widrow and Stearns (1985) is used. Instantaneous estimates of the amplitude values $a_k(t_i)$ at the time instances t_i (weights of the adaptive linear combiner) have been found using the least mean square (LMS) algorithm (10) for the cost function (8), when $N = 7$:

$$J(t) = e^2(t), \tag{8}$$

where

$$e(t) = S_C(t) - \hat{S}_C(t) = S_C(t) - \sum_{k=0}^{N} A_k Q_k(t) \tag{9}$$

$$a_k(t_i) = 2\mu_{a_k} \int_0^{t_i} e(\tau) Q_k(\tau)\, \mathrm{d}\tau, \tag{10}$$

where μ_{a_k} is a real positive number which determines the speed of the cost function (8) minimization process. In practical cases, the process minimization speed can be increased by introducing the high-pass filter in series with the integrator from (10), giving the transfer function

$$\mathrm{TF}_k(s) = \frac{1}{\tau_{\mathrm{int}} s} \frac{\tau_z s + 1}{\tau_p s + 1}, \qquad \text{where i.e.} \quad \tau_z > \tau_{\mathrm{int}} > \tau_p \qquad \text{and} \qquad \tau_{\mathrm{int}} = 1/2\mu_{a_k}. \tag{11}$$

4.3. Synthesis of the CBISM

As a result of the above-described developments, the cardiac BI signal model $\hat{S}_C(t)$ at the output of the $\mathrm{SSLL_C}$ is expressed as

$$\hat{S}_C(t) = \sum_{k=0}^{N} A_k Q_k(t) \tag{12}$$

where

$$A_k = a_k(t_i). \tag{13}$$

5. Bio-impedance signal decomposer (BISD)

The adaptive BISD—intended for the separation of two low frequency signals: the cardiac and respiratory BI components—is designed as a two-component SSLL operating in the ASOB with a Jacobi weighting function to achieve better results than in Krivoshei *et al* (2007a), where the non-symmetrical triangular signal is used as a CBISM, and in Krivoshei *et al* (2007b), where the triangular function in power two is used as a weighting function in the standard Gram–Schmidt process. A block diagram of the proposed BISD is shown in figure 5(a).

The cardiac BI signal $S_C(t)$ is tracked by the $\mathrm{SSLL_C}$, which is described by Krivoshei *et al* (2007a) and which is also considered in the previous section together with the proposed ASOB.

Since the respiratory BI signal is much less deterministic than the cardiac one, the signal modelling procedure is more complicated. The present version of the BISD uses the FIR (finite impulse response) low-pass filter $\mathrm{LPF_R}$ with a constant cut-off frequency $f_{\mathrm{cut}} = 1.5$ Hz to suppress the remainder part of the cardiac BI signal model $\hat{S}_C(t)$, subtracted from the input cardiac signal $S_C(t)$. The second low-pass filter $\mathrm{LPF_C}$ is used in the upper branch of the two-component SSLL to compensate the delay of the respiratory signal in the $\mathrm{LPF_R}$, and to suppress the high frequency noise. Moreover, an additional lead shift of phase $\varphi(0)$ of the CBISM towards the 'future' (figure 5(b)) is required to compensate the delay of the cardiac signal $S_C(t)$ in the $\mathrm{LPF_C}$.

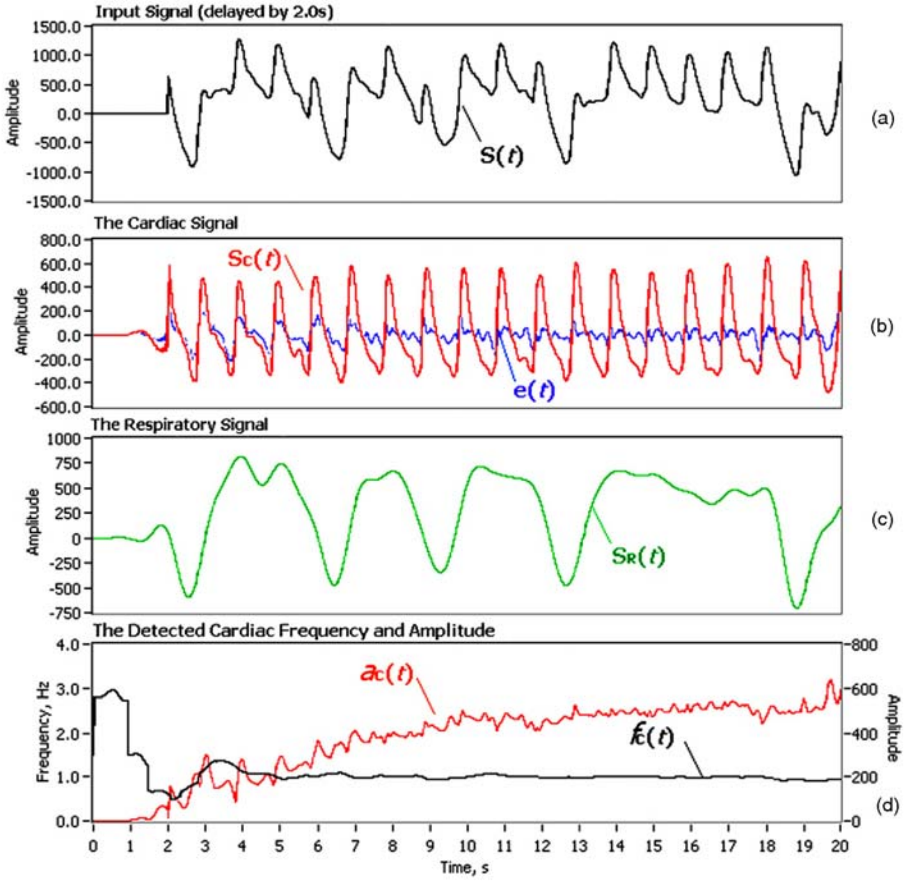

Figure 6. Time domain responses of the proposed signal decomposer BISD to the BI data of patient 1 (just after switching on the signals).

6. Results

The proposed method and the signal decomposer BISD based on this method are both accomplished as a digital software system operating at 200 Hz clock frequency (PC version, programmed in C++, LabView user interface).

The collection of bio-impedance (BI) signals recorded in clinical conditions was used for testing the proposed method. The impedance measurements were carried out by using the CircMon device (JR Medical Ltd, Estonia) operating at a frequency of 30 kHz and having a tetrapolar configuration of electrodes (together eight standard ECG electrodes on hands and feet). Initially the BI signal is sampled at a rate of 1 kHz and further is decimated to 200 Hz using a 5-point averaging filter. The signal collection used contains the values of BI signals as digital codes of integer numbers, obtained from the digital output of the CircMon device.

Figures 6 and 7 present the time responses of the BISD to the input signals obtained from two patients. Each of the figures consists of four plots:

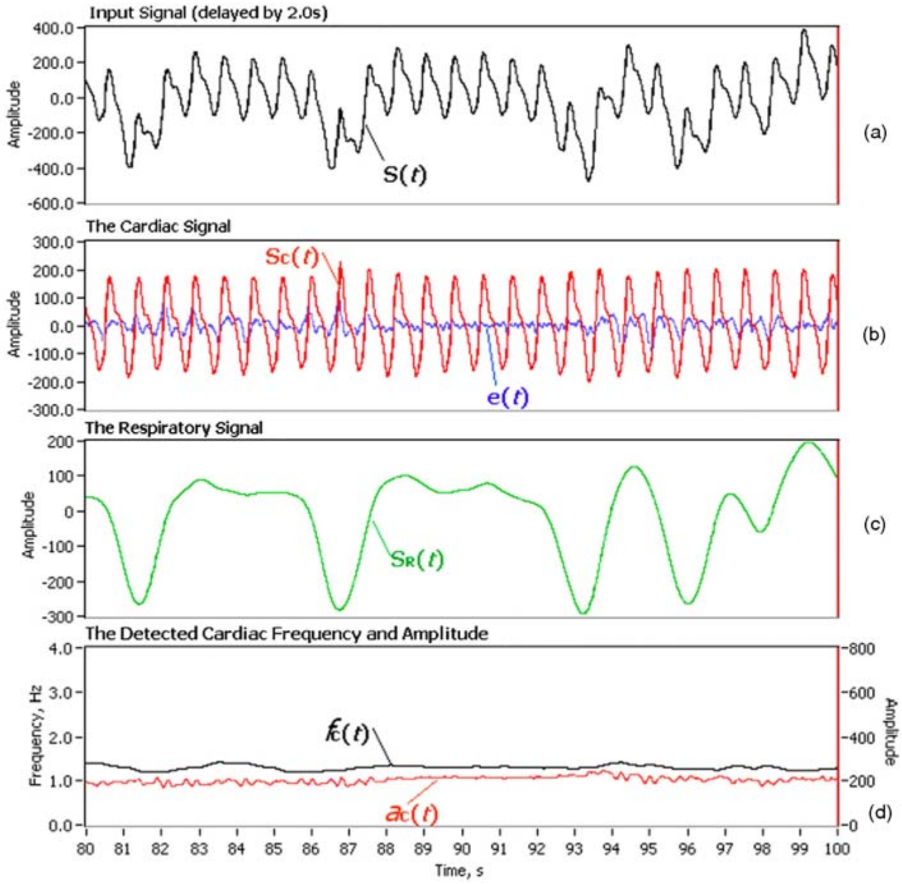

Figure 7. Time domain responses of the proposed signal decomposer BISD to the BI data of patient 2.

(a) The input signal $S(t)$, delayed by 2 s;
(b) The obtained cardiac component $S_{\mathrm{C}}(t)$ (a red line), and the difference $e(t)$ between the $S_{\mathrm{C}}(t)$ and its model $\hat{S}_{\mathrm{C}}(t)$ (a blue line);
(c) The obtained respiratory component $S_{\mathrm{R}}(t)$;
(d) The estimates of instantaneous frequency $f_{\mathrm{C}}(t_i)$ (a black line), and instantaneous amplitude value $a_{\mathrm{C}}(t_i) = \sqrt{a_1^2(t_i) + a_2^2(t_i)}$ of the $S_{\mathrm{C}}(t)$ (a red line).

7. Discussion and conclusions

The developed method for the separation of the cardiac and respiratory components of the bioimpedance BI signal is based only on the initial raw input. However, additional information about the heart rate, derived from other (e.g. ECG) signals, can be used if available, but this is certainly not obligatory. Such an approach eliminates the direct dependence on the ECG and other complementary information, but allows us to use the additional data to increase the speed and reliability of the decomposition process. Improved methods and algorithms for effective using of the additional information from different sources are under development by our research group.

The methods which process the BI based and optional data about the heart rate are closely connected to the development of the signal shape locked loop ($\mathrm{SSLL_C}$) for tracking the cardiac signal. The complexity of the problem does not allow us to consider this thoroughly in the present paper. The role of the $\mathrm{SSLL_C}$ in the bio-impedance signal decomposer (BISD) is described briefly in section 4; a more detailed explanation can be found in Krivoshei *et al* (2007a).

The model of the cardiac BI signal used is based on the application specific orthonormal basis (ASOB) designed by the authors. This model is intended to represent the cardiac BI signal using only two components, $Q_1(t)$ and $Q_2(t)$, of the full ASOB set. We proposed the signal model with constant and equal power exponents $A = B = 5$ in the Jacobi function (5). Such a choice is sufficient for the first stage modelling. However, because the waveforms of cardiac signals (not only the heart rate) are also non-stationary, adaptive modelling is required, in principle. To compensate this insufficiency, more components of the ASOB can be introduced, e.g., using of five or six components can already solve the problem. A more perspective way is to use the signal model with adaptively tunable parameters A and B, which has recently been proposed by Krivoshei *et al* (2008).

Since the available BI signal records were acquired in stationary clinical conditions, the motion artefacts are almost absent. Therefore the artefact problem is not studied in the paper, only the respiratory signal has been taken into account as a disturbance to the cardiac signal.

In conclusion, the proposed method allow us to separate the cardiac and respiratory BI signal components effectively in non-stationary conditions with only 2 s of delay time. Figures 6 and 7 show that especially the respiratory signal component can be extremely non-stationary and may change very fast (figure 6). Despite the promising results further research is needed to make the algorithms simpler and more reliable, and also robust enough for implementation in wearable medical devices, including testing in different pathological cases.

Acknowledgments

This work was supported by the Estonian Science Foundation (grants no. G7212, G7243 and G5614), Enterprise Estonia through the Competence Centre ELIKO and EITSA. The authors express their thanks to Dr Jürgen Lamp from JR Medical Ltd for providing practical information and giving valuable advice.

References

Barros A K, Yoshizawa M and Yasuda Y 1995 Filtering noncorrelated noise in impedance cardiography *IEEE Trans. Biomed. Eng.* **42** 324–7

Chen J Z, Lin Z and McCallum R W 1993 Cancelation of motion artifacts in electrogastrogram: a comparision of time-, transform- and frequency-domain adaptive filtering *Proc. Conf. SoutheastCon'93*

Cotter G, Schachner A, Sasson L, Dekel D and Moshkovitz Y 2006 Impedance cardiology revisited *Physiol. Meas.* **27** 817–27

Grimnes S and Martinsen Ø G 2000 *Bioimpedance and Bioelectricity Basics* (London: Academic)

Hu W, Sun H H and Wang X 1997 A study on methods for impedance cardiography *Proc. 19th Int. Conf. IEEE/EMBS 97* pp 2074–7

Hurwitz B E, Shyu L Y, Reddy S P, Schneiderman N and Nagel J H 1990 Coherent ensemble averaging techniques for impedance cardiography *Proc. 3rd Annu. IEEE Symp. Comp. Based Med. Syst.*

Hyvärinen A, Karhunen J and Oja E 2001 *Independent Component Analysis* (New York: Wiley)

Kim D W, Song C G and Lee M H 1992 A new ensemble averaging technique in impedance cardiography for estimation of stroke volume during treadmill exercise *Front. Med. Biol. Eng.* **4** 179–88

Krivoshei A 2006 A bio-impedance signal synthesiser (BISS) for testing of an adaptive filtering system *Proc. Int. Biennal Baltic Electronics Conf. BEC 2007* pp 225–8

Krivoshei A, Min M, Parve T and Ronk A 2006 An adaptive filtering system for separation of cardiac and respiratory components of bioimpedance signal *Proc. Int. Workshop on Medical Measurements and Applications MeMeA 2006* pp 10–5

Krivoshei A, Min M and Kukk V 2007a Signal-shape locked loop (SSLL) as an adaptive separator of cardiac and respiratory components of bio-impedance signal *Proc. Int. Workshop on Medic. Meas. and Applic. MeMeA 2007* pp 47–52

Krivoshei A, Kukk V and Birjukov A 2007b Bio-impedance signal decomposer (BISD) as an adaptive signal model based separator of cardiac and respiratory components *ICEBI 2007, IFMBE Proc.* **17** 209–12

Krivoshei A, Kukk V and Min M 2008 An adaptively tunable model of the cardiac signal for the bio-impedance signal decomposer (BISD) *Proc. Int. Workshop on Medic. Meas. and Applic. MeMeA 2008* pp 49–52

Muzi M, Jeutter D C and Smith J J 1986 Computer-automated impedance-derived cardiac indexes *IEEE Trans. Biomed. Eng.* **33** 42–7

Ouyang J, Gao X and Zhang Y 1998 Wavelet-based method for reducing respiratory interference in thoracic electrical bioimpedance *Proc. 20th Ann. Int. Conf. IEEE Eng. in Medic. and Biol. Soc.* **20** 1446–9

Pandey V K and Pandey P C 2005 Cancellation of respiratory artifact inimpedance cardiography *Proc. 27th Annual Conf. Engineering in Medicine and Biology* pp 5503–6

Pandey V K and Pandey P C 2007 Wavelet based cancellation of respiratory artifacts in impedance cardiography *Proc. 15th Int. Conf. on Digital Signal Processing* pp 191–4

Wang X, Sun H H and Van De Water J M 1995 An advanced signal processing technique for impedance cardiography *IEEE Trans. Biomed. Eng.* **42** 224–30

Widrow B and Stearns S D 1985 *Adaptive Signal Processing* (Upper Saddle River, NJ: Prentice-Hall)

Woltjer H H, Bogaard H J and de Vries P M J M 1996 The intra- and interobserver variability of impedance cardiography in patients at rest and during exercise *Physiol. Meas.* **17** 171–8

Yamamoto Y, Mokushi K, Tamura S, Mutoh Y, Miyashita M and Hamamoto H 1988 Design and implementation of a digital filter for beat-by-beat impedance cardiography *IEEE Trans. Biomed. Eng.* **35** 1086–90

Zhang Y, Qu M, Webster J G, Tompkins W J, Ward B A and Bassett D R 1986 Cardiac output monitoring by impedance cardiography during treadmill exercise *IEEE Trans. Biomed. Eng.* **33** 1037–42

G appendix

ELULOOKIRJELDUS

1. Isikuandmed

Ees- ja perekonnanimi:	Andrei Krivošei
Sünniaeg ja -koht:	27.04.1979, Kohtla-Järve, Eesti
Kodakondsus:	Eesti

2. Kontaktandmed

Aadress:	Olevi 35-38, 30325, Kohtla-Järve, Eesti
Telefon:	(+372) 533 23 719
E-posti aadress:	andrei.krivoshei@gmail.com

3. Hariduskäik

Õppeasutus (nimetus lõpetamise ajal)	**Lõpetamise aeg**	**Haridus (eriala/kraad)**
Järve Vene Gümnaasium	Juuni 1997	Gümnaasiumi haridus
Virumaa Kõrgkool	Juuni 2000	Lõpemata kõrgharidus
Tallinn Tehnikaülikool	Juuni 2003	Tehnikateaduste bakalaureus
Tallinn Tehnikaülikool	Juuni 2005	Tehnikateaduste magister

4. Keelteoskus (alg-, kesk- või kõrgtase)

Keel	Tase
Vene	Kõrgtase
Eesti	Kõrgtase
Inglise	Kesktase

5. Täiendusõpe

Õppimise aeg	Täiendusõppe läbiviija nimetus
03.09.07-07.09.07	”Low-Noise, Low-Offset Analog IC Design” *Swiss, Lausanne, Swiss Federal Institute of Technology - EPFL*
27.08.07-31.08.07	”Practical Aspects in Mixed-Mode ICs” *Swiss, Lausanne, Swiss Federal Institute of Technology - EPFL*
25.06.07-29.06.07	”Practical Approach to Delta-Sigma Design” *Swiss, Lausanne, Swiss Federal Institute of Technology - EPFL*

6. Teenistuskäik

Töötamise aeg	Tööandja nimetus	Ametikoht
Jan’2005 – praegu	ELIKO TAK OÜ	Insener (part-time)
Jul’2003 – Dec’2004	Tevalo AS	Müüja ja konsultant
Jun’2001 – Aug’2001	Analoog Disaini AS	Praktikant

7. Teadustegevus

“Electronic components and subsystems for mission critical embedded systems” (SF0142737s06)

“Mitmekomponendiliste ja mitme kandjaga mõõtesignaalide süntees ja analüüs: signaalide sünkroon- ja adaptiivtöötluse meetodite ja vahendite arendus” (ETF7243)

“Südame täitumismahuga seostuv energiatarve” (ETF7212)

Osalensin IKT Doktorikoolis

8. Kaitstud lõputööd

“*Adaptive system of filters for post-processing in bio-impedance measurement technique*”, Tehnikateaduste magistri kraad 2005

“*Switched Capacitor (SC) filters for a Bio-impedance measurement system*”, Tehnikateaduste bakalaureuse kraad 2003

9. Teadustöö põhisuunad

Digitaalne signaali töötlus
Adaptiivne signaali töötlus
Bioimpedants signaali töötlus
Biomeditsiniline signaali töötlus

Kuupäev: 31.07.2009

H appendix

CURRICULUM VITAE

1. Personal data

Name:	Andrei Krivošei
Date and place of birth:	27.04.1979, Kohtla-Järve, Estonia

2. Contact information

Address:	Olevi 35-38, 30325, Kohtla-Järve, Estonia
Phone:	(+372) 533 23 719
E-mail:	andrei.krivoshei@gmail.com

3. Education

Educational institution	Graduation year	Education (field of study/degree)
Järve Vene Gümnaasium	Juuni 1997	Secondary
Virumaa Kõrgkool	Juuni 2000	Unfinished
Tallinn University of Technology	Juuni 2003	B. Sc.
Tallinn Tehnikaülikool	Juuni 2005	M. Sc.

4. Language competence/skills (fluent; average, basic skills)

Language	Level
Russian	Native
Estonian	Very good
English	Good

5. Special Courses

Period	Educational or other organisation
03.09.07-07.09.07	”Low-Noise, Low-Offset Analog IC Design” *Swiss, Lausanne, Swiss Federal Institute of Technology - EPFL*
27.08.07-31.08.07	”Practical Aspects in Mixed-Mode ICs” *Swiss, Lausanne, Swiss Federal Institute of Technology - EPFL*
25.06.07-29.06.07	”Practical Approach to Delta-Sigma Design” *Swiss, Lausanne, Swiss Federal Institute of Technology - EPFL*

6. Professional Employment

Period	Organisation	Position
Jan’2005 – praegu	ELIKO TAK OÜ	Research & Development Engineer (part-time)
Jul’2003 – Dec’2004	Tevalo AS	Shop assistant and consultant
Jun’2001 – Aug’2001	Analoog Disaini AS	Trainee

7. Scientific work

“Electronic components and subsystems for mission critical embedded systems” (SF0142737s06)

“Mitmekomponendiliste ja mitme kandjaga mõõtesignaalide süntees ja analüüs: signaalide sünkroon- ja adaptiivtöötluse meetodite ja vahendite arendus” (ETF7243)

“Südame täitumismahuga seostuv energiatarve” (ETF7212)

Osalensin IKT Doktorikoolis

8. Defended theses

“*Adaptive system of filters for post-processing in bio-impedance measurement technique*”, B. Sc. 2005

“*Switched Capacitor (SC) filters for a Bio-impedance measurement system*”, M. Sc. 2003

9. Main areas of scientific work/Current research topics

Digital Signal Processing
Adaptive Signal Processing
Bio-impedance signal processing
Biomedical signal processing

Date: 31.07.2009

List of publications

Krivoshei A 2006a A Bio-Impedance Signal Synthesiser (BISS) for Testing of an Adaptive Filtering System *Proc. Int. Biannual Baltic Electronics Conf. BEC 2006* 225–8.

Krivoshei A, Min M, Parve T and Ronk A 2006b An Adaptive Filtering System for Separation of Cardiac and Respiratory Components of Bioimpedance Signal *Proc. Int. Workshop on Medical Measurements and Applications MeMeA 2006* 10–5.

Krivoshei A, Min M and Kukk V 2007a Signal-Shape Locked Loop (SSLL) as an Adaptive Separator of Cardiac and Respiratory Components of Bio-Impedance Signal *Proc. Int. Workshop on Medic. Meas. and Applic. MeMeA 2007* 47–52.

Krivoshei A, Kukk V and Birjukov A 2007b Bio-Impedance Signal Decomposer (BISD) as an Adaptive Signal Model Based Separator of Cardiac and Respiratory Components *Proc. On ICEBI 2007, IFMBE* **17** 209–12.

Krivoshei A, Kukk V and Min M 2008a An Adaptively Tunable Model of the Cardiac Signal for the Bio-Impedance Signal Decomposer (BISD) *Proc. Int. Workshop on Medic. Meas. and Applic. MeMeA 2008* 49–52.

Krivoshei A, Kukk V and Min M 2008b Decomposition method of electrical bio-impedance signal into cardiac and respiratory components *Physiological Measurement* **29**(6) S15 - S25.

Annus P, Krivoshei A and Min M 2008a Excitation Current Source for Bioimpedance Measurement Applications: Analysis and Design *Proc. Int. Instrumentation and Measurement Technology Conf. I2MTC 2008* 848–53.

References

Annus P, Krivoshei A and Min M 2008a Excitation Current Source for Bioimpedance Measurement Applications: Analysis and Design *Proc. Int. Instrumentation and Measurement Technology Conf. I2MTC 2008* 848–53.

Annus P, Min M and Ojarand J 2008b Shortened square wave waveforms in synchronous signal processing. *Proc. Int. Instrumentation and Measurement Technology Conf. I2MTC 2008* 1259–62.

Atzler E and Lehmann G 1932 Über ein Neues Verfahren zur Darstellung der Herztätigkeit (Dielektrographie) *Arbeitsphysiol.* **6** 636–80.

Barros A K, Yoshizawa M and Yasuda Y 1995 Filtering Noncorrelated Noise in Impedance Cardiography *IEEE Trans. Biomed. Eng*. **42** 324–7.

Chen J Z, Lin Z and McCallum R W 1993 Cancelation of motion artefacts in electrogastrogram – a comparison of time-, transform- and frequency-domain adaptive filtering *Proc. Conf. SoutheastCon'93.*

Cotter G, Schachner A, Sasson L, Dekel D and Moshkovitz Y 2006 Impedance cardiology revisite *J. Physiol. Meas*. **27** 817–827.

Dell'Orto S, Valli P and Greco M E 2004 Sensors for Rate Adaptive Pacing *Indian Pacing and Electrophysiology J.* **4**(3) 137–45.

Geddes L A 1972 *Electrode and the Measurement of Bioelectric Events* (NY: Wily-Interscience).

Geddes L A and Baker L E 1975 *Principles of Applied Biomedical Instrumentation (Second Edition)* (NY: Wily-Interscience).

Grimnes S and Martinsen Ø G 2008 *Bioimpedance & Bioelectricity Basics* (London: Academic Press).

Hu W, Sun H H and Wang X 1997 A study on methods for impedance cardiography *Proc. 19th Int. Conf. IEEE/EMBS 97* 2074–77.

Hurwitz B E, Shyu L Y, Reddy S P, Schneiderman N and Nagel J H 1990 Coherent ensemble averaging techniques for impedance cardiography *Proc. 3rd Annu. IEEE Symp. Comp. Based Med. Syst.*

Hyvärinen A and Oja E 2000 Independent Component Analysis: Algorithms and Applications *Neural Networks* **13**(4-5) 411–30 .

Hyvärinen A, Karhunen J and Oja E 2001 *Independent Component Analysis* (John Wiley & Sons).

Kennelly A E 1893 Impedance *Transactions of the American Institute of Electrical Engineers* **10** 175–232.

Kim D W, Song C G and Lee M H 1992 A new ensemble averaging technique in impedance cardiography for estimation of stroke volume during treadmill exercise *Frountiers Med. Biol. Eng.* **4** 179–188.

Krivoshei A 2006a A Bio-Impedance Signal Synthesiser (BISS) for Testing of an Adaptive Filtering System *Proc. Int. Biennial Baltic Electronics Conf. BEC 200*6 225–8.

Krivoshei A, Min M, Parve T and Ronk A 2006b An Adaptive Filtering System for Separation of Cardiac and Respiratory Components of Bioimpedance Signal *Proc. Int. Workshop on Medical Measurements and Applications MeMeA 2006* 10–5.

Krivoshei A, Min M and Kukk V 2007a Signal-Shape Locked Loop (SSLL) as an Adaptive Separator of Cardiac and Respiratory Components of Bio-Impedance Signal *Proc. Int. Workshop on Medic. Meas. and Applic. MeMeA 2007* 47–52.

Krivoshei A, Kukk V and Birjukov A 2007b Bio-Impedance Signal Decomposer (BISD) as an Adaptive Signal Model Based Separator of Cardiac and Respiratory Components *ICEBI 2007, IFMBE Proc.* **17** 209–12.

Krivoshei A, Kukk V and Min M 2008a An Adaptively Tunable Model of the Cardiac Signal for the Bio-Impedance Signal Decomposer (BISD) *Proc. Int. Workshop on Medic. Meas. and Applic. MeMeA 2008* 49–52.

Krivoshei A, Kukk V and Min M 2008b Decomposition method of electrical bio-impedance signal into cardiac and respiratory components *Physiological Measurement* **29**(6) S15 - S25.

Kubicek W G, Karnegis J N, Patterson R P *et al* 1966 Development and evaluation of an impedance cardiac output system *Aerospace Med.* **37** 1208–12.

Kubicek W G 1968 *Minnesota Impedance Cardiograph Model 303. Instruction Manual* (Minneapolis: Univ. of Minnesota Press).

Malmivuo J and Plonsey R 1995 *Bioelectromagnetism: Principles and Applications of Bioelectric and Biomagnetic Fields* (NY:Oxford University Press).

McFetridge-Durdle J A, Routledge F S, Parry M J E, Dean C R T and Tucker B 2008 Ambulatory impedance cardiography in hypertension: A validation study *European Journal of Cardiovascular Nursing* **7** 204–13.

Min M, Parve T and Kink A 1999 Thoracic Bioimpedance as a Basis for Pacing Control (at Electrical Bioimpedance Methods: Applications to Medicine and Biotechnology) *Annals of the NY Academy of Science* **873** 155–66.

Min M, Märtens O and Parve T 2000 Lock-in measurement of bio-impedance variations *Meas. J. IMEKO* **21**(1) 21–8.

Min M, Parve T, Kukk V and Kuhlberg A 2002 An Implantable Analyzer of Bio-Impedance Dynamics: Mixed Signal Approach *IEEE Ttans. On Instrum. And Meas.* **51**(4) 674–8.

Min M, Pliquett U, Nacke T, Barthel A, Annus P and Land R 2008 Broadband excitation for short-time impedance spectroscopy *Physiological Measurement* **29**(6) S185–S192.

Mond H L, Stratmore N, Kertes P, Hunt D and Baker G 1988 Rate responsive pacing using a minute ventilation sensor *Pace* **11**(suppl. II) 1866–74.

Muzi M, Jeutter D C and Smith J J 1986 Computer-Automated Impedance-Derived Cardiac Indexes *IEEE Trans. Biomed. Eng.* **33** 42–7.

Newman D G and Callister R 1999 The non-invasive assessment of stroke volume and cardiac output by impedance cardiography: a review *Aviat. Space Environ. Med.* **70**(8) 780–9.

Nyboer J, Bagno S, Barmett A *et al* 1940 Radiocardiograms: electrical impedance changes in heart in relation to electrocardiograms and heart sounds *Journal Clin. Invest.* **19** 963.

Nyboer J 1950 Electrical impedance plethysmography: a physical and physiologic approach to peripheral vascular study *Circulation* **2** 811–21.

Ouyang J, Gao X and Zhang Y 1998 Wavelet-based method for reducing respiratory interference in thoracic electrical bioimpedance *Proc. 20th Ann. Int. Conf. of IEEE Eng. In Medic. and Biology Society* **20** 1446–9.

Paavle T, Min M and Parve T 2008 Using of Chirp Ecxitation for Bioimpedance Estimation: Theoretical Aspects and Modeling *Proc. Int. Biennial Baltic Electronics Conf. BEC 200*8 325–8.

Pandy V K and Pandey P C 2005 Cancellation of Respiratory Artifact inImpedance Cardiography *Proc. 27th Annual Conf. Eng. In Medicine and Biol.* pp 5503–6

Pandy V K and Pandey P C 2007 Wavelet based cancellation of respiratory artifacts in impedance cardiography *Proc. 15th Int. Conf. on Dig. Sign. Process.* 191–4.

Patterson R P 1989 Fundamentals of Impedance Cardiography *IEEE Eng. In Medicine And Biology Mag.* 35–8.

Rohrmann S and Hopp H 2008 Cardiovascular indicators of disgust *International Journal of Psychophysiology* **68** 201–8.

Rossel, Cohen K P and Webster J G 1995 Reduction of Motion Artifacts Using a Two-Frequency Impedance Plethysmograph and Adaptive Filtering *IEEE Trans. On Biomed. Engineering* **42**(10) 1044–8.

Salo R W 2001 *An improved computational model for intracardiac impedance plethysmography* PhD Thesis (Fridley, Minnesota).

Sigman E, Kolin A, Katz L N and Jochim K 1937 Effect of motion on the electrical conductivity of the blood *Am. J. Physiol.* **118** 708–19.

Sodolski and Kutarski 2007 Impedance cardiography: A valuable method of evaluating haemodynamic parameters *Cardiology Journal* **14**(2) 115–26.

Wang X, Sun H H and Van De Water J M 1995 An Advanced Signal Processing Technique for Impedance Cardiography *IEEE Trans. Biomed. Eng.* **42** 224–230.

Webster J G 1995 *Design of Cardiac Pacemakers* (NJ: IEEE Press).

West J B 1988 *Respiratory Physiology: The Essentials* (Moskva: Mir) [Russian edition].

Widrow B and Stearns S D 1985 *Adaptive Signal Processing* (NJ: Prentice Hall).

Woltjer H H, Bogaard H J and M de Vries P M J 1996 The intra- and interobserver variability of impedance cardiography in patients at rest and during exercise *J. Physiol. Meas.* **17** 171-8.

Yamamoto Y, Mokushi K, Tamura S, Mutoh Y, Miyashita M and Hamamoto H 1988 Design and Implementation of a Digital Filter for Beat-by-Beat Impedance Cardiography *IEEE Trans. Biomed. Eng.* **35** 1086-90.

Zhang Y, Qu M, Webster J G, Tompkins W J, Ward B A and Bassett D R 1986 Cardiac Output Monitoring by Impedance Cardiography During Treadmill Exercise *IEEE Trans. Biomed. Eng.* **33** 1037-42.

Zlochiver S, Freimark D, Arad M, Adunsky A and Abboud S 2006 Parametric EIT for monitoring cardiac stroke volume *Physiol. Meas.* **27** S139–S146.

DISSERTATIONS DEFENDED AT TALLINN UNIVERSITY OF TECHNOLOGY ON *INFORMATICS AND SYSTEM ENGINEERING*

1. **Lea Elmik**. Informational modelling of a communication office. 1992.

2. **Kalle Tammemäe**. Control intensive digital system synthesis. 1997.

3. **Eerik Lossmann**. Complex signal classification algorithms, based on the third-order statistical models. 1999.

4. **Kaido Kikkas**. Using the Internet in rehabilitation of people with mobility impairments – case studies and views from Estonia. 1999.

5. **Nazmun Nahar**. Global electronic commerce process: business-to-business. 1999.

6. **Jevgeni Riipulk**. Microwave radiometry for medical applications. 2000.

7. **Alar Kuusik**. Compact smart home systems: design and verification of cost effective hardware solutions. 2001.

8. **Jaan Raik**. Hierarchical test generation for digital circuits represented by decision diagrams. 2001.

9. **Andri Riid**. Transparent fuzzy systems: model and control. 2002.

10. **Marina Brik**. Investigation and development of test generation methods for control part of digital systems. 2002.

11. **Raul Land**. Synchronous approximation and processing of sampled data signals. 2002.

12. **Ants Ronk**. An extended block-adaptive Fourier analyser for analysis and reproduction of periodic components of band-limited discrete-time signals. 2002.

13. **Toivo Paavle**. System level modeling of the phase locked loops: behavioral analysis and parameterization. 2003.

14. **Irina Astrova**. On integration of object-oriented applications with relational databases. 2003.

15. **Kuldar Taveter**. A multi-perspective methodology for agent-oriented business modelling and simulation. 2004.

16. **Taivo Kangilaski**. Eesti Energia käiduhaldussüsteem. 2004.

17. **Artur Jutman**. Selected issues of modeling, verification and testing of digital systems. 2004.

18. **Ander Tenno**. Simulation and estimation of electro-chemical processes in maintenance-free batteries with fixed electrolyte. 2004.

19. **Oleg Korolkov**. Formation of diffusion welded Al contacts to semiconductor silicon. 2004.

20. **Risto Vaarandi**. Tools and techniques for event log analysis. 2005.

21. **Marko Koort**. Transmitter power control in wireless communication systems. 2005.

22. **Raul Savimaa**. Modelling emergent behaviour of organizations. Time-aware, UML and agent based approach. 2005.

23. **Raido Kurel**. Investigation of electrical characteristics of SiC based complementary JBS structures. 2005.

24. **Rainer Taniloo**. Ökonoomsete negatiivse diferentsiaaltakistusega astmete ja elementide disainimine ja optimeerimine. 2005.

25. **Pauli Lallo.** Adaptive secure data transmission method for OSI level I. 2005.

26. **Deniss Kumlander**. Some practical algorithms to solve the maximum clique problem. 2005.

27. **Tarmo Veskioja**. Stable marriage problem and college admission. 2005.

28. **Elena Fomina**. Low power finite state machine synthesis. 2005.

29. **Eero Ivask**. Digital test in WEB-based environment 2006.

30. **Виктор Войтович**. Разработка технологий выращивания из жидкой фазы эпитаксиальных структур арсенида галлия с высоковольтным p-n переходом и изготовления диодов на их основе. 2006.

31. **Tanel Alumäe**. Methods for Estonian large vocabulary speech recognition. 2006.

32. **Erki Eessaar**. Relational and object-relational database management systems as platforms for managing softwareengineering artefacts. 2006.

33. **Rauno Gordon**. Modelling of cardiac dynamics and intracardiac bio-impedance. 2007.

34. **Madis Listak**. A task-oriented design of a biologically inspired underwater robot. 2007.

35. **Elmet Orasson**. Hybrid built-in self-test. Methods and tools for analysis and optimization of BIST. 2007.

36. **Eduard Petlenkov**. Neural networks based identification and control of nonlinear systems: ANARX model based approach. 2007.

37. **Toomas Kirt**. Concept formation in exploratory data analysis: case studies of linguistic and banking data. 2007.

38. **Juhan-Peep Ernits**. Two state space reduction techniques for explicit state model checking. 2007.

39. **Innar Liiv**. Pattern discovery using seriation and matrix reordering: A unified view, extensions and an application to inventory management. 2008.

40. **Andrei Pokatilov**. Development of national standard for voltage unit based on solid-state references. 2008.

41. **Karin Lindroos**. Mapping social structures by formal non-linear information processing methods: case studies of Estonian islands environments. 2008.

42. **Maksim Jenihhin**. Simulation-based hardware verification with high-level decision diagrams. 2008.

43. **Ando Saabas**. Logics for low-level code and proof-preserving program transformations. 2008.

44. **Ilja Tšahhirov**. Security protocols analysis in the computational model – dependency flow graphs-based approach. 2008.

45. **Toomas Ruuben**. Wideband digital beamforming in sonar systems. 2009.

46. **Sergei Devadze**. Fault Simulation of Digital Systems. 2009.